STUDY OF THE MORPHOLOGY OF CROSSLINKED POLYETHYLENE AND OF POLYMER MELTS UNDER SHEAR

Andrew J. Peacock, M.Sc.,B.Sc.,A.K.C.

University of Southampton

A thesis submitted in support of
candidature for the degree of
Doctor of Philosophy

July, 1984

Acknowledgements

I would like to express my gratitude to the following people, without whom this thesis would not have been possible.

Dr. P. J. Hendra for supervision, advice and encouragement throughout.

Dr. H. A. Willis and Dr. M. E. A. Cudby for many fruitful discussions and much beneficial advice.

All the members of the Polymer Properties Group at the University of Southampton for discussions, advice and help.

My mother for diligently preparing the typescript.

Contents

Contents (cont'd)

Contents (cont'd)

List of Figures

List of Figures (cont'd)

List of Tables

UNIVERSITY OF SOUTHAMPTON

ABSTRACT

FACULTY OF SCIENCE

CHEMISTRY

Doctor of Philosophy

STUDY OF THE MORPHOLOGY OF CROSSLINKED POLYETHYLENE AND OF POLYMER MELTS UNDER SHEAR

by Andrew James Peacock

The aim of the work was to study the morphology of various polymers under a variety of conditions. The research followed various lines. The morphology of crosslinked polyethylene and its implications with respect to that of linear polyethylene was studied by Raman spectroscopy, differential scanning calorimetry, electron microscopy, small angle light scattering and nuclear magnetic resonance. The efficiency of the crosslinking reaction was evaluated. The morphology of flowing molten polymers was investigated by Raman spectroscopy. Hot stretched crosslinked polyethylene was studied by vibrational spectroscopy as an aid to investigating the structure of flowing melts.

The following results are reported:

The morphology of crosslinked polyethylene is very similar to that of linear polyethylene. This supports Flory's view of the crystallization process.

The efficiency of crosslinking polyethylene with dicumyl peroxide is approximately 81.5%.

Orientation of polymer molecules by flow under the wide range of temperatures and shear rates investigated was found to be negligible.

Stretching crosslinked polyethylene at temperatures above its crystalline melting point results in preferential extension of a small proportion of polymer chains with little effect on others.

Chapter 1

INTRODUCTION

1.1 HISTORY, PRODUCTION, PROPERTIES AND USES OF POLYETHYLENE

The first preparation of polyethylene on record is that by Von Pechmann in 1898 who decomposed diazomethane:

$$nCH_2N_2 \longrightarrow \text{-}(CH_2)\text{-}_n$$

At the time it was not appreciated that a polymer had been produced.

In 1925 various paraffin waxes were identified from the reaction of carbon monoxide with hydrogen. The highest of these had molecular weights in the region of 20,000.

Low density polyethylene was discovered in 1931 at the laboratories of Imperial Chemical Industries while investigating the reaction of ethylene with benzaldehyde at high pressures. Attempts to repeat this preparation sometimes resulted in runaway exothermic reactions causing explosions. This brought a halt to this line of research.

By 1935 improved experimental techniques allowed the continuation of work on the polymerisation of ethylene at Imperial Chemical Industries. The reaction was initiated by traces of oxygen acting as a free radical initiator. In 1936 Fawcett and others took out the first patent for polyethylene manufacture.

A pilot plant was established in 1938 and commercial production began in 1939. Polyethylene found immediate and almost exclusive use as an electrical insulator in Radar establishments. Manufacturing capacity was rapidly increased to fulfil the requirements for the materiél of war.

High density polyethylene was discovered by Ziegler in 1953, while investigating the reaction of ethylene with alkyl aluminium. A small amount of nickel from the reaction vessel formed a complex with the alkyl aluminium which acted as a catalyst to produce polyethylene. The first production plant was built in 1955. The number of known Ziegler-Natta catalysts now exceeds 200.

Phillips Petroleum in the USA produced a linear polyethylene in 1955 from ethylene using a supported chromium oxide catalyst. This product reached commercial production in 1957 at Pasadena.

Standard Oil developed a similar process to that of Phillips Petroleum using a molybdenum oxide catalyst. The first commercial plant using this process commenced production in Japan in 1961.

Typical production conditions and properties for polyethylene are given in Table 1.

		High density polyethylene	
	Low density polyethylene	Ziegler-Natta	Phillips, Standard Oil
Reaction conditions	1000-3000 atmospheres $\sim 250^{\circ}C$	5 atmospheres $\sim 80^{\circ}C$	20-50 atmospheres 50-70$^{\circ}C$
Mechanism	Free radical	Transition metal halide metal alkyl complex catalyst	Supported metal oxide catalyst
Crystallinity (%)	50-60	65-75	75-85
Density (gcm^{-3})	0.91-0.94	0.95-0.96	0.96-0.98
Side chains	20-50 short side chains per 1000 carbon atoms	5-7 long chain branches per 1000 carbon atoms	Less than 2 long chain branches per 1000 carbon atoms
Melting point ($^{\circ}C$)	~ 110	~ 130	~ 135
Vicat softening point ($^{\circ}C$)	80-100	120-125	125-130
Number average molecular weight	10,000-40,000	5,000-15,000	10,000-30,000
$\bar{M}w / \bar{M}n$	20-50	4-15	4-15
Tensile strength (MNm^{-2})	10-15	25	30
Youngs modulus (MNm^{-2})	0.2×10^3	1×10^3	1×10^3

Table 1 Typical production conditions and properties of various types of polyethylene.

Ethylene may be readily copolymerised with many other monomers to produce copolymers. Suitable monomers include ethyl acetate, propylene and butene.

The physical properties of polyethylene are functions of four variables introduced during polymerization, these are: molecular weight, molecular weight distribution, long chain branching and short chain branching.

Branchpoints on the polyethylene backbone are generally not incorporated into crystalline regions. This results in a lower degree of crystallinity as the number of branches increases, and hence decreased density. Many properties are dependent on the degree of crystallinity and hence these are affected by chain branches. With decreasing branching comes increasing stiffness, tensile strength, tear strength and chemical resistance. This last is a function of decreasing permeability with increased crystallinity and the reduction of the number of tertiary carbon-hydrogen bonds available for attack. Flexibility, clarity and impact strength decrease as density and crystallinity increase.

The molecular weight, molecular weight distribution and long chain branching all affect the rheological properties of polyethylene. A broadening of the molecular weight distribution and increasing long chain branching facilitate processing, but are detrimental to tensile properties. The greater the molecular weight the greater is the viscosity of the melt while the physical properties are generally improved.

Polyethylene is susceptible to environmental stress cracking, but this decreases with increasing crystallinity and molecular weight.

Due to its non-polar nature the electrical insulation properties of polyethylene are excellent.

Polyethylene has a low coefficient of friction.

Although many of the individual properties of polyethylene are only moderately good they combine to confer a desirable melange of qualities on the material. Coupled with its relatively low cost and ease of processing polyethylene becomes an economical choice of material for a wide range of products. Polyethylene has the largest weight usage of all the organic synthetic polymers. Polyethylene is in use in a wide variety of applications as evidenced by Table 2.

	Low density polyethylene (Tonnes)	High density polyethylene (Tonnes)
Film and sheet	2,770,000	180,000
Injection moulding	270,000	480,000
Blow moulding	110,000	690,000
Wire and cable coating	150,000	-
Pipe	110,000	130,000
Extrusion coating	250,000	-
Monofilaments	-	50,000
Miscellaneous	130,000	80,000
Total	3,800,000	1,600,000

Table 2 Approximate consumption of polyethylene in Western Europe in 1983. (1)

In the past ten years the consumption of high density polyethylene relative to low density polyethylene has increased greatly.

For many potential uses polyethylene has a modulus and softening point which either separately, or in conjunction, prove to be too low to allow its application. Polypropylene is often used as an alternative material as it has a higher softening point and is of a similar cost, however it suffers severely from environmental stress cracking, low chemical resistance, and a high brittle point($0^{o}C$) precluding external use.

There is a major interest in improving the properties of polyethylene to extend its range of applications. Improvements may be of many kinds, including: manipulation of average molecular weight and molecular weight distribution during polymerisation, controlled crystallization, molecular orientation during processing, copolymerisation, blending with other grades of polyethylene or other thermoplastics, fibre reinforcement, the grafting on of side chains to confer chemical activity and crosslinking of various types.

1.2 MORPHOLOGY OF POLYETHYLENE

Early x-ray diffraction studies on polyethylene showed sharply defined rings surrounded by a diffuse halo, indicative of a partially crystalline structure. To explain this phenomenon the fringed micelle model was postulated. See Figure 1.

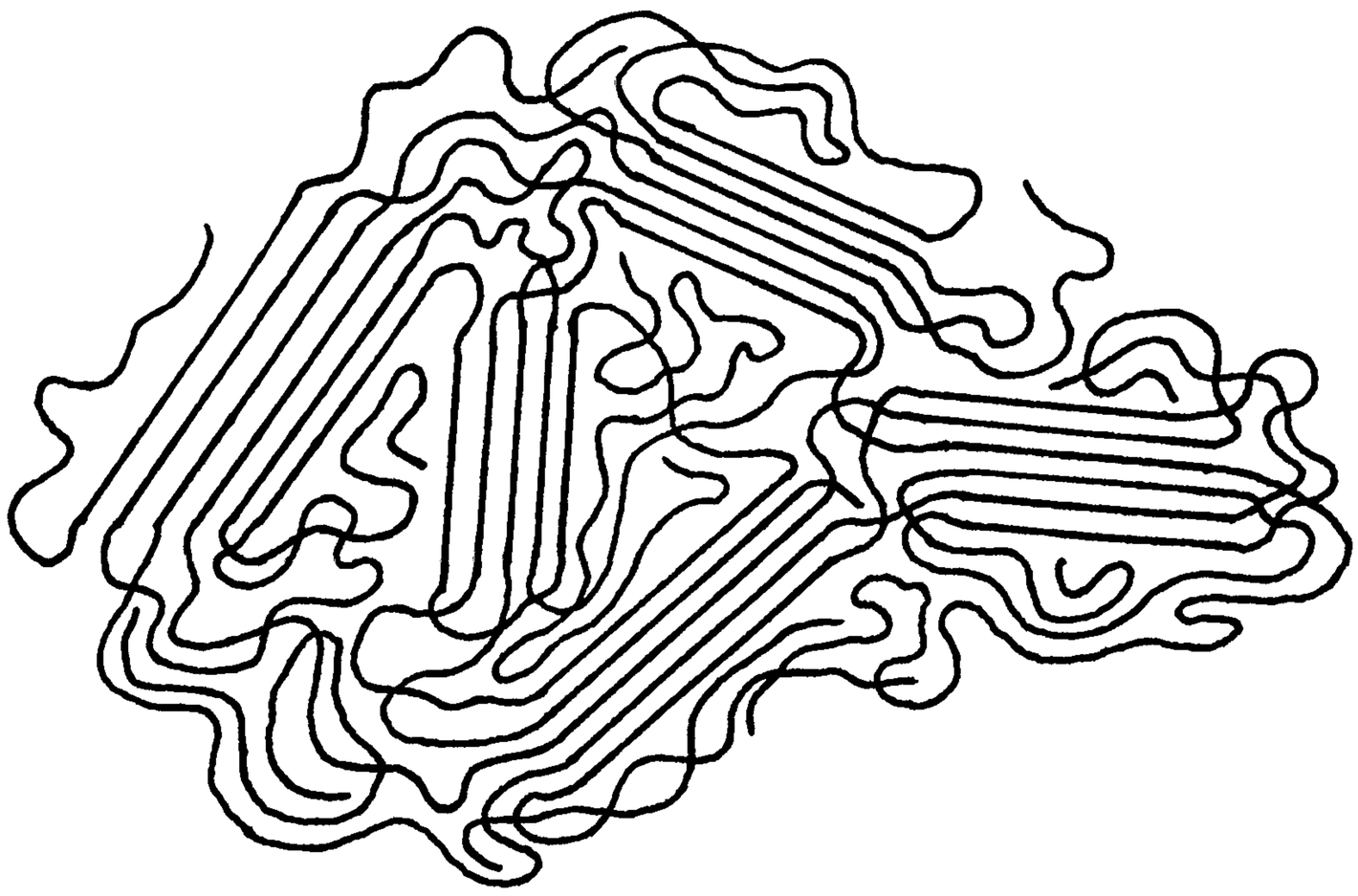

Figure 1 Schematic representation of fringed micelle model

In this model polymer chains are incorporated into a number of discrete crystallites arranged at random. As polymer chains leave the crystalline regions they traverse an amorphous region before entering another crystallite. The term 'fringed micelle' comes from the arrangement of the chains as they leave the end of the crystallites. This model was widely accepted up to the late 1950s when the discovery of polymer lamellae cast doubt upon it.

Dilute solutions of polyethylene in xylene ($< 1\%$) may crystallize to give single crystals (2,3). These crystals are planar - or nearly so - having a thickness of 10-20nm with lateral dimensions of up to several μm. Contrary to expectation the polymer chains were found to run approximately perpendicular to the gross plane of the crystal (3). As the length of the polymer chain may be up to 100 times that of the lamellar thickness the chain must pass through the crystal many times. Various models have been proposed for the organisation of the surface of single crystals. Some of the models proposed are shown schematically in Figure 2.

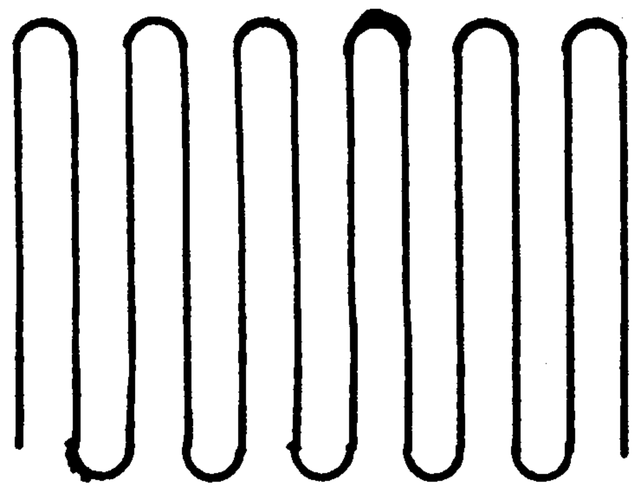

Sharp folds with adjacent re-entry (4)

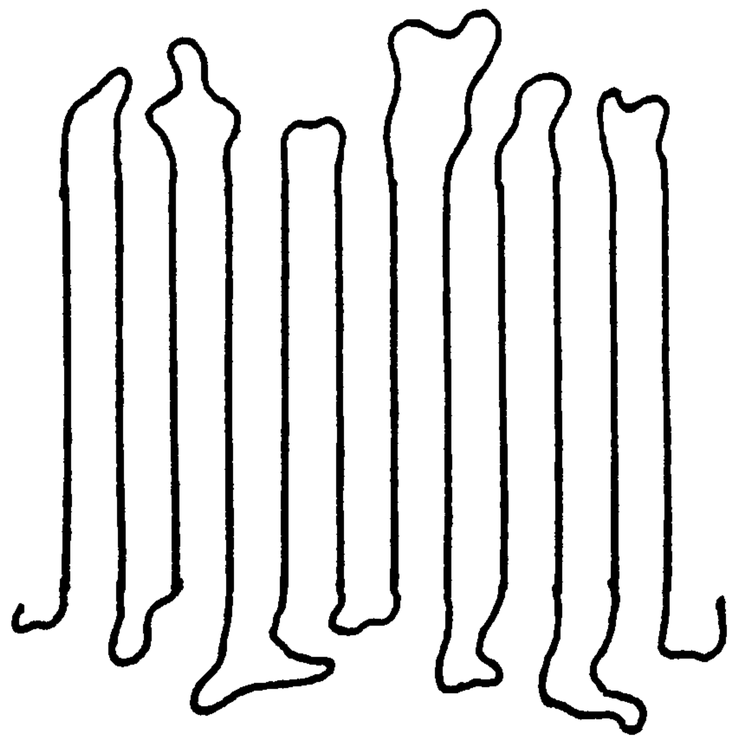

Loose loops with adjacent re-entry (5)

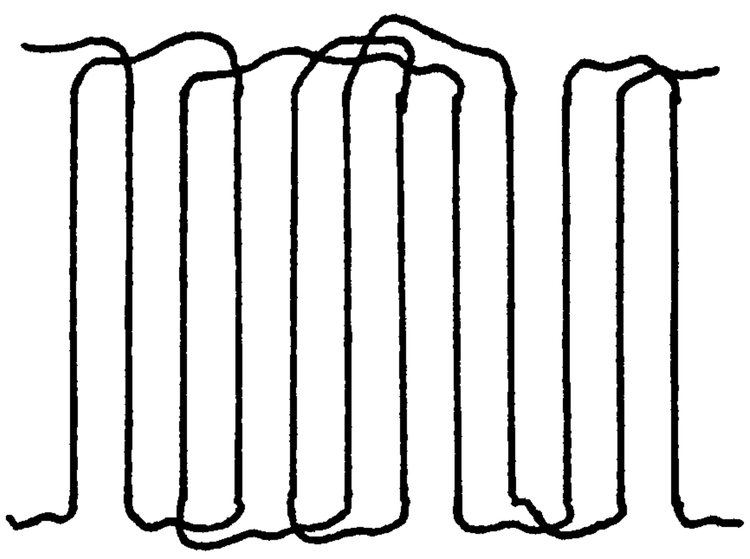

Switchboard model (6)

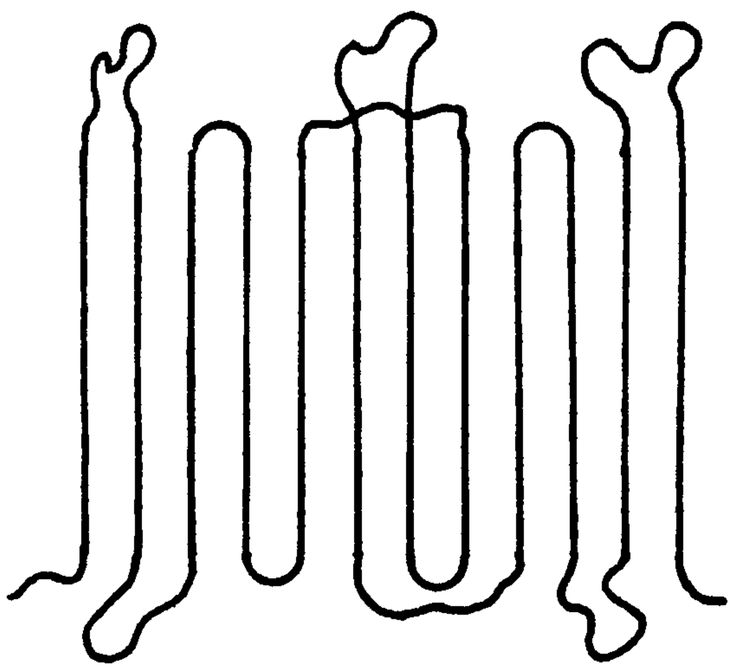

Composite model (7)

Figure 2 Schematic representations of models of the surface of single crystals.

Bassett's model (4) with sharp folds and adjacent re-entry is now accepted for the vast majority of polymer single crystals.

The discovery of lamellae in polymer single crystals prompted a renaissance of research into the morphology of bulk crystallized polyethylene. Reports of parallel lamellar-like structures appeared soon after the discovery of single crystals (8,9,10). From small angle x-ray diffraction and electron microscopy studies of fractured surfaces the thickness of melt crystallized lamellae was found to be in good agreement with that found for single crystals. Thus the fringed micelle model lost favour. Recently however the fringed micelle model has again been suggested as a structure for crystallites where they compose $< 15\%$ of the total volume of the polymer.

The existence of lamellae in melt crystallized polyethylene has not been disputed for twenty years. However the morphology of the lamellar surfaces and that of the disordered region between lamellae is still hotly debated to this day. The first view, advanced by Geil in 1960 (11), was that the surface of bulk

crystallized lamellae was similar to that of single crystals, consisting of tight folds with adjacent re-entry. According to this model, a polymer chain does not inhabit both the crystalline and amorphous regions. See Figure 3.

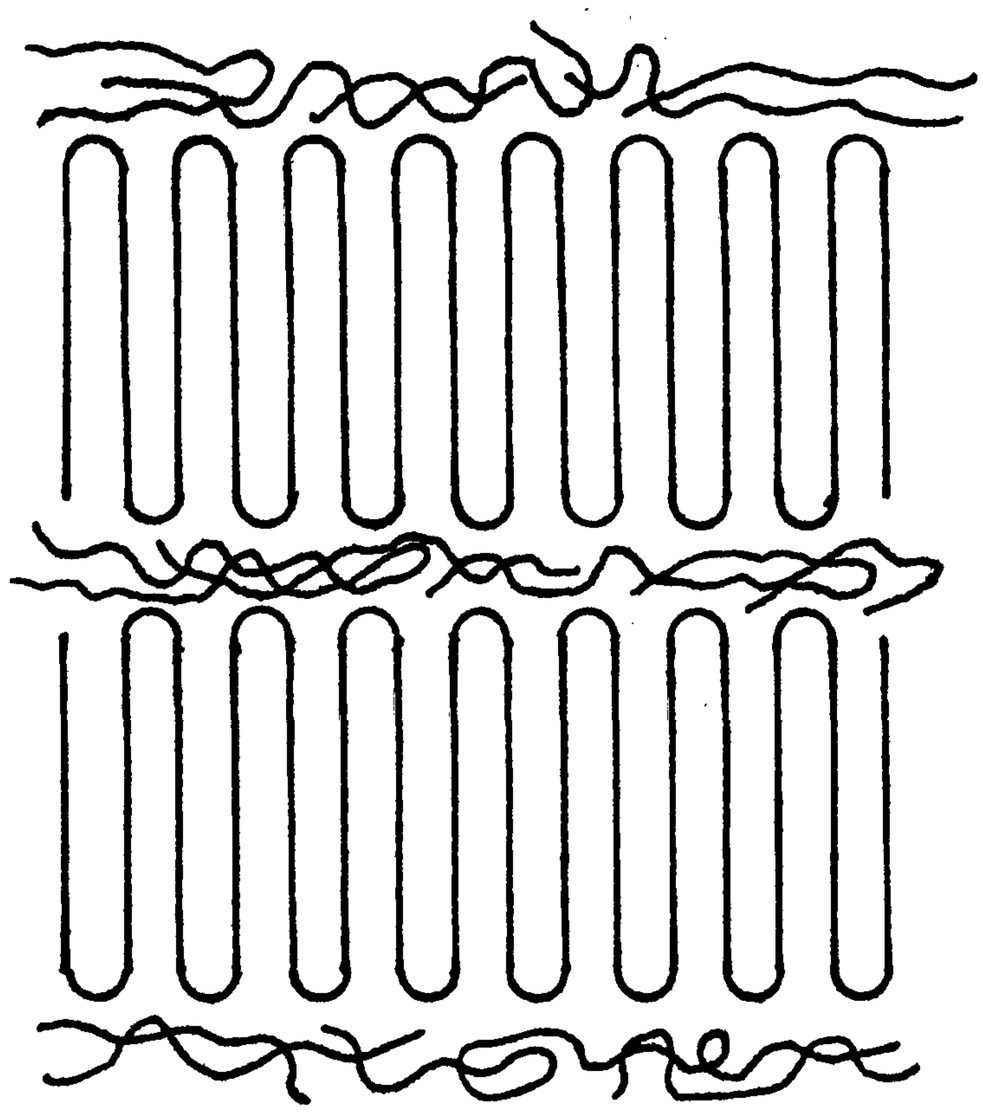

Figure 3 Schematic representation of Geil's model for lamellar organisation in melt crystallized polyethylene.

This model was opposed by Flory in 1962 (12), who, working from the principles of crystallization predicted that the lamellae would have loose loops, with a varying stem length and chains translating the interlamellar zones. See Figure 4.

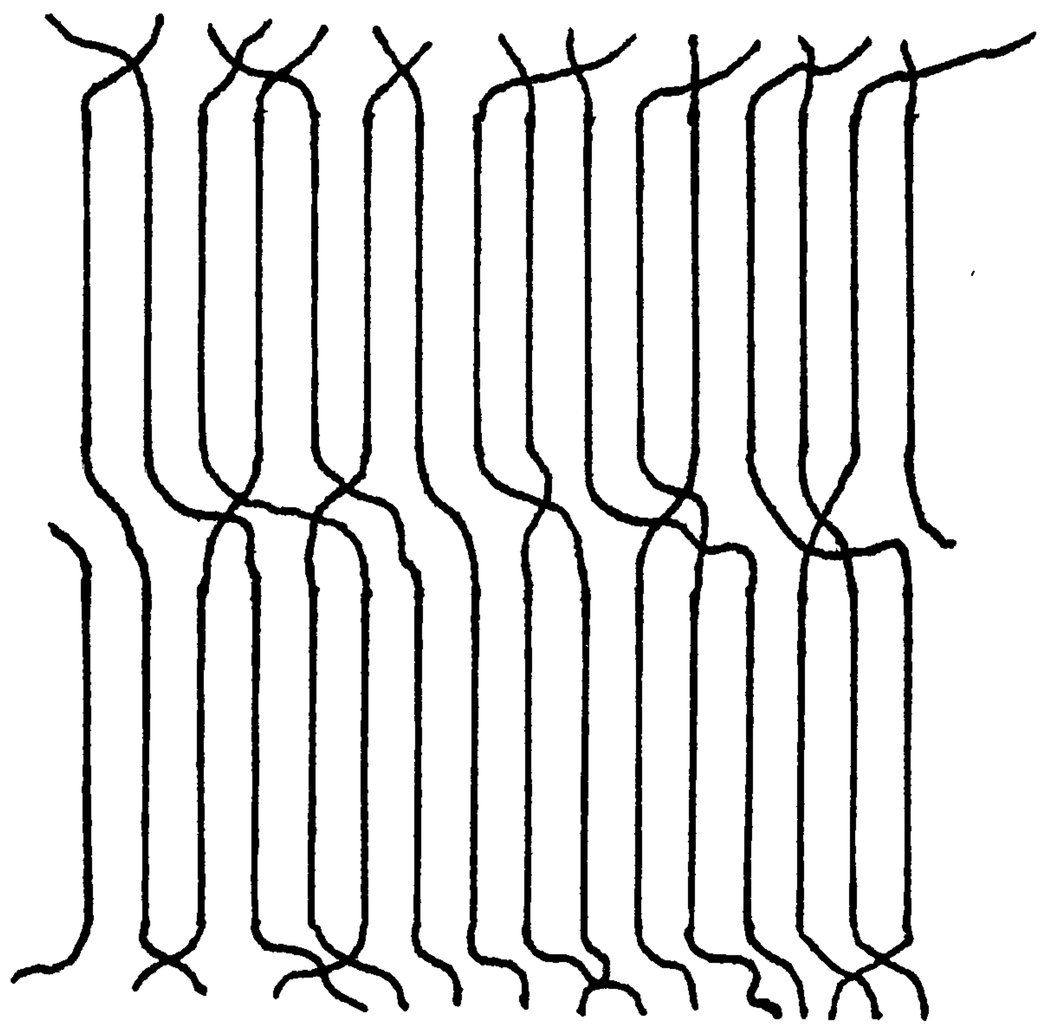

Figure 4 Schematic representation of Flory's model for lamellar organisation in melt crystallized polyethylene.

Since it was first proposed, Flory's model has been opposed on various theoretical grounds, the most obvious being that of a severe density anomaly occurring at the lamellar surface (13). Experimental evidence on the whole tends to support the view of Flory. Small angle neutron scattering studies would appear to show that a polyethylene chain maintains an overall random walk configuration when passing from the melt to the crystalline state (14,15,16). This indicates that the polymer chains do not take up a chain folded configuration. The two opposing factions champion different views on the kinetics of crystallization to support their own ideas on the morphology of polyethylene (17,18,19). De Gennes believes that the mobility of polyethylene chains in the crystallising melt is so great that there is sufficient time for the chains to be drawn from the amorphous melt and laid down in an orderly fashion on the growing face of the lamellae. (This is the mainspring of the argument in support of adjacent re-entry with tight folds and will be returned to later). Flory and Yoon maintain that crystallization of the melt is so rapid that there is insufficient time to allow large scale movement of polymer chains.

More recently various compromise models have been proposed, the two most notable of which are the central core model (20) shown in Figure 5 and the variable cluster model (21) shown in Figure 6.

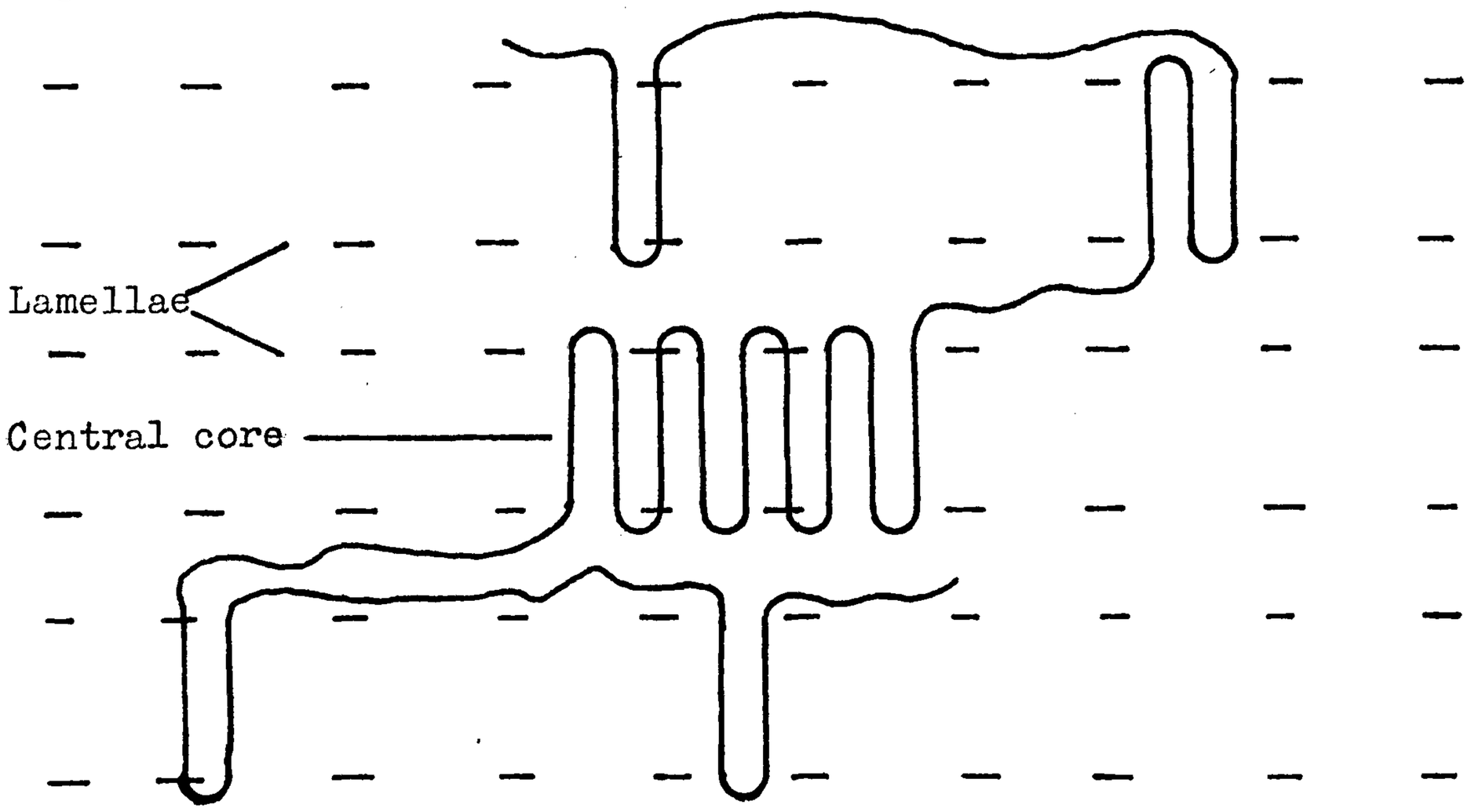

Figure 5 Schematic representation of the central core model.

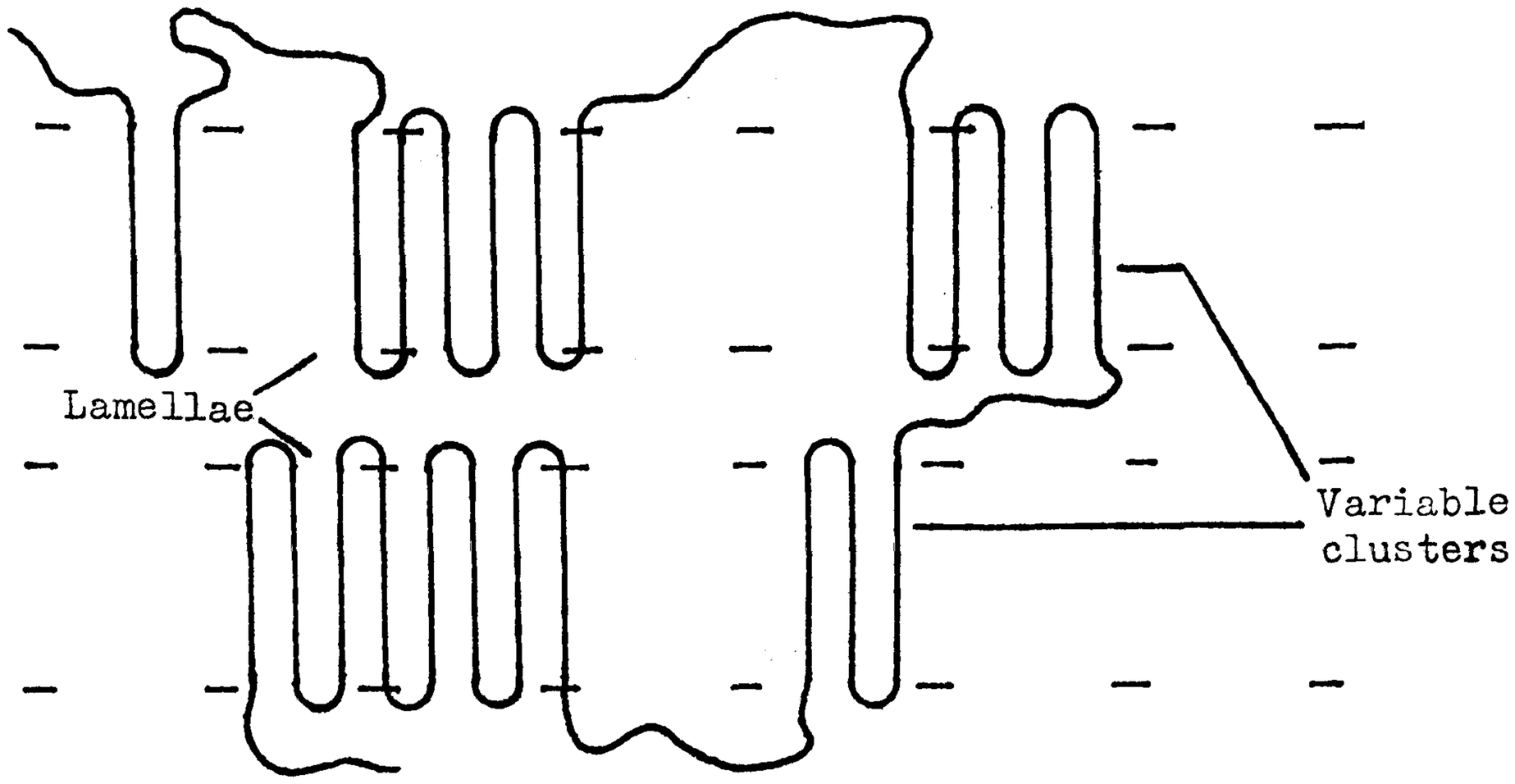

Figure 6 Schematic representation of the variable cluster model.

These two models are built up from the assumption that the probability of adjacent re-entry is ≥ 0.65. This figure is derived from the small angle neutron scattering data of Schelten et al (14) and Sadler and Keller (22).

The exact nature of the morphology of bulk crystallized polyethylene is of great interest from a technological standpoint. The morphology of polyethylene determines its bulk physical properties, hence an understanding of its exact nature would facilitate design of new products and would enable it to be used in new roles. As polyethylene has the greatest weight use of all synthetic organic polymers and the lowest cost such an achievement would be of great significance.

1.3 CROSSLINKING OF POLYETHYLENE

As mentioned in section 1.1 crosslinking is a method of improving certain physical properties of polyethylene. Crosslinking involves the formation of links between adjacent polymer chains. These links may be direct covalent links between two carbon atoms or via a short intervening chain. There are three main types of crosslinking: radiation crosslinking to produce covalent carbon-carbon bonds between chains, peroxide crosslinking also producing carbon-carbon links and graft crosslinking resulting in chains being linked by short intervening chains.

1.3.1 Radiation Crosslinking of Polyethylene

When polymers are irradiated they may either crosslink

or suffer degradation of various kinds, depending on the polymer, type of radiation, and conditions (23). Ethylene has a relatively high heat of polymerisation and hence polyethylene has a low degradation/crosslinking ratio, ~ 0.2 at $22^{o}C$. This means that when irradiated it will crosslink with negligible radiation damage (24).

When ionizing radiation strikes a polyethylene chain carbon-hydrogen bonds are broken, generating hydrogen atoms and macroradicals:

$$R\text{-}H \longrightarrow R\cdot + H\cdot$$

The hydrogen atom can abstract a further hydrogen atom from a chain to generate a second macroradical:

$$R'\text{-}H + H\cdot \longrightarrow R'\cdot + H_2$$

Two adjacent macroradicals can then combine to form a crosslink:

$$R\cdot + R'\cdot \longrightarrow R\text{-}R'$$

or disproportionate:

$$R\cdot + R'\cdot \longrightarrow R\text{-}H + R''\text{-}CH=CH''$$

It is also possible that a macroradical in an excited state will stimulate the formation of a radical on an adjacent chain:

$$R\cdot{}^{*} + R'H \longrightarrow (R\ldots\cdot H\ldots\cdot R') \longrightarrow R\cdot + R'\cdot + H\cdot$$

The two macroradicals being in close proximity stand a good chance of reacting (25).

The degree of crosslinking may be varied by altering the radiation dose.

All evidence points to the fact that no crosslinks are formed within the crystalline lattice of polyethylene, but occur on lamellar surfaces or in disordered regions (26,27,28).

1.3.2 Peroxide Crosslinking of Polyethylene

Peroxide crosslinking of polyethylene is achieved by generating free-radicals on chains which combine to form covalent carbon-carbon bonds.

A wide variety of organic peroxides is available for crosslinking polyethylene (23,29), but all initiate crosslinking by the same mechanism. Commercially the most

commonly used peroxide is dicumyl peroxide, but many others are used for specialised purposes.

Organic peroxides decompose homolytically on heating to produce two free radicals:

$$R\text{-}O\text{-}O\text{-}R \longrightarrow 2R\text{-}O\bullet \qquad R=\text{alkyl or aryl}$$

(+ some side products)

These free radicals then abstract hydrogen atoms from polyethylene chains:

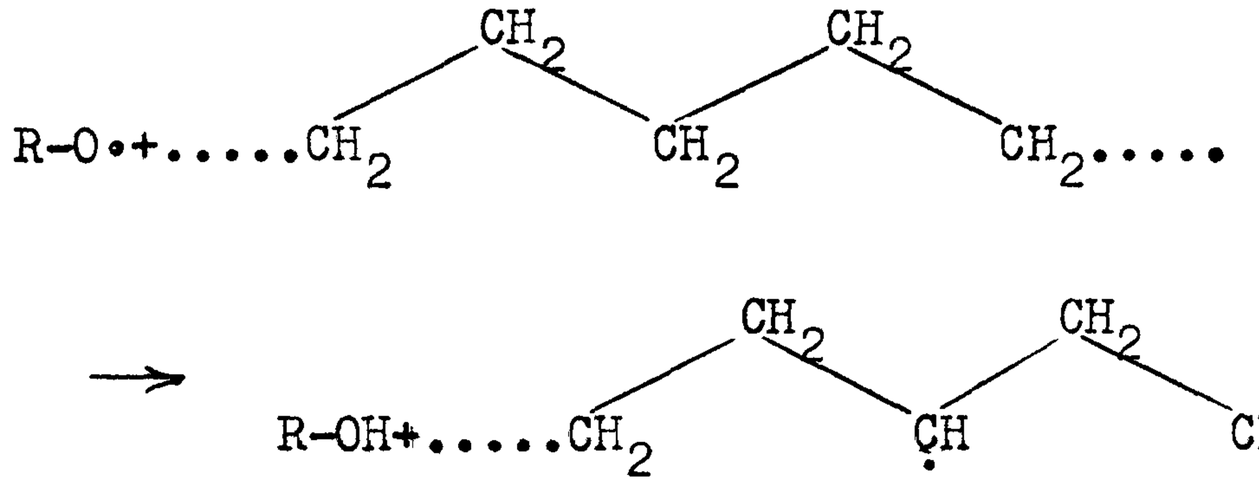

When unpaired electrons from adjacent chains meet they react to form a covalent carbon-carbon bond.

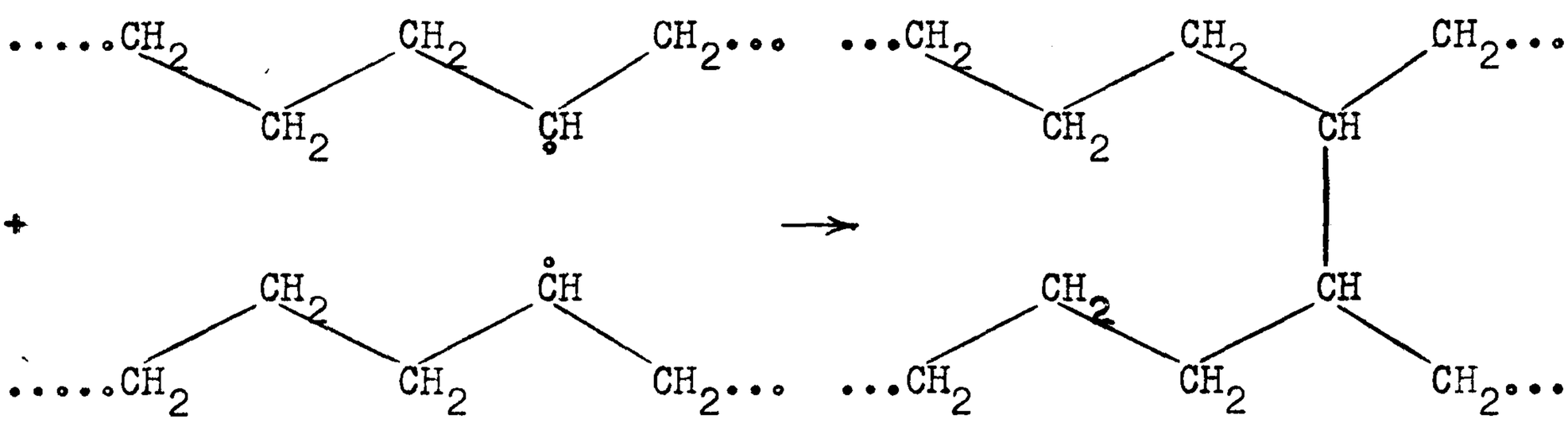

This reaction may be inter- or intramolecular. Depending on the amount of peroxide used some or all of the polyethylene chains will be tied into a three dimensional matrix. This is portrayed schematically in Figure 7.

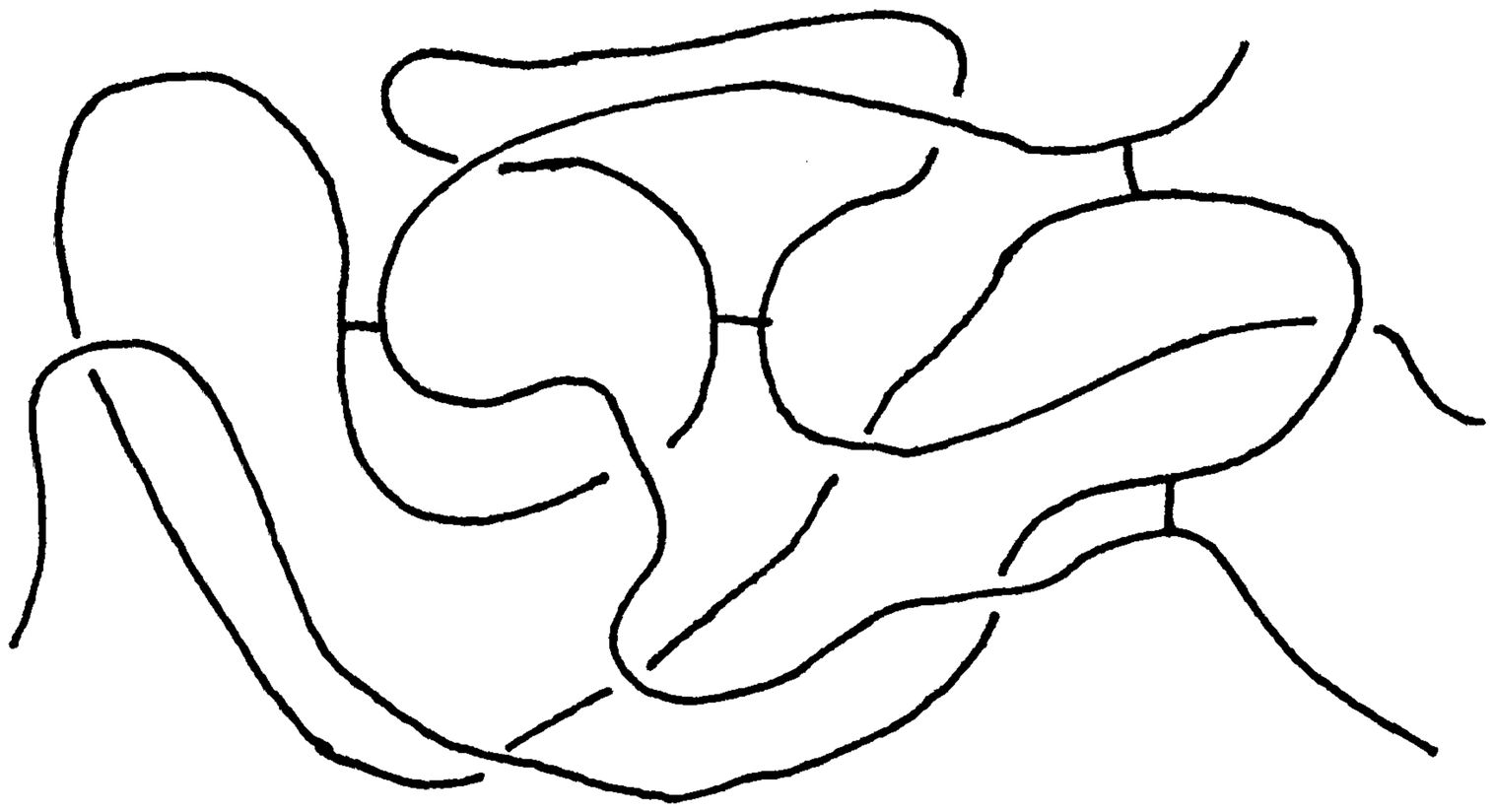

Figure 7 Schematic representation of peroxide crosslinking of polyethylene in an amorphous region.

Crosslinks are never incorporated into the crystalline matrix because they would cause distortion of the unit cell.

The ease of generation of radicals on the polyethylene chains depends on the type of polyethylene used. Hydrogen atoms attached to tertiary carbon atoms will be abstracted far more readily than those attached to secondary carbon atoms. This results in the crosslinking rate for branched polyethylene being much higher than that for linear polyethylene. Vinyl groups are also readily attacked (30) (of this more later).

Production of peroxide crosslinked polyethylene usually follows the scheme given below. The base resin is mixed thoroughly with the peroxide and all additives at a temperature at which the peroxide will not decompose to any detrimental extent. A very high degree of dispersion of peroxide throughout the polyethylene is required if crosslinking is to be uniform in the final product. Mixing on a laboratory scale is normally accomplished by kneading in a small Banbury Mixer or on a two roll mill. Strict control must be maintained over conditions at this stage to ensure that premature decomposition of the peroxide does not occur. Crosslinking is brought about by heat causing the peroxide to decompose producing free radicals which react with the polymer chains.

1.3.3 Graft Crosslinking of Polyethylene

There are various methods of crosslinking polyethylene involving grafts; the two most notable are the organo-silane method and chlorosulphonation.

Organo-silane crosslinkable polyethylene is a two component material consisting of a graft copolymer and a masterbatch containing the catalyst, this being dibutyltindilaurate. The structure of the copolymer is:

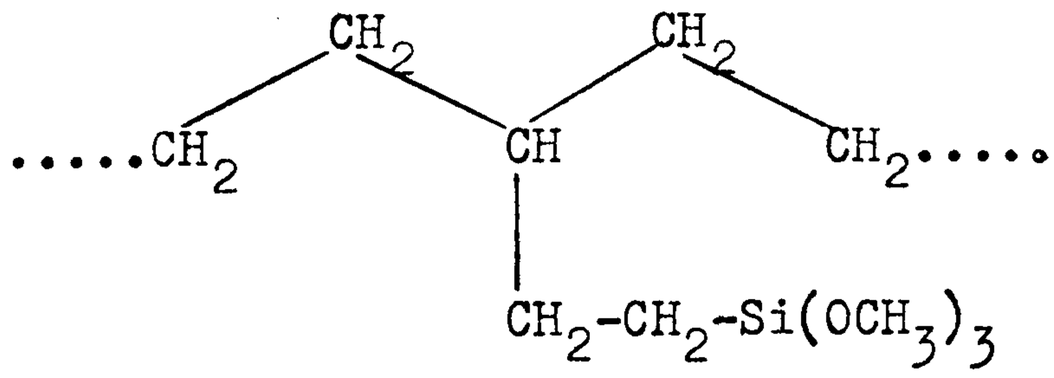

In the presence of water and the catalyst the organo-silane side groups will react with 1-3 others evolving methanol to form crosslinking bridges.

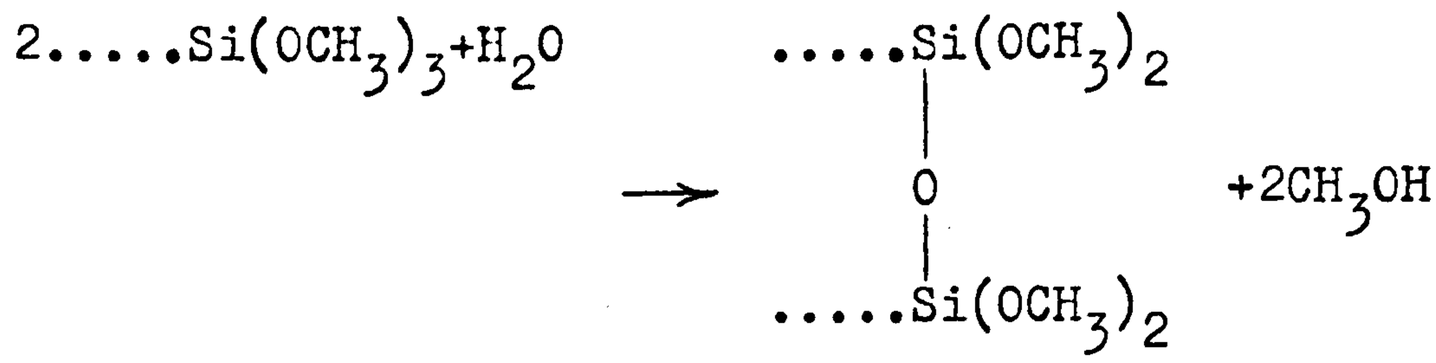

In the chlorosulphonation crosslinking method polyethylene is treated with chlorine and sulphur dioxide to produce sulphonyl chloride and chloride side groups. Crosslinking takes place through the introduced side groups by reaction with a metal oxide and water within the graft copolymer. The resulting products are rubbers, whose properties are dependent on the degree of crosslinking. The product is marketed under the trade name of Hypalon.

The mechanism of crosslinking is thought to be:

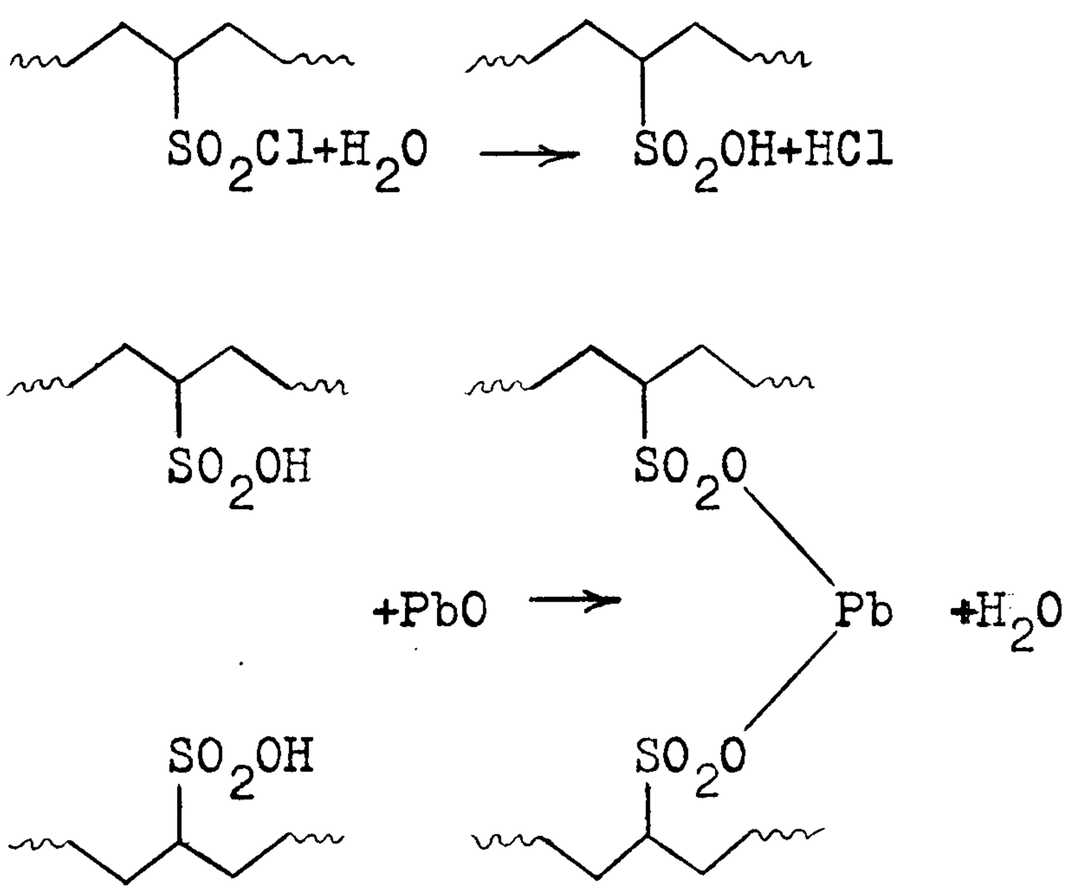

1.3.4 Properties of Crosslinked Polyethylene

Crosslinking improves many properties of polyethylene, some of which are listed below:

a) Slightly increased tensile strength.

b) Increased toughness.

c) Improved abrasion resistance.

d) Improved dimensional stability at elevated temperatures up to and beyond the crystalline melting point.

e) Greatly improved resistance to environmental stress cracking reagents.

f) Greatly improved resistance to creep.

g) Improved chemical resistance.

h) Improved thermal resistance.

Many of these properties are of great value to certain industrial concerns. By far the largest usage of crosslinked polyethylene is as an electrical insulator for cables carrying heavy loads. Resistance to deformation by heat is such that continuous service is possible at temperatures up to 90°C with short circuit emergency loads resulting in temperatures as high as 250°C for short periods.

Crosslinking reduces crystallinity because crosslinks are not incorporated into lamellae.

Of particular interest to this thesis is the behaviour of crosslinked polyethylene as a rubber above its crystalline melting point and the ability to link all polymer chains into a single matrix with variable lengths of backbone between crosslinks.

1.4 CROSSLINKING AS A TOOL FOR ELUCIDATING THE MORPHOLOGY OF POLYETHYLENE

Crosslinking confers a number of interesting properties on polyethylene that make it a useful and informative tool in the continuing study of polyethylene morphology. By adjusting the degree of crosslinking certain properties may be systematically varied. Above the crystalline melting point of polyethylene crosslinked polyethylene retains its dimensional stability opening up new areas for investigating the effect of physical perturbations on a polymer melt. The properties of polyethylene which are controllable by crosslinking are chiefly those that are affected by the limitations on chain movement imposed by the crosslinks.

When heated, crosslinked polyethylene does not melt, but rather acts as a rubber. This is of benefit when carrying out spectroscopic studies of thin films at elevated temperatures. One particular aspect of this effect that was studied was the modelling of flowing polyethylene by stretched crosslinked polyethylene at high temperatures. Both Raman and infrared spectroscopy were undertaken on hot stretched films.

As the polymer chains in crosslinked polyethylene are effectively tied into a three dimensional matrix each chain element is attached to three or six others dependent upon whether or not it has a chain end. An effective chain is the

length of polymer backbone between crosslinks, and the average size of an effective chain is used as a measure of the crosslink density. Figure 8 shows a chain element attached to three others, and Figure 9 an effective chain attached to six others.

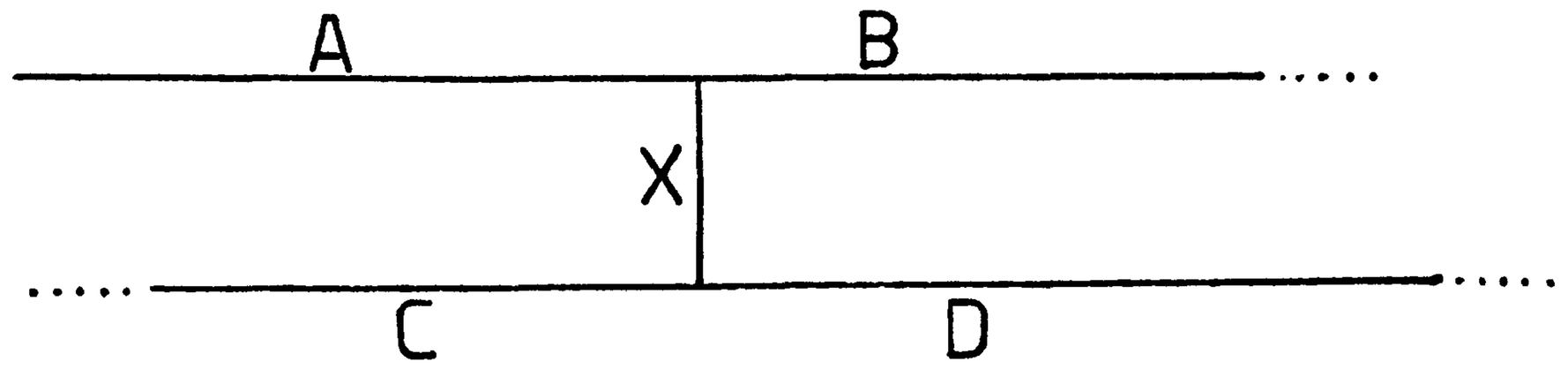

Figure 8 Chain element 'A' attached to chain elements 'B', 'C' and 'D' at crosslink X.

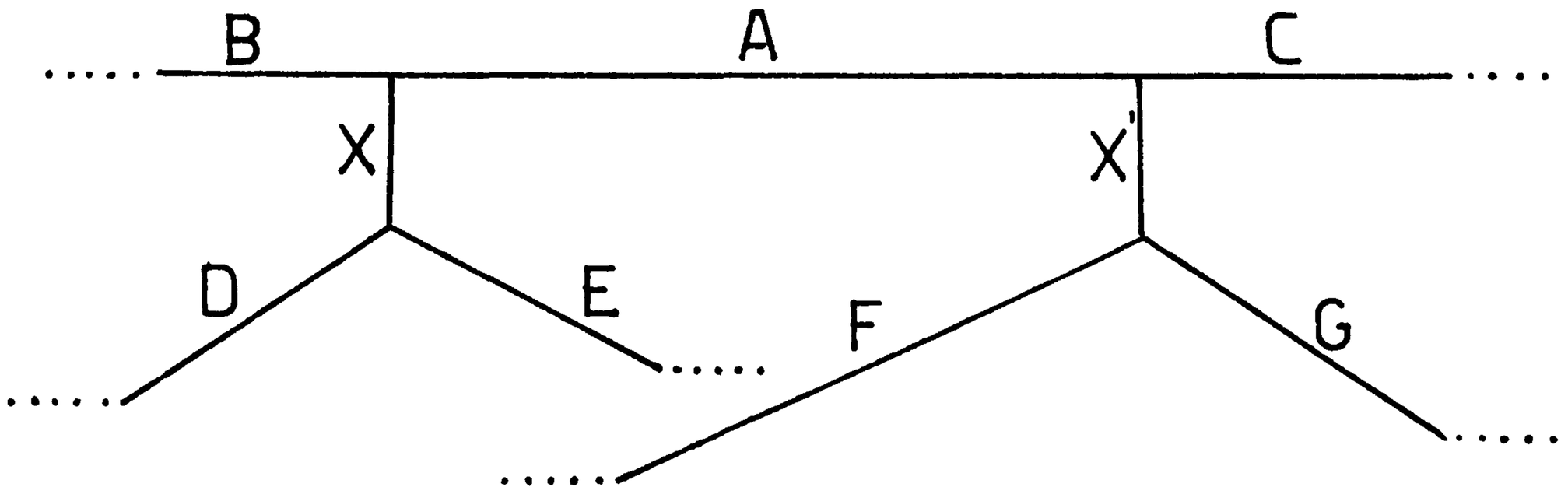

Figure 9 Effective chain 'A' attached to chain elements 'B', 'C', 'D', 'E', 'F' and 'G' at crosslinks X and X'.

As may be readily envisaged, such an arrangement will impose limitations on the movement of chains during crystallization. The greater the crosslink density, the greater will be the restriction on the movement of individual effective chains. This will decrease the proportion of polymer chains with sufficient freedom to take up an alignment suitable for crystallization. Coupled with the fact that crosslinks cannot be incorporated into a crystalline matrix

the result is a lowered degree of crystallinity. This may have the effect of decreasing the numbers of crystallites formed and/or reducing the dimensions of crystallites. A possible effect could actually be the increase of numbers of crystallites, but these would be of a much reduced size and would probably have a less well ordered arrangement than that found in conventionally melt crystallized linear polyethylene. The limitation of chain movement would, of course, totally impede the reptation of polymer chains required during crystallization to produce certain types of lamellar morphology.

Crosslinking will trap polymer chains in one position with respect to those around them. If a distinction between the effect of inter- and intramolecular bonds could be found the size and shape of polyethylene molecules at different temperatures and under different conditions could be investigated.

1.5 EXTRUSION AND POLYMER FLOW

Extrusion is one of the major methods of processing thermoplastics. It finds use in its own right and as part of the injection and blow moulding processes. The purpose of extrusion is threefold; it melts, homogenises and transports polymer. The process of extrusion is illustrated schematically in Figure 10 overleaf.

The rate of flow of polymer in a tube may be considered to be parabolic as shown in Figure 11.

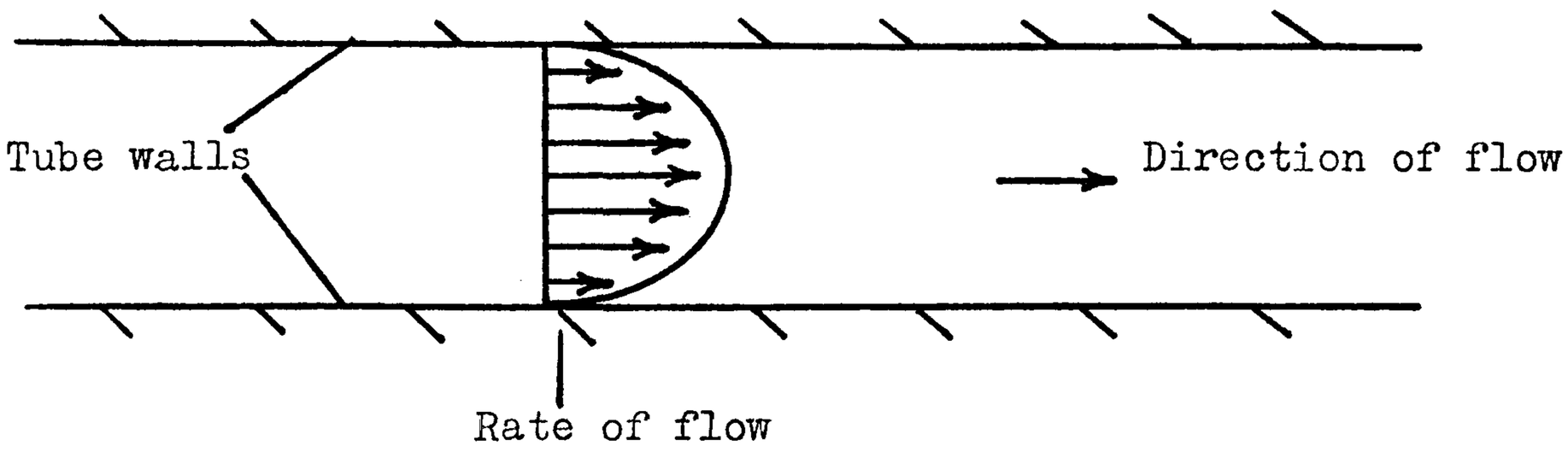

Figure 11 Melt flow in a tube.

The flow of polymer melt in a tube is a function of the tube profile, viscosity of the polymer and the pressure producing the flow. The greatest shear is at the tube walls and hence it is here that the greatest alignment of molecules takes place.

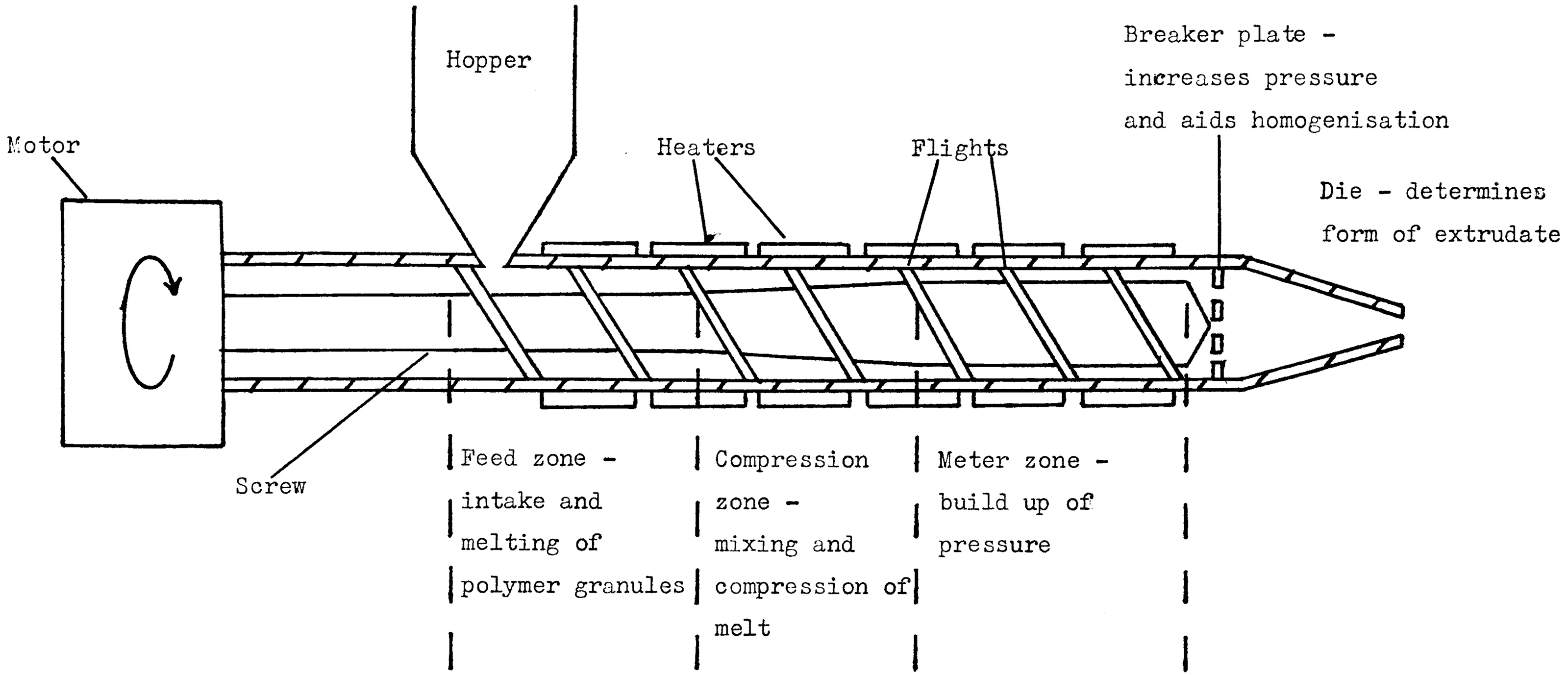

Figure 10 Schematic representation of extrusion

For flow in a circular tube the shear rate may be calculated from:

$$\dot{\gamma} = \frac{4Q}{d^3}$$

where: $\dot{\gamma}$ = Apparent shear rate at wall (s^{-1})
Q = Output ($cm^3 s^{-1}$)
d = Diameter (cm)

For flow in a rectangular tube,

$$\dot{\gamma} = \frac{6Q}{wh^2}$$

where: w = width of tube (cm)
h = height of tube (cm)

As may readily be seen the smaller the dimensions of a tube for a given output the greater is the shear rate at the wall.

Polymer melts are visco-elastic in nature. Due to this a change in tube profile can still have an effect some way downstream, up to 10 x the tube width.

Chapter 2

EXPERIMENTAL TECHNIQUES

2.1 INTRODUCTION

During the course of the research described in this thesis a great many different experimental techniques were employed. There are too many of these to allow anything but a brief description of each, except where a technique is novel or required the design and production of specialised equipment. It is hoped that the reader will bear with this approach, and if sufficient interest is generated will consult the more exhaustive texts referred to.

In this chapter only those techniques which pertain to more than one line of research described in the subsequent chapters will be described. Other relevant experimental procedures will be described in the chapters referring to individual investigations.

2.2 CROSSLINKING OF POLYETHYLENE

Crosslinking of polyethylene was carried out chemically using dicumyl peroxide. Rigidex 006-60 a linear polyethylene was crosslinked to varying degrees. This material is manufactured by British Petroleum Ltd. using a variant of the Phillips process. The molecular weight distribution was kindly provided by the manufacturer; this is illustrated in Figure 12. The number average molecular weight is 19,500 and the weight average molecular weight 130,000. There are less than 2 long chain branches per 1,000 carbon atoms. Each chain bears 1 terminal vinyl group. The dicumyl peroxide used was a general purpose reagent supplied by British Drug Houses Ltd. This was found to have a purity of 98.5% ($\pm$ 0.5) using the analytical method of Mair and Graupner (31).

In the absence of suitable compounding equipment for blending dicumyl peroxide and polyethylene directly the dicumyl peroxide was dissolved into a solution of polyethylene in xylene and the solvent was removed.

A weighed quantity of polymer ($\sim$10g) was dissolved in xylene (0.2dm^3) at 125-130°C overnight. This solution was cooled to 100°C yielding a viscous fluid. An accurately weighed portion of dicumyl peroxide (0.025-1.0g) was added and stirred in thoroughly for 10 minutes. At 100°C the half life of dicumyl peroxide is approximately 83 hours, thus

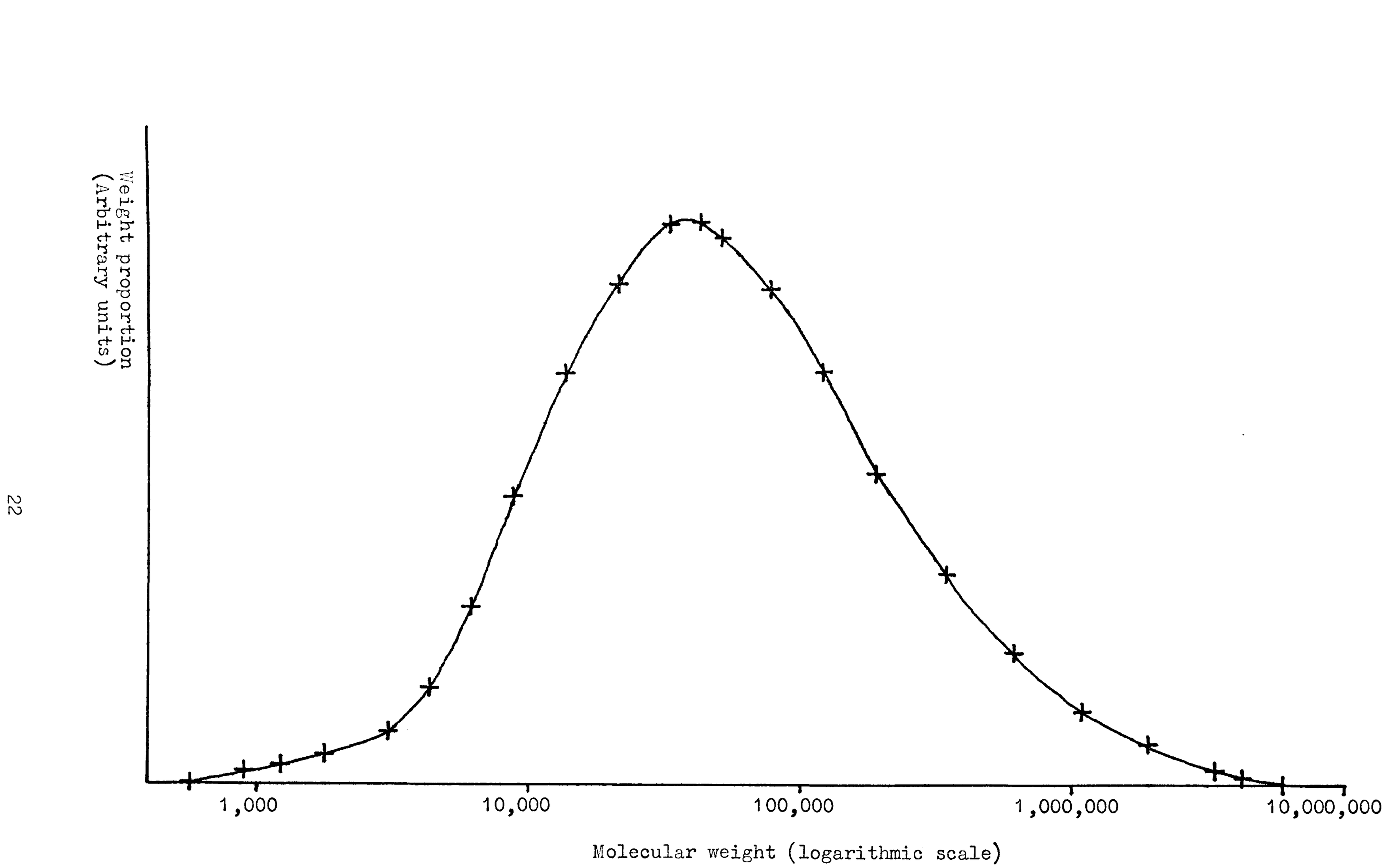

Figure 12 Molecular weight distribution of Rigidex 006-60

decomposition is negligible during mixing. The mixture was transferred to an evaporating basin lined with aluminium foil and was placed in a vacuum oven preheated to 80°C to remove the solvent. Vacuum was provided by a rotary oil pump. Xylene was collected in a solvent trap cooled in an ice/water mixture. Under these conditions about 90% of the solvent was removed within 4 hours. Constant weight is achieved by 48 hours. At 80°C the half life of dicumyl peroxide is approximately 1,500 hours, resulting in approximately 3% decomposition after 48 hours. The resulting product is a friable mass with a bulk density of about 0.1gcm^{-3}.

Decomposition of dicumyl peroxide to effect crosslinking is brought about by heating the polyethylene and peroxide blend in a hot press for 10 minutes at 180°C at approximately 100 pounds per square inch to produce a film. Under these conditions decomposition is >99.8% complete. Samples crosslinked at ambient pressure foamed due to the release of gaseous reaction products.

Difficulty was encountered with this procedure at first. Some samples did not crosslink at all and others to only a small degree. This was explained by three factors, poor heat control causing premature decomposition of the dicumyl peroxide, the effect of anti-oxidant in the base resin, and impurities from the xylene reacting preferentially with the dicumyl peroxide.

To ensure correct heat control the temperature of the materials was monitored carefully at each stage. The polymer originally used was a commercially available grade which had been pre-pelletised and had anti-oxidant incorporated. The manufacturer kindly provided ex-reactor samples of Rigidex 006-60 in powder form. Analar xylene was substituted for the general purpose reagent previously used. With these three modifications the crosslinking procedure worked satisfactorily.

2.3 RAMAN SPECTROSCOPY (32,33,34)

2.3.1 The Raman Effect

When light is incident on a transparent or semi-transparent medium some light scattering inevitably occurs. The most

intense scatter is of the same frequency as the incident light (i.e. elastic scatter) and is caused by reflection or refraction at inhomogeneities within the sample - this is the Tyndall effect. Even in a nominally clear sample scatter occurs due to absorption and re-emission of energy. Re-emitted light is normally of the same frequency as the absorbed, but some may have a changed frequency (i.e. inelastic scatter). Raman scatter is the most faint of the inelastic scattering effects and it is this that we are concerned with here.

Raman scatter is caused by incident light exciting a molecule into a polarized - or virtual - state, and the decay of this state to one other than its original. The virtual state is identical to the original state except for polarization. (See Figure 13.

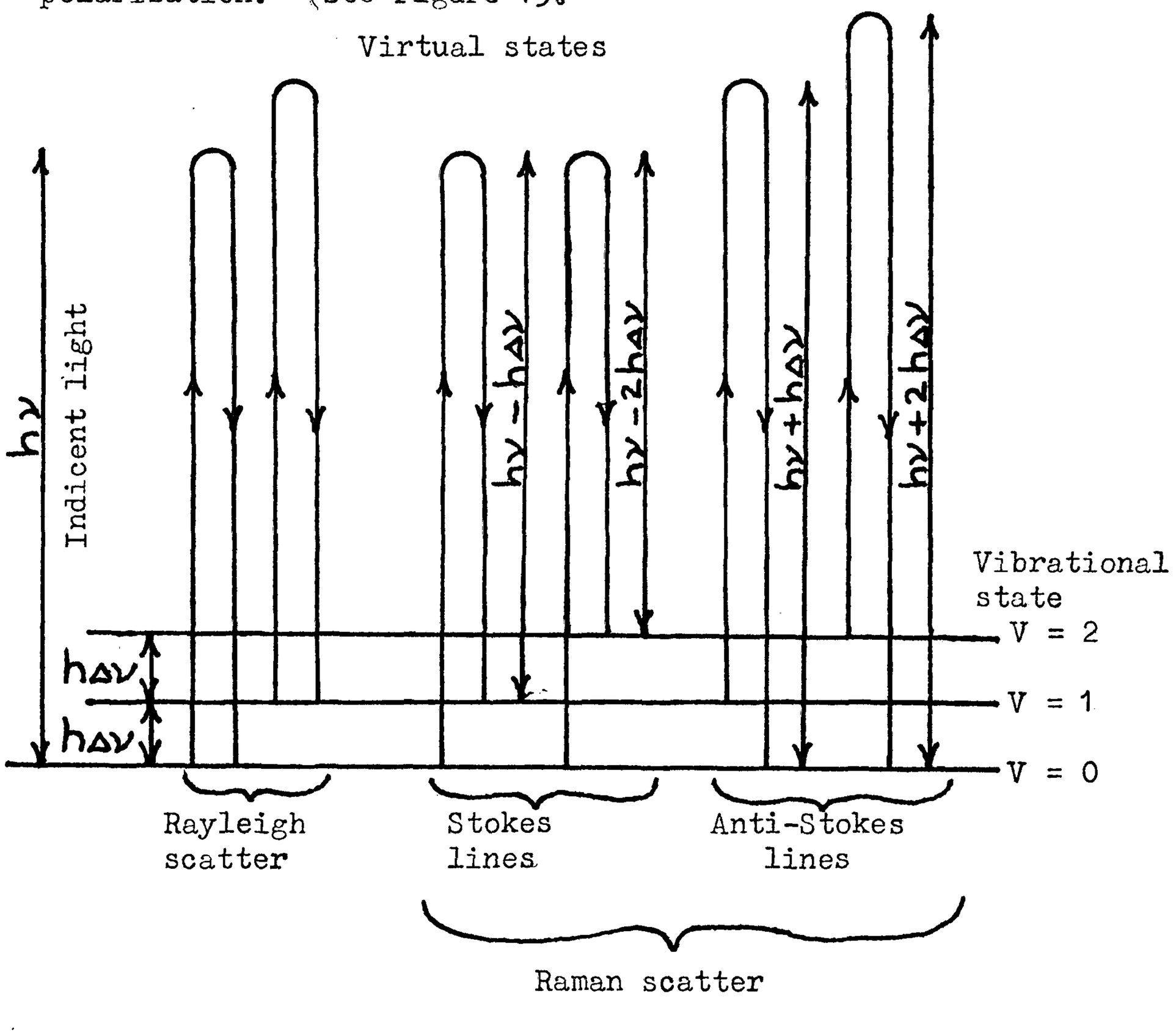

Figure 13 Diagrammatic representation of the origination of Rayleigh and Raman scatter in polymers.

The decay of the polarised state is rapid, the half-life is approximately 10^{-14} seconds. The intensity of the Rayleigh scatter is approximately 10^{6} times that of the Raman scatter. The difference in intensity between the Stokes and Anti-Stokes lines is a function of the population density of the vibrational states. The energy difference between the incident light and the Raman scatter is equivalent to the energy difference between vibrational states. Thus a study of the frequency shifts yields information about vibrational states in molecules.

Not all molecular vibrations are Raman active, only those which have a non-zero value of $\delta\alpha/\delta q$ at $q=0,\pi$ during the vibration are Raman active. See Figure 14.

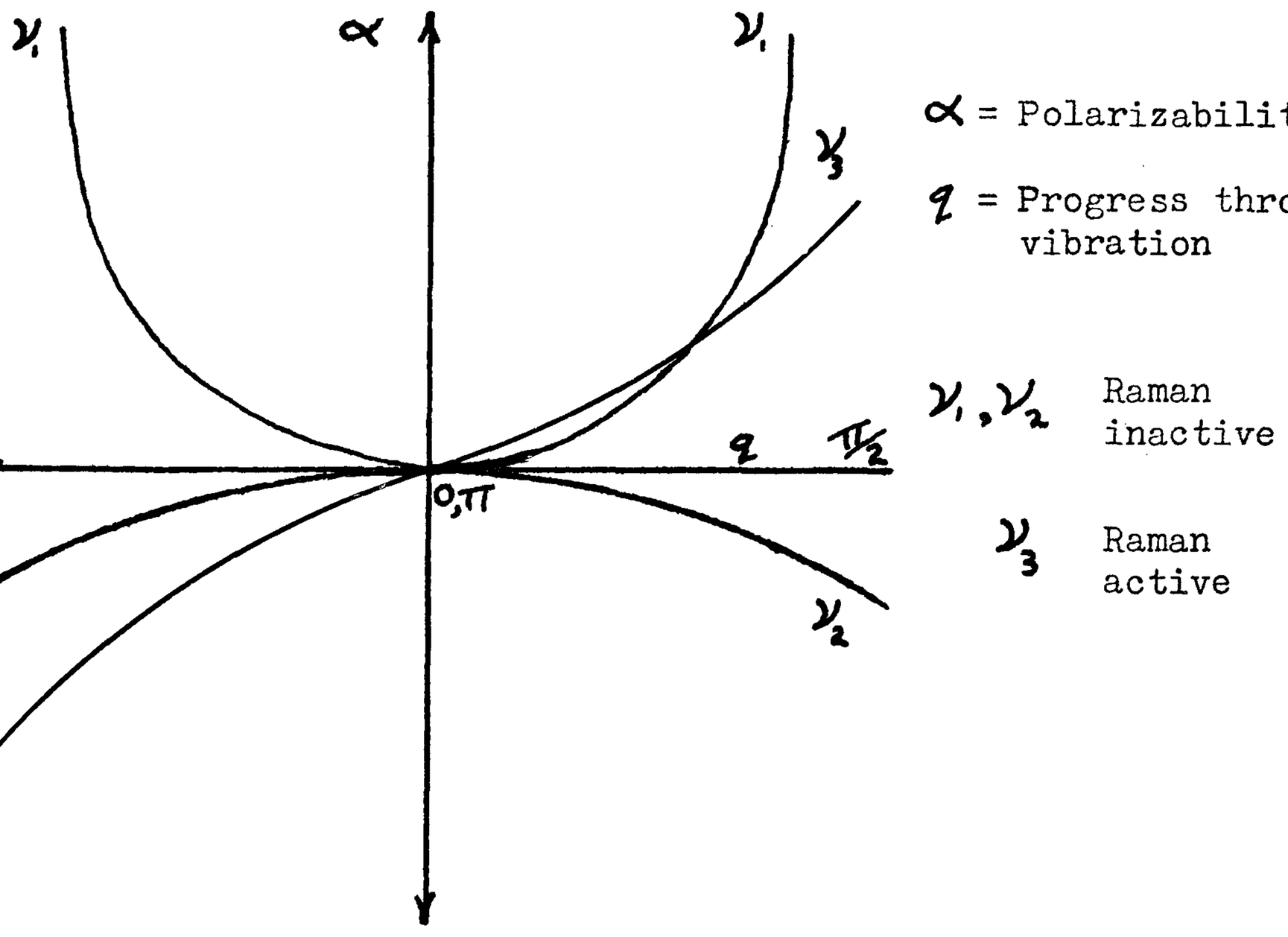

Figure 14 Polarizability versus progress of vibration and relation to Raman activity.

The vibrations of polymers that are of interest to particular experiments are described in the relevant chapters.

2.3.2 Raman Instrumentation

Two Raman spectrometers were used, one a scanning instrument and the other a spectograph.

The majority of work was carried out on a Coderg T800

Scanning Raman Spectrometer. This instrument employs a pre-monochromator to filter the exciting laser beam and three monochromators to analyze the scattered light. Detection of scattered light is carried out by a photomultiplier tube, this is coupled via a digital to analogue converter to a chart recorder. With this instrument it is possible to record spectra to within 5 wavenumbers of the exciting line. The exciting radiation was provided by an argon ion laser operating at 514.5nm.

The other instrument used was an Anaspec LR-36 spectrograph. The arrangement of this instrument is most unusual. The scattered light is dispersed by a short focal length spectrograph, the output of which goes through a second long focal length spectrograph arranged for subtractive dispersion. Output from the second spectrograph falls on a diode array photodetector in its exit slit plane. A range of up to 850 wavenumbers may be sampled at one time. Data may be output to a magnetic floppy disc, or to a chart recorder for digital or analogue plotting. All functions are computer controlled. This instrument suffers from a number of serious design limitations, including non-linearity of the diode array, susceptibility to stray light, and only being able to record spectra down to a frequency shift of 200 wavenumbers. In its favour are its rapid collection of data and superlative data manipulating capabilities. On the whole, for all but fairly routine work on strong Raman scatterers this instrument proved to be inferior to the Coderg T800.

2.4 FOURIER TRANSFORM INFRA-RED SPECTROSCOPY

Only a brief outline of the theory of Fourier transform infra-red spectroscopy will be given. An exhaustive discussion of the theory is to be found in Bell's book (35) and a survey of chemical applications in Griffith's book (36).

At the heart of the optical system of a Fourier transform infra-red spectrometer is a Michelson interferometer. The principles of this are illustrated in Figure 15.

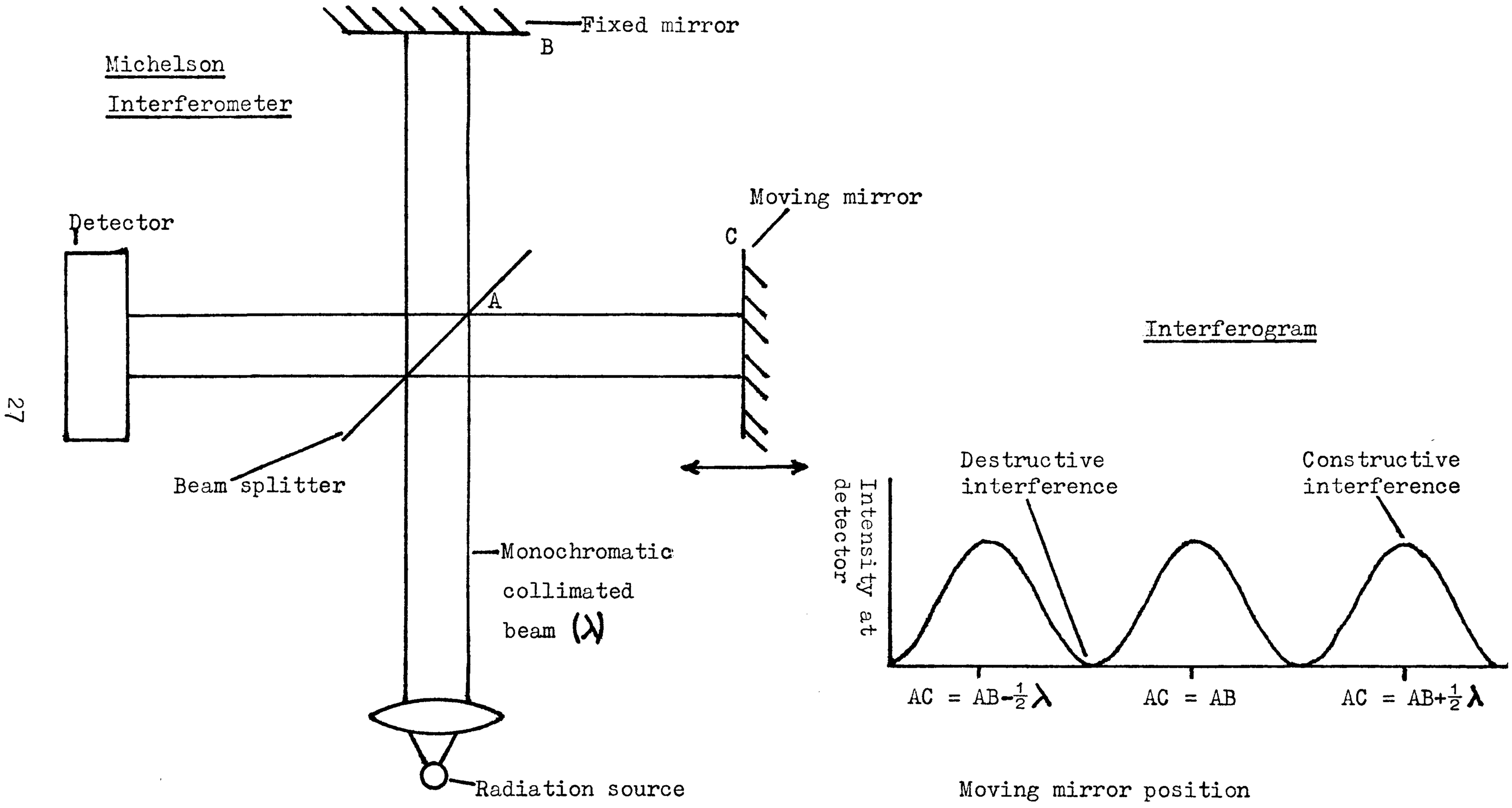

Figure 15 Principles of the Michelson Interferometer

The frequency of the modulated sine wave is determined by the velocity of the moving mirror and the number of waves by the throw of the mirror. For a broad band infra-red source the modulated sine waves for all frequencies are summed with all the concomitant constructive and destructive interference to give an interferogram - a typical example of which is shown in Figure 16.

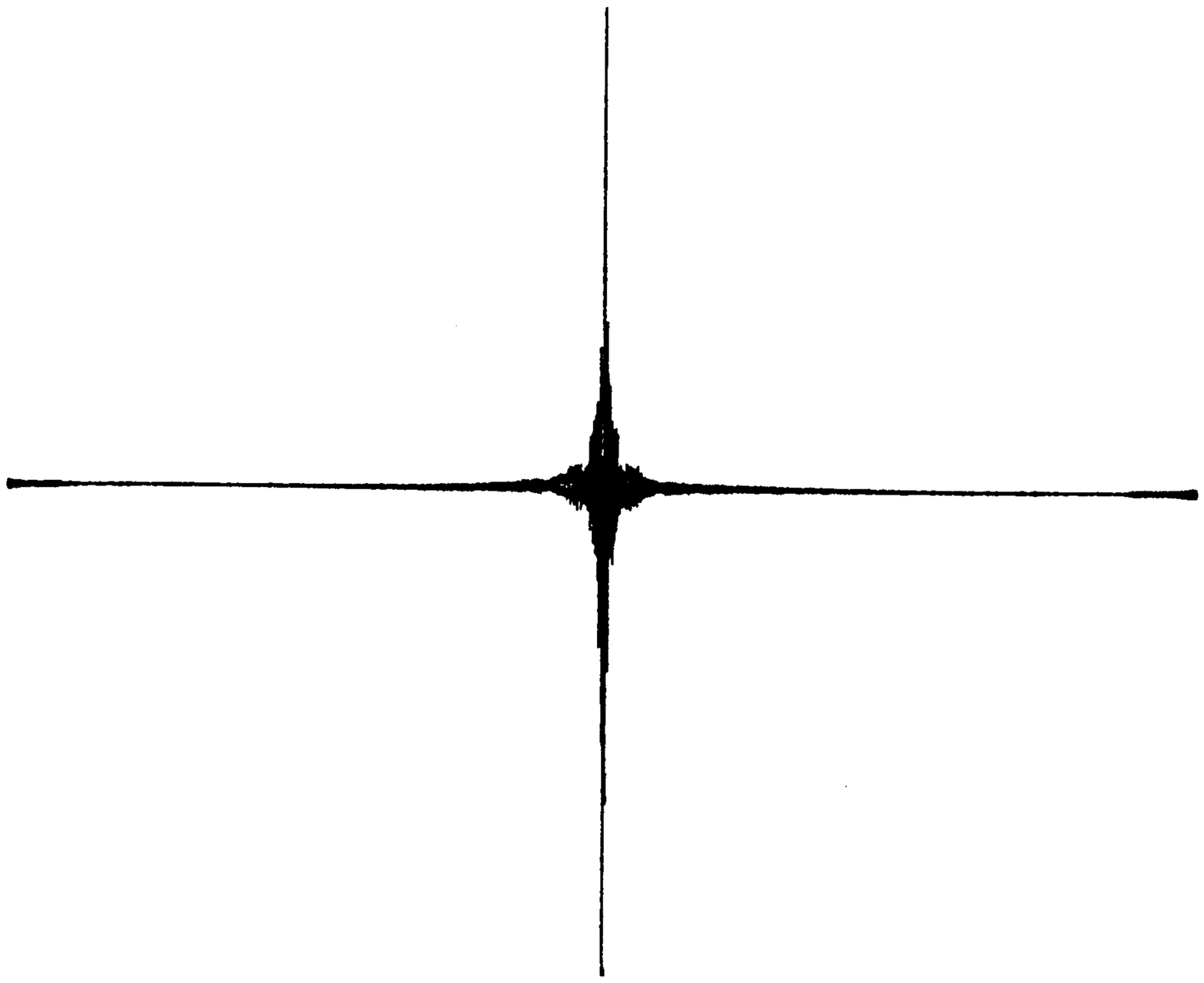

Figure 16 Typical interferogram.

The maximum signal occurs when the path length between the beam splitter and the two mirrors is identical.

When a sample is placed between the beam splitter and the detector a modified interferogram is produced. Analysis of the modified interferogram in comparison with the original by the mathematical process of Fourier transformation yields the familiar infra-red spectrum. The resolution of the instrument depends on the length of throw of the moving mirror.

The major improvements of Fourier transform infra-red spectroscopy over conventional dispersive spectroscopy are,

a greatly increased signal to noise ratio with a high degree of precision, and accuracy in the determination of the frequency of data points. These improvements arise principally from the Felgett - or multiplex - advantage and the Jaquinot - or throughput - advantage. The Felgett advantage is that of observing all frequencies at once: each point on the interferogram contributes information on all infra-red frequencies. Thus data is acquired very quickly allowing multiple scans to improve signal to noise ratio. The Jaquinot advantage refers to the fact that there are no slits in a interferometric instrument as there are in a dispersive spectrometer. This means that the overall infra-red throughput is greatly increased, with a corresponding increase in response at the detector.

2.4.1 Nicolet MX-1

The instrument used in this investigation was a Nicolet MX-1. The total scan time was 60 seconds with a 12 second Fourier transform time. This allowed 35 scans of the moving mirror. The resolution used was 2 wavenumbers, the frequency of the data points was known to an accuracy of 0.01 wavenumbers. Data was output to a magnetic floppy disc or protrayed by a Nicolet Zeta digital plotter. The frequency range and scale of the spectra as plotted were widely variable. Subtraction of spectra could be carried out on the instrument. Band head position could be determined digitally by the instrument. All functions were controlled by touch sensitive controls.

Chapter 3

GEL CONTENT OF CROSSLINKED POLYETHYLENE VERSUS CONCENTRATION OF DICUMYL PEROXIDE

3.1 INTRODUCTION

Initial attempts to crosslink polyethylene were not amazingly successful (see 2.2). Some thought was given to this problem and it was decided that it would be beneficial to evaluate the efficiency of the crosslinking reaction.

Examination of the literature indicates that several attempts have been made to determine the efficiency of crosslinking polyethylene with dicumyl peroxide (30,37,38,39). The efficiency of the crosslinking reaction is defined as the average number of crosslinks formed for each molecule of dicumyl peroxide used. The results afforded have been dependent upon the type and grade of polyethylene used. Thus, Hulse et al (30) reported values in the range 20-40% when crosslinking linear polyethylene bearing less than 0.07 vinyl groups per 1,000 carbon atoms, and a value of 76% for a linear polyethylene bearing 0.5 vinyl groups per 1,000 carbon atoms. Dannenberg et al (37), and Simunkova et al (38), using branched polyethylene as the base resin both claimed an efficiency of 100%. Methods used to evaluate the efficiency of crosslinking have included spectroscopy, analysis of reaction products, and the study of the dimerisation of model compounds such as n-tetradecane.

As the concentration of dicumyl peroxide used to effect crosslinking is increased the gel content increases. The gel content is a measure of the fraction of material chemically bound into a network and hence insoluble to extraction. The relationship between dicumyl peroxide used and the gel content is not linear; at low concentrations of dicumyl peroxide the gel content rises rapidly with increasing concentration, but rises more slowly as the concentration of dicumyl peroxide increases further. See Figure 17.

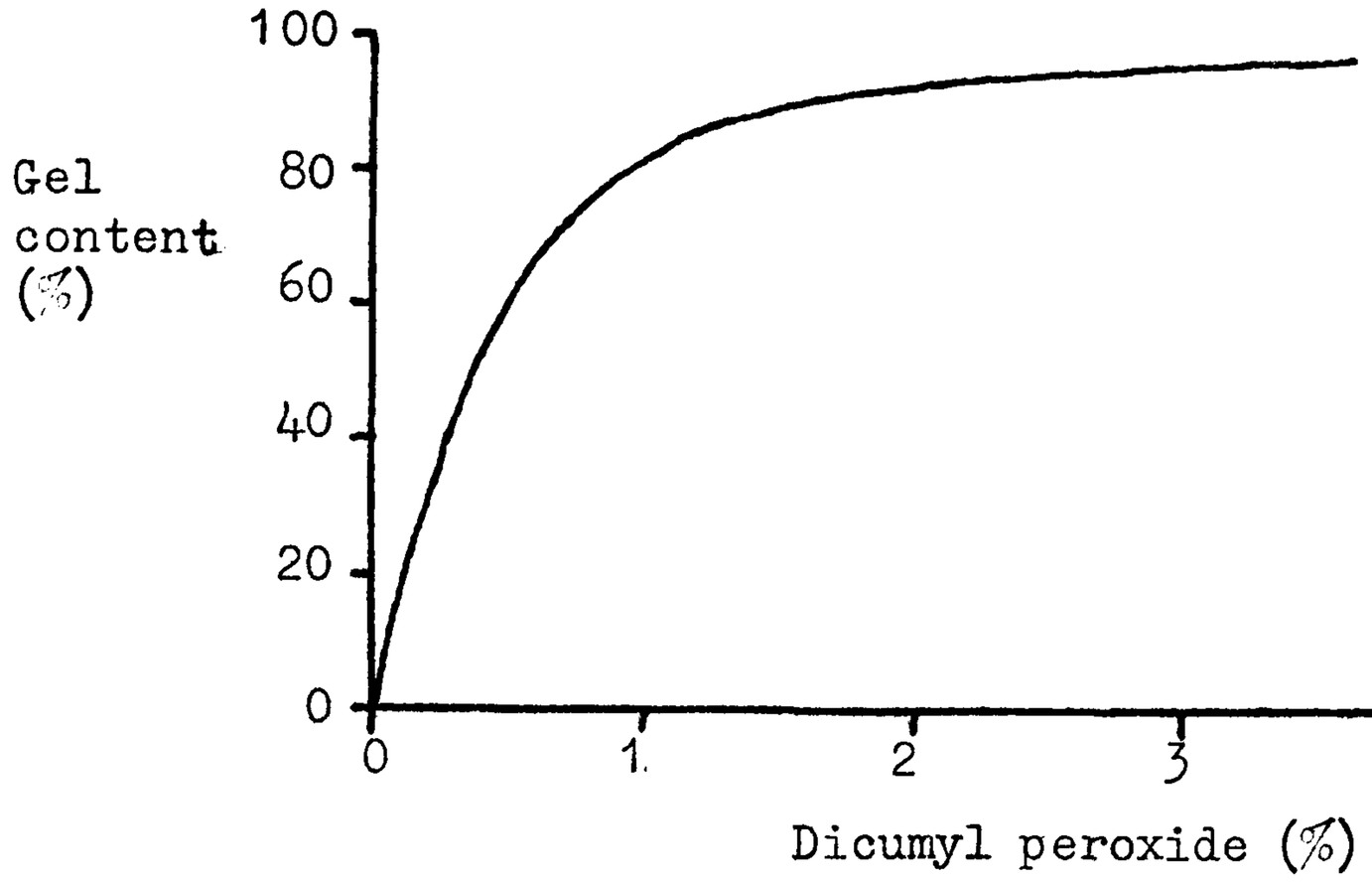

Figure 17 Typical plot of gel content vs concentration of dicumyl peroxide crosslinking agent.

It can readily be seen that deviations in the efficiency of crosslinking will alter the relationship between gel content and concentration of dicumyl peroxide, particularly at low concentrations.

A comparison of the experimentally determined plot of gel content versus concentration of dicumyl peroxide with that predicted from the molecular weight distribution and the concentration of dicumyl peroxide will yield a value of crosslinking efficiency. To this end a computer programme was written that could predict gel content, and a series of gel content analyses was carried out.

3.2. GEL CONTENT ANALYSIS

Gel content analysis is used to determine the fraction of a sample of crosslinked polyethylene insoluble above the crystalline melting point of polyethylene.

Gel content analysis is normally carried out using xylene or tetralin. Satisfactory results had previously been obtained using xylene (40), so this was chosen as the solvent. Specimens of crosslinked polyethylene were simply immersed in xylene under reflux (137-140°C) for 48 hours. Specimens were typically within the range 0.05-0.15g with a thickness of 0.1-0.4mm. The volume of xylene used was large enough to prevent significant

error due to soluble material failing to diffuse out of the swollen crosslinked polyethylene network. It is desirable to keep specimens as thin as possible to minimise the time required for all soluble material to diffuse out of the network. After removal from the solvent specimens were dried in a vacuum oven at 80°C for 48 hours, by which time constant weight was achieved.

$$\text{Gel content } (\%) = \frac{\text{Original mass of specimen - Final mass of specimen}}{\text{Original mass of specimen}} \times 100$$

For each sample of crosslinked polyethylene at least two separate determinations of gel content were carried out. Errors are greatest at low values of gel content: accuracy is typically $\pm 3\%$ at values of less than 50% gel content, dropping to $\pm$ 1% at values in excess of 90%.

A series of experiments was carried out to determine the gel content of specimens of Rigidex 006-60 crosslinked with various concentrations of dicumyl peroxide varying from 0.25-9.84%. The results of these experiments are given in Table 3 and shown in Figure 18.

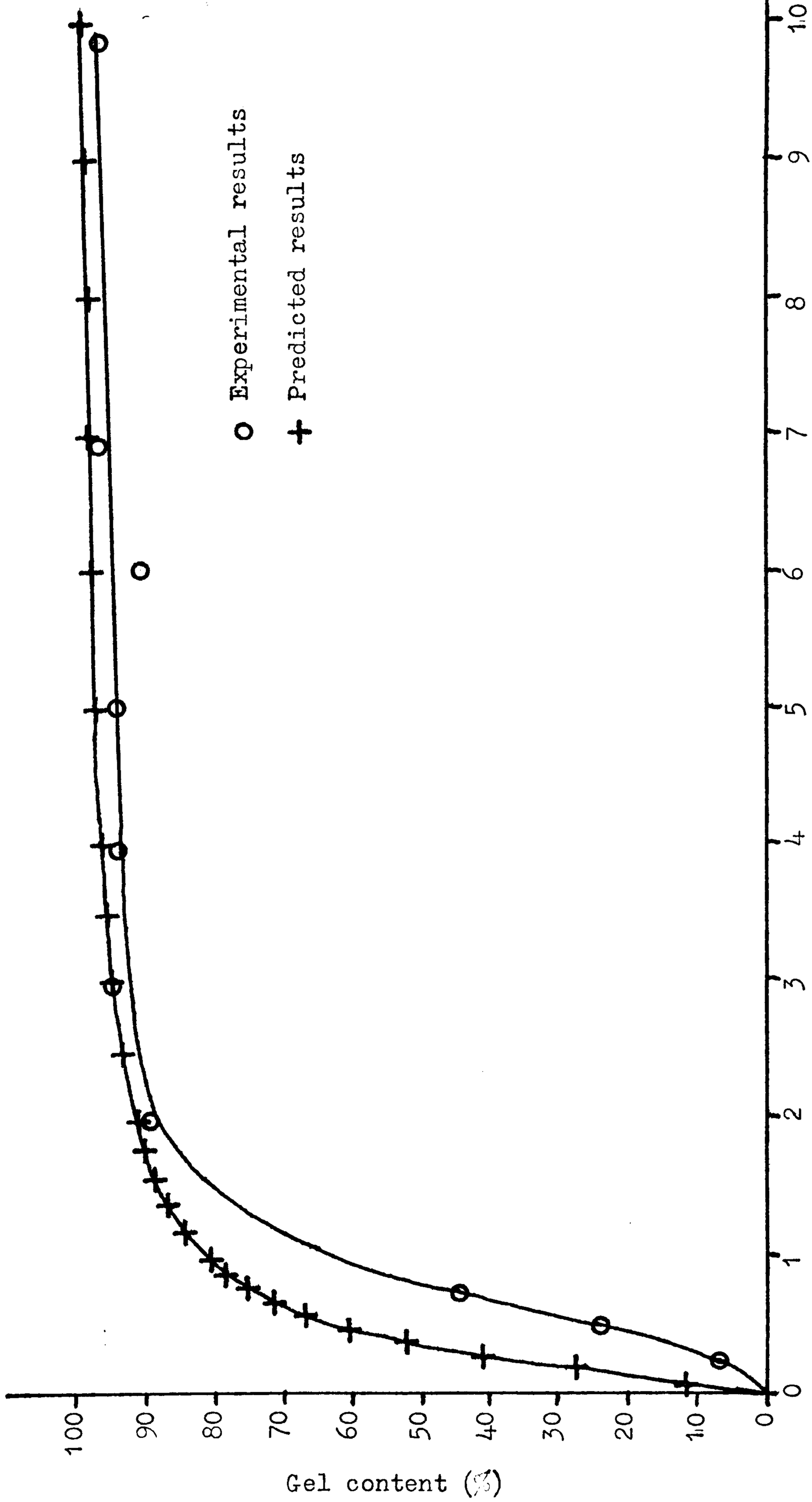

Figure 18 Plots of gel content vs concentration of crosslinking agent for Rigidex 006-60.

Concentration of dicumyl peroxide (%)	Gel content (%)
0	0
0.25	7.0 ± 2.0
0.50	24.6 ± 3.0
0.74	44.8 ± 3.0
1.98	89.3 ± 2.0
2.96	94.9 ± 1.0
3.94	94.5 ± 1.0
5.00	94.6 ± 1.0
6.01	91.2 ± 1.0
6.89	97.2 ± 1.0
9.84	96.8 ± 1.0

Table 3 Experimentally determined values of gel content vs concentration of crosslinking agent for Rigidex 006-60

3.3 COMPUTER PREDICTION OF GEL CONTENT

A computer programme was written to predict gel content from various criteria relating to the polymer and the concentration of dicumyl peroxide. The programme was written in BASIC to run on a Commodore 3032 PET desk-top computer. Although relatively slow, this computer had the advantage that it was readily available, little used, and situated in a position with relatively little disturbance.

Assuming that crosslinks are inserted at random along the length of a polymer chain, it is possible to calculate the probability that a chain of a given length will have a certain number of crosslinks for a given molecular concentration of dicumyl peroxide. Hence, if the molecular weight distribution is known, it is possible to calculate the fraction of chains containing 0,1,2,3...n crosslinks. With this information it is then possible to calculate the probability that a chain with a given number of crosslinks will not be bound into an insoluble matrix. For instance, a chain which is linked to 4 others will remain soluble if each of the chains it is attached to have no further crosslinks, see Figure 19.

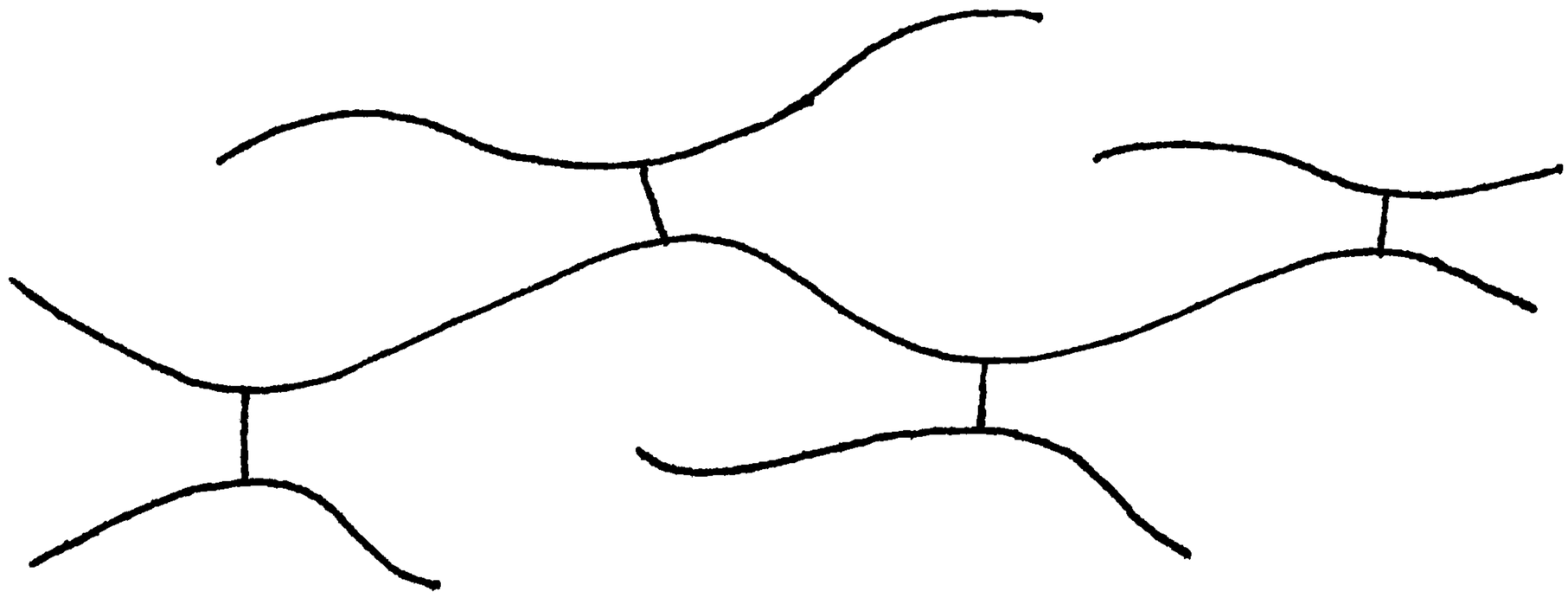

Figure 19 Soluble group of crosslinked polyethylene chains

When the total mass of all such soluble groups is added to the mass of chains which are not crosslinked at all the total soluble fraction is known. The predicted gel content is simply 100 - the percentage soluble.

In practice the value of n is taken to be 6. Separate computer predictions indicated that all chains with more than this number of crosslinks can be assumed to be part of the insoluble fraction without resulting in significant error.

All crosslinks are assumed to occur intermolecularly. The soluble fraction is dominated by those chains having 0, 1 or 2 crosslinks. When there is only 1 crosslink on a chain it must perforce be intermolecular. The size of molecules which have only 2 crosslinks will tend to be relatively small, therefore they will have a relatively large area of contact with surrounding chains, thus facilitating intermolecular bonding. At very low concentrations of dicumyl peroxide $<0.1\%$ this assumption will not hold true as much larger molecules, with relatively less contact with adjacent chains, will have only 2 crosslinks.

The possible effect of entanglements is ignored. Entanglements involving loops from adjacent molecules entwining would only affect the gel content if they involved short chains with the entanglement trapped as shown in Figure 20. The subject of chain entanglement is not clear, but is was thought that the number of entanglements being trapped in such a manner would be insignificant.

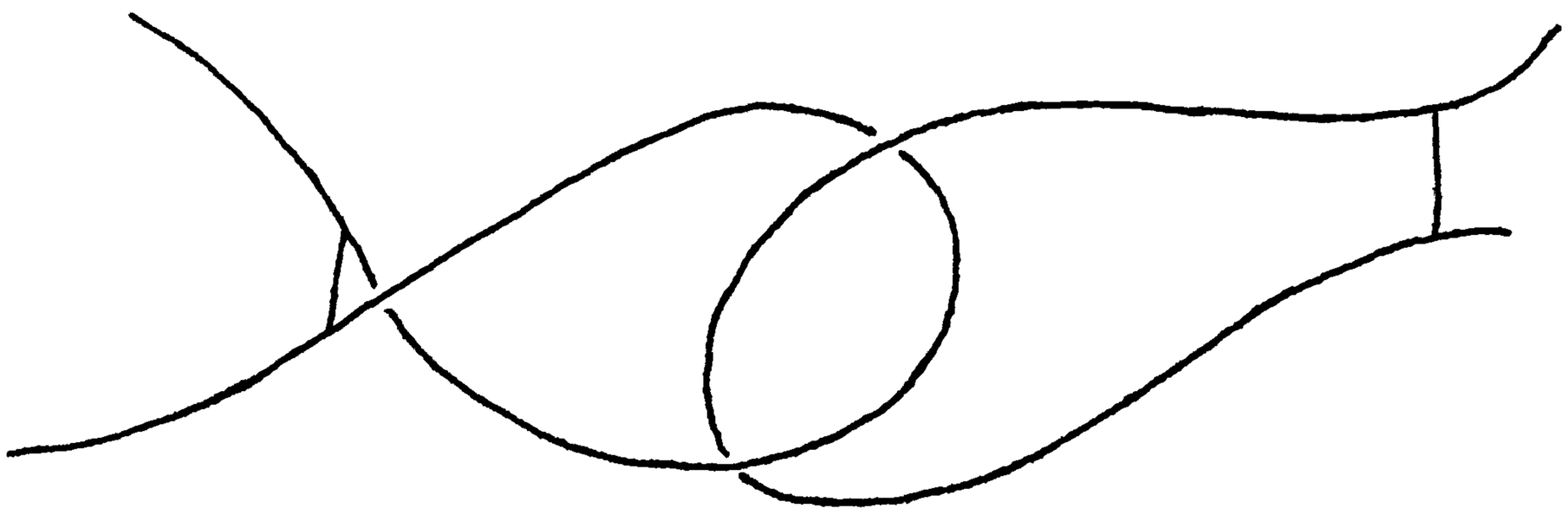

Figure 20 Trapped entanglement

Results of predicted gel content versus concentration of dicumyl peroxide used to effect crosslinking for Rigidex 006-60 are given in Table 4 and shown in Figure 18.

Concentration of dicumyl peroxide (%)	Predicted gel content (%)
0.0	0.0
0.1	11.9
0.2	27.9
0.3	41.8
0.4	52.7
0.5	60.9
0.6	67.2
0.7	72.0
0.8	75.8
0.9	78.8
1.0	81.2
1.2	84.8
1.4	87.3
1.6	89.2
1.8	90.7
2.0	91.8
2.5	93.9
3.0	95.3
3.5	96.2
4.0	96.9
4.5	97.4
5.0	97.8
6.0	98.3
7.0	98.7
8.0	99.0
9.0	99.2
10.0	99.3

Table 4 Predicted gel content vs concentration of crosslinking agent for Rigidex 006-60

3.4 PRELIMINARY COMPARISON OF EXPERIMENTAL RESULTS WITH COMPUTER PREDICTIONS

From Figure 18 it can be seen that the general shapes of the computer prediction of gel content versus concentration of dicumyl peroxide, and that determined experimentally are similar. The difference between the slopes of the two curves gives a

measure of the crosslinking efficiency. The values of concentration of dicumyl peroxide required to produce various values of gel content are shown in Table 5. The ratio of the computer predicted value of dicumyl peroxide to the experimentally determined value gives the efficiency.

Gel content (%)	Experimentally determined value of dicumyl peroxide (%)	Computer predicted value of dicumyl peroxide (%)	Efficiency (%)
10	0.31±0.01	0.08±0.01	25.8±4.2
20	0.46±0.01	0.14±0.01	30.4±2.9
30	0.57±0.01	0.21±0.01	36.8±2.5
40	0.68±0.01	0.28±0.01	41.2±2.1
50	0.80±0.01	0.37±0.01	46.3±1.8
60	0.93±0.01	0.50±0.01	53.8±1.6

Table 5 Concentrations of dicumyl peroxide required to produce various values of gel content, and efficiency at this point.

There are two major discrepancies between the shapes of the experimental and predicted curves. 1. The experimental curve shows a fairly small slope at first, which rapidly increases: figures for the crosslinking efficiency show a corresponding increase. 2. After approaching closely in the region of $2\frac{1}{2}$ to $3\frac{1}{2}$% dicumyl peroxide the two curves deviate. These discrepancies indicate that the model on which the computer predictions are made is imperfect. The first discrepancy indicates that there is a competing reaction at first, which decreases in importance with increasing dicumyl peroxide. The second discrepancy may be accounted for if certain of the decomposition products from dicumyl peroxide (such as phenol and acetophenone) remain within the crosslinked polymer and are leached out during solvent extraction, thereby resulting in an anomalously low value of gel content.

One possible reaction competing with crosslinking is that of preferential reaction of chain ends. Such a reaction would not result in an insoluble network until virtually all chain ends had been reacted. The possibility of such a reaction occurring was investigated.

3.5 CONSIDERATION OF CHAIN END ADDITION

It had been reported (30, 41) that vinyl groups increase the efficiency of crosslinking. With this in mind enquiries were made of British Petroleum concerning the concentration of vinyl groups in Rigidex 006-60. British Petroleum reported that each polymer chain bears a terminal vinyl group at one end. Fourier transform infra-red spectroscopy confirmed the existence of terminal vinyl groups, and established that no other vinyl groups were present. With a number average molecular weight of 19300 the concentration of vinyl groups is equivalent to 0.70% dicumyl peroxide. A quantitative study of the concentration of vinyl groups in unextracted samples of crosslinked polyethylene was carried out. The results of this study are given in Table 6 and shown in Figure 21.

Concentration of dicumyl peroxide (%)	Absorbance mm^{-1} of vinyl group at $910cm^{-1}$	Fraction of original vinyl groups left
0	0.88±0.01	1
0.25	0.65±0.01	0.739±0.020
0.50	0.48±0.01	0.545±0.017
0.74	0.35±0.01	0.398±0.016
1.98	0.11±0.01	0.125±0.013
2.96	0.09±0.01	0.102±0.013
3.94	0.05±0.01	0.057±0.012
5.00	0.04±0.01	0.045±0.012
6.01	0.05±0.01	0.057±0.012
6.89	0	0
9.84	0	0

Table 6 Variation of numbers of vinyl groups in crosslinked Rigidex 006-60 with increasing crosslinking agent.

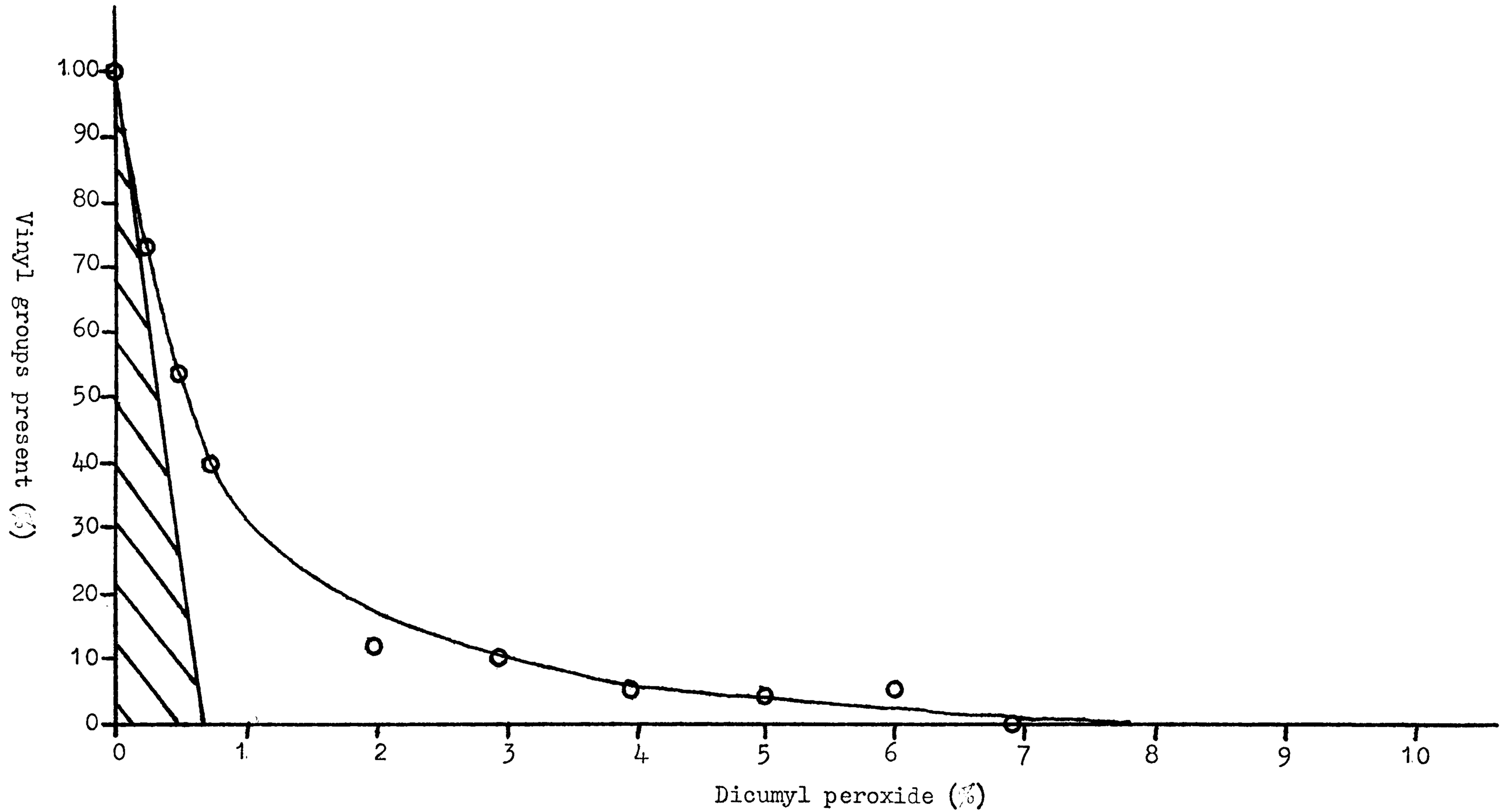

Figure 21 Relationship between numbers of vinyl groups in crosslinked Rigidex 006-60 and the concentration of crosslinking agent.

The hatched area in Figure 21 indicates the concentration of dicumyl peroxide required to react with any given proportion of the vinyl groups. The area between the hatched area and the curve indicates the concentration of dicumyl peroxide available for crosslinking. This discovery put a whole new complexion on the picture of the crosslinking process.

Reaction of dicumyl peroxide with terminal vinyl groups results in the joining of chain ends, which is not considered to be crosslinking, but rather chain extension. This chain extension reaction results in a reprofiling of the molecular weight distribution. The greater the proportion of vinyl groups reacted, the greater the change in the molecular weight distribution. It is possible to write a computer programme that will predict the change in molecular weight distribution, from the proportion of terminal vinyl groups reacting to give chain extension. This was done. The reprofiled molecular weight distribution is fed into the original computer programme along with the concentration of dicumyl peroxide available for crosslinking, thus generating a revised prediction of gel content. The revised set of values of gel content versus concentration of dicumyl peroxide is given in Table 7 and shown in Figure 22 with the experimental values obtained previously.

Original concentration of dicumyl peroxide (%)	Concentration of dicumyl peroxide available for crosslinking (%)	Revised prediction of gel content (%)
0	0	0
0.25	0.07±0.02	8.8±3
0.5	0.18±0.02	30.5±3
0.75	0.33±0.02	53.7±2
1.0	0.53±0.01	71.2±1.5
1.25	0.74±0.01	80.2±0.5
1.5	0.96±0.01	86.6±0.5
1.75	1.18±0.01	89.9±0.3
2.0	1.42±0.01	92.3±0.2
2.5	1.89±0.01	95.6±0.1
3.0	2.37±0.01	96.6±0.1
3.5	2.85±0.01	97.3
4.0	3.33±0.01	98.5
5.0	4.32±0.01	99.3
6.0	5.31±0.01	99.6
7.0	6.31±0.01	99.8
8.0	7.30	99.8
9.0	8.30	99.9
10.0	9.30	99.9

Table 7 Revised prediction of gel content with reprofiled molecular weight distribution

The correlation between the shapes of the two curves in Figure 22 is excellent. From the ratio of the values of the concentration of dicumyl peroxide required to produce various values of gel content the efficiency of the overall crosslinking reaction for Rigidex 006-60 may be calculated. See Table 8.

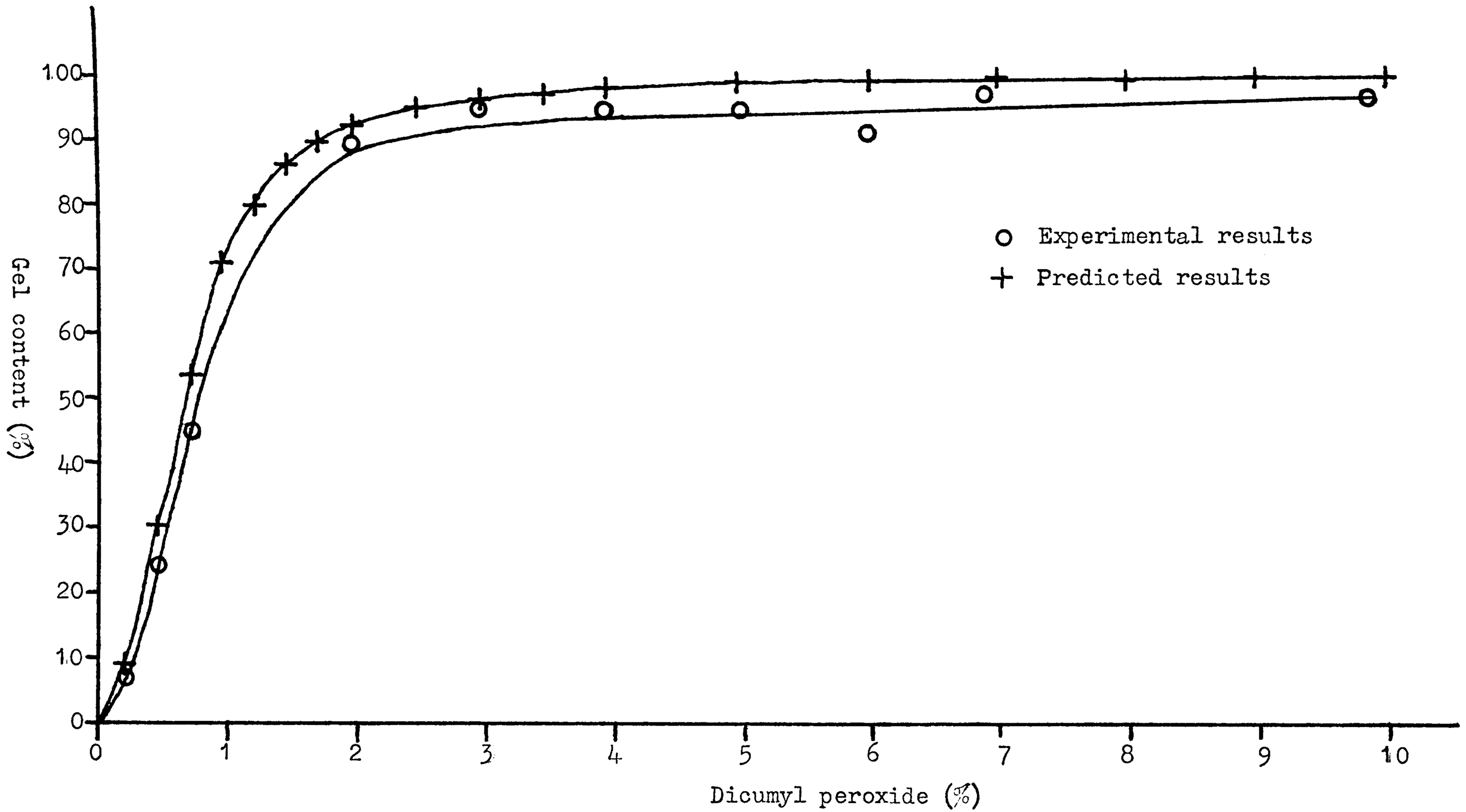

Figure 22 Plots of revised gel content vs concentration of dicumyl peroxide.

Gel content (%)	Experimentally determined value of dicumyl peroxide (%)	Computer predicted value of dicumyl peroxide (%)	Efficiency (%)
10	0.31±0.01	0.27±0.01	87.1±6.2
20	0.46±0.01	0.39±0.01	84.8±4.1
30	0.57±0.01	0.50±0.01	87.7±3.4
40	0.68±0.01	0.60±0.01	88.2±2.8
50	0.80±0.01	0.71±0.01	88.8±2.3
60	0.93±0.01	0.83±0.01	89.2±2.1
		Average efficiency	87.6%

Table 8 Concentrations of dicumyl peroxide required to produce various values of gel content in Rigidex 006-60 with a modified molecular weight distribution.

The efficiency as calculated in Table 8 is not the true value of crosslinking efficiency. It is dependent upon the amount of dicumyl peroxide used up in chain extension (and hence the molecular weight distribution) and the efficiency of the crosslinking reaction.

To obtain the true crosslinking efficiency of dicumyl peroxide with linear polyethylene it is necessary to subtract the concentration of dicumyl peroxide required for the reaction with vinyl groups from the total dicumyl peroxide value and replot the results. Thus a new pair of curves is generated which is shown in Figure 23. Once again the correlation between the shapes of the two curves is excellent. From the values of the concentration of dicumyl peroxide required to produce various gel content values the efficiency of the reaction producing crosslinks may be calculated. See Table 9.

Gel content (%)	Experimentally determined value of dicumyl peroxide (%)	Computer predicted value of dicumyl peroxide (%)	Efficiency (%)
10	0.09±0.01	0.07±0.01	77.8±20
20	0.16±0.01	0.12±0.01	75.0±11
30	0.22±0.01	0.19±0.01	86.4± 9
40	0.28±0.01	0.24±0.01	85.7± 7
50	0.37±0.01	0.30±0.01	81.1± 5
60	0.47±0.01	0.39±0.01	83.0± 4
		Average efficiency	81.5%

Table 9 Corrected concentrations of dicumyl peroxide required to produce various values of gel content in Rigidex 006-60 with a modified molecular weight distribution.

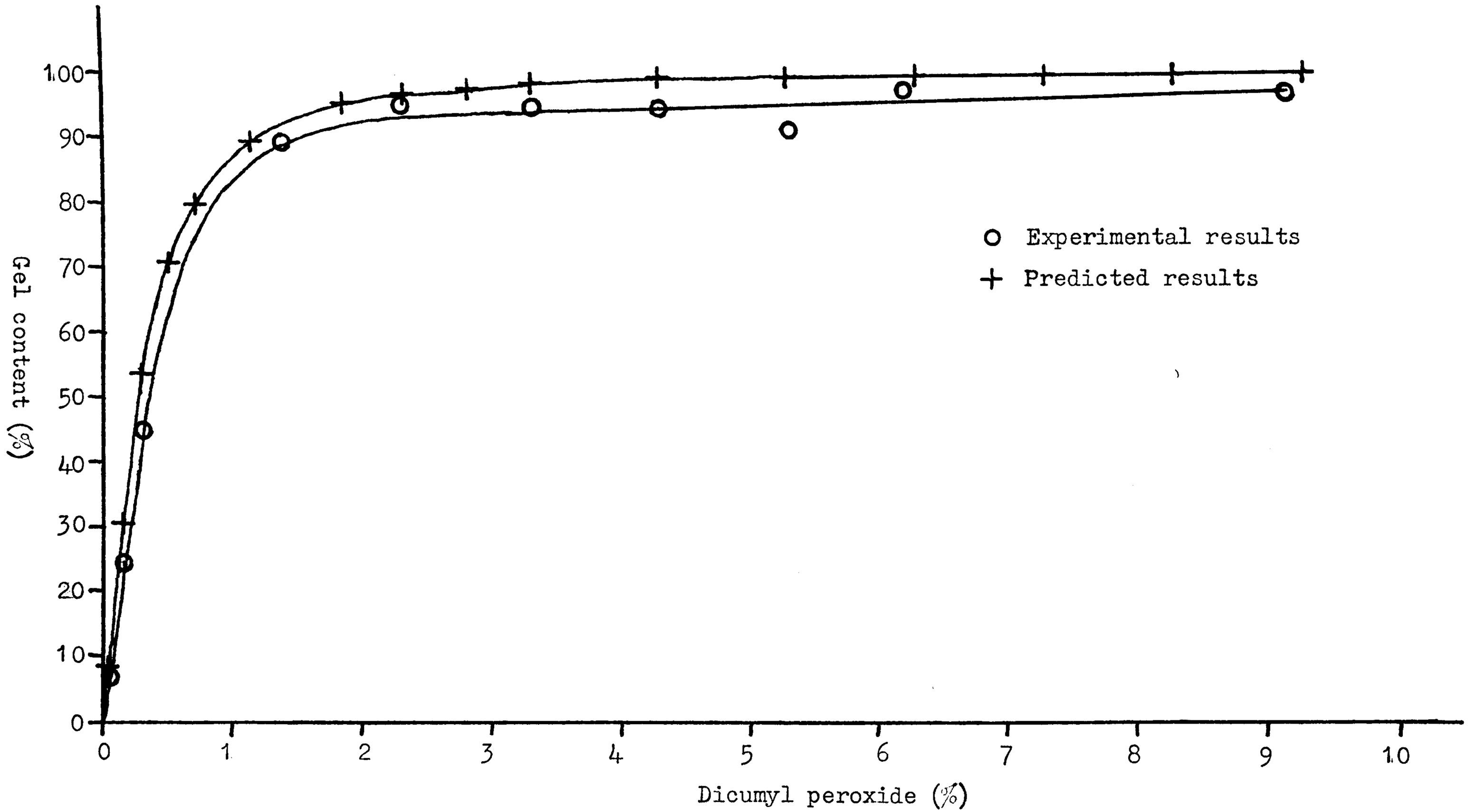

Figure 23 Plots of revised gel content vs revised concentrations of dicumyl peroxide.

3.6 COMPARISON OF CROSSLINKING EFFICIENCIES

The distinction between the two efficiencies calculated in Section 3.5 is that the overall efficiency of 87.6% is dependent on the concentration of vinyl groups and hence the molecular weight distribution, and is therefore specific to Rigidex 006-60, while the other efficiency of 81.5% is specific to the crosslinking reaction and is applicable to linear polyethylene in general.

The overall efficiency of reaction of dicumyl peroxide with Rigidex 006-60 as determined by gel content analysis is higher than that for pure crosslinking because it is a combination of reactions at random and specific sites. Reaction at the terminal vinyl groups is preferred over that producing crosslinks. This gives rise to longer chains which have more sites for crosslinking and so are statistically more likely to be bound into the insoluble network.

In the absence of terminal vinyl groups the experimentally determined curve for gel content versus concentration of dicumyl peroxide would be much closer to that originally predicted, as shown in Figure 18. This is because the preferred reaction with vinyl groups involves much larger proportions of low molecular weight fractions than would be involved if cumyloxy radicals attacked non-specific sites at random along the polymer chains.

The value of 81.5% efficiency for the crosslinking reaction is much higher than previously reported for linear polyethylene. Hulse et al (30) reported a value of only 24% efficiency for Phillips type linear polyethylene in which vinyl groups have been removed by hydrogenation. This difference is unresolved, but one is led to suspect that Hulse and his co-workers encountered some form of inhibition to crosslinking of which they were unaware.

Chapter 4

ASPECTS OF THE MORPHOLOGY OF CROSSLINKED POLYETHYLENE

4.1 DETERMINATION OF THE DEGREE OF CROSSLINKING

4.1.1 Definition of the degree of crosslinking

The degree of crosslinking may be expressed in two ways: 1. It may be given as the average separation of crosslinks expressed in terms of either molecular weight, or the equivalent number of monomeric units. When a polymer is only lightly crosslinked this definition is problematic because not all chains are bound into the crosslinked network by more than one crosslink. Also free chain ends are not accounted for. 2. The quantity may also be given as the crosslink density i.e. the average molecular weight, or number of monomeric units, per crosslink.

As each crosslink connects two chains the value of the average separation of crosslinks is half that of the crosslink density for a given sample.

The average separation of crosslinks may be determined experimentally, and the crosslink density calculated from the efficiency of the crosslinking reaction.

4.1.2 Gel Equilibrium Experiments

Fully crosslinked polyethylene does not dissolve, but rather will swell in appropriate solvents at elevated temperatures to form a gel. The extent to which a specimen swells is determined by the degree of crosslinking and the solvent/polymer interaction parameter.

The average separation of crosslinks may be calculated from the swelling ratio using the Flory-Rehner equation (42,43):

$$V = -\frac{Vr + \mu Vr^2 + \ln(1-Vr)}{Vo\left(Vr^{\frac{1}{3}} - Vr/2\right)}$$

where: Vr=Volume fraction of polymer in gel

V=Concentration of effective chains (mol cm^{-3})

μ=Huggins solvent/polymer interaction parameter

Vo=Molar volume of solvent (cm^3)

$$Vr = \frac{1}{\left(\frac{Ms\rho p}{\rho sMp}\right)+1}$$

where: Ms=Mass of solvent in gel (g)

Mp=Mass of polymer in gel (g)

ρs=Density of solvent (gcm^{-3})

ρp=Density of polymer (gcm^{-3})

$$Mc = \frac{\rho p}{V}$$

where: Mc=Average molecular weight of effective chains ≡ average separation of crosslinks

The Flory-Rehner equation was developed from statistical mechanics theory. It fails to take into account network imperfections or the existence of lengths of chain terminated by a crosslink at only one end. Flory proposed a modification to make allowance for such imperfections (44):

$$Mc' = \frac{MxMc}{(M+2Mc)}$$

where: Mc'=True value of average molecular weight of effective chains

M=Number average molecular weight of polymer prior to crosslinking

This modification has been demonstrated to be valid (45) and is used in this work.

Experimentally gel equilibrium measurement provides few difficulties, and is a tried and tested method for the rapid evaluation of the degree of crosslinking of many types of rubber.

An accurately weighed specimen of crosslinked polyethylene which had previously been solvent extracted to constant weight was immersed in boiling xylene (137-141 °C) for a minimum of two hours. By this time swelling equilibrium is achieved. It is then removed from the solvent and immediately placed into a pre-weighed, airtight screw top jar. This is necessary to prevent loss of solvent exuded as the gel cools. The bottle and solvent/polymer gel is weighed to ascertain the mass of the swollen gel. From this, the ratio (Q) of the mass of solvent to the mass of polymer in the gel is calculated. The average separation of crosslinks is obtained from the modified Flory-Rehner equation.

For this work the appropriate parameters for solving the Flory-Rehner equation are:

$$\mu = 0.31 \quad (46,47)$$
$$V_o = 139.3 \text{ cm}^3 \text{ at } 140^\circ C$$
$$\rho_p = 0.806 \text{ gcm}^{-3} \text{ at } 140^\circ C$$
$$\rho_s = 0.761 \text{ gcm}^{-3} \text{ at } 140^\circ C$$

Appropriate allowance is made to take into account the loss of ungelled material during solvent extraction which increases the number average molecular weight (M) of the remaining crosslinked chains.

Errors in the evaluation of the swelling ratio are approximately $\pm$ 5% resulting in an error in the evaluation of the average separation of crosslinks varying from $\pm$ 10% when Q is less than 3, rising to $\pm$ 15% at values of Q of 10 and over.

Although swelling measurements are widely used to characterise rubbers, doubts with respect to its applicability to crosslinked polyethylene (which later were proved unfounded) were expressed. This led to the decision to evaluate the degree of crosslinking by another method.

4.1.3 Calculation of Crosslink Density from the Quantity of Crosslinking Agent Employed

As explained in Chapter 3 it is possible to evaluate the efficiency of crosslinking linear polyethylene with dicumyl peroxide. From a knowledge of the quantity of dicumyl peroxide added, the efficiency of the reaction, and the amount of dicumyl peroxide that is taken up by the chain extension reaction the crosslink density may be calculated:

$$\rho_c = \frac{Md \times 100}{(D-F) \times E}$$

where: ρ_c=Crosslink density expressed in terms of molecular weight per crosslink

Md=Molecular weight of dicumyl peroxide

D=Weight % of dicumyl peroxide added

F=Weight % of dicumyl peroxide taken up by chain extension

E= Efficiency of the crosslinking reaction

which simplifies to:

$$\rho_c = \frac{33150}{(D-F)}$$

4.1.4 Average Separation of Crosslinks and Crosslink Density versus % Dicumyl Peroxide used as the Crosslinking Agent

The values of average separation of crosslinks versus % dicumyl peroxide added as calculated from gel equilibrium are given in Table 10 and shown in Figure 24. The values of crosslink density versus % dicumyl peroxide added predicted from the efficiency of the reaction are given in Table 11 and shown in Figure 24, coaxially with the gel equilibrium results.

% dicumyl peroxide	Q	Average separation of crosslinks (molecular weight)
0.25	80.1	85000
0.50	47.2	42600
0.74	22.3	25900
0.74	28.6	28300
0.98	22.0	22000
1.24	29.6	21400
1.24	23.6	20200
1.49	14.9	16000
1.98	3.57	3800
1.98	4.20	4700
2.96	2.84	2700
2.96	2.46	2100
3.94	3.36	3300
3.94	3.25	3200
4.93	3.66	3800
4.93	3.91	4200
5.91	3.31	3300
6.89	2.55	2300
6.89	1.94	1500
9.84	1.81	1400
9.84	1.38	900

Table 10 Average separation of crosslinks versus % dicumyl peroxide used.

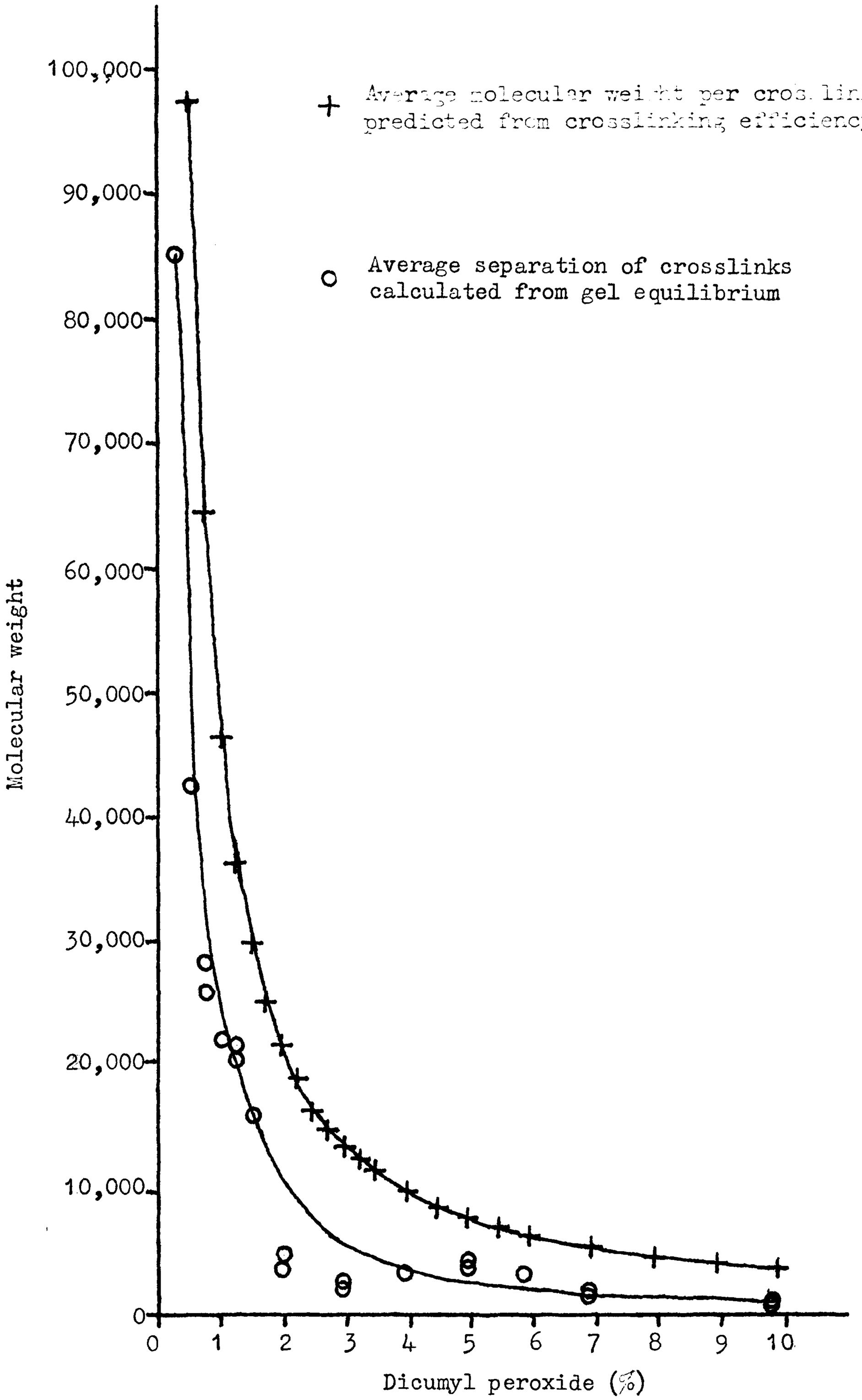

Figure 24 Average separation of crosslinks as calculated from gel equilibrium and average molecular weight per crosslink predicted from crosslinking efficiency vs % dicumyl peroxide used for crosslinking.

% dicumyl peroxide	Average molecular weight per crosslink
0.25	194700
0.5	97300
0.75	64400
1.0	46500
1.25	36300
1.5	29800
1.75	25100
2.0	21700
2.25	19000
2.5	16800
2.75	15000
3.0	13600
3.25	12500
3.5	11500
4.0	9940
4.5	8700
5.0	7760
5.5	6970
6.0	6330
7.0	5350
8.0	4620
9.0	4060
10.0	3610

Table 11 Average molecular weight per crosslink vs dicumyl peroxide used

A comparison of the two sets of data shows a fairly good agreement when one takes into account the fact that the values of average molecular weight per crosslink are twice the average separation of crosslinks. This confirms that the Flory-Rehner analysis of gel equilibrium in rubbers is applicable to crosslinked polyethylene.

4.2 DIFFERENTIAL SCANNING CALORIMETRY

4.2.1 Principles of Differential Scanning Calorimetry

Differential scanning calorimetry applied to polymers yields a measure of the degree of crystallinity, and the temperatures at which transitions take place. These results must be treated with some degree of caution.

The principle of differential scanning calorimetry is that the sample and a reference are heated or cooled at the same rate, and the difference in the amount of heat required to maintain identical temperatures is recorded as a function of temperature. The resulting thermogram may show exotherms, endotherms, and changes of specific heat capacity. In the case of polyethylene, exotherms are associated with crystallization, and endotherms with melting. A change of slope indicates a change of specific heat capacity, associated with a transition relating to small scale movement of polymer chains.

The area of an endotherm is proportional to the amount of heat required for the melting process. This is based on a two phase model of morphology which postulates that each part of a polymer chain inhabits either a perfectly crystalline lattice, or a wholly amorphous region. This model is open to question; if one accepts that the morphology of polyethylene crystallized from the melt is chain folded with negligible interlamellar links then it is acceptable, but, if the melt crystallized material adopts a morphology in which many chains traverse the interlamellar zones there will be a partially ordered transition zone between the crystalline lamellae and the truly amorphous regions. As differential scanning calorimetry only measures the heat required to raise the temperature it cannot distinguish between the melting of a crystalline lattice and the disordering of a partially ordered phase. In this work, any contribution of the disordering of a partially ordered phase is considered to have negligible effect on the size of the endotherm. This is of course not strictly true, but is acceptable as all results are considered relative to the others.

The melting point is normally taken as the position of the endotherm peak maximum. This is not strictly correct as the peak position is affected very slightly by the rate of heating and the size of the sample. These effects are related, and are due to a thermal lag caused by the poor heat conducting properties of polyethylene. To minimise these effects a slow heating rate should be used with a small sample size. Unfortunately fulfilling these conditions leads to other problems; a slow heating rate may allow the sample to anneal, and a small sample results in relatively larger errors

associated with weighing the sample and integrating the area of endotherm. Clearly a compromise must be attempted. To this end a standard heating rate of 20°C min^{-1} was used, and a small range of sample size (8-12mg) was chosen.

Errors in the estimation of the melting point arise due to slight variations in the calibration of the instrument and inexactitudes related to determining the peak position of the endotherm. These are of the order of ± 1°C. Errors in calculating the degree of crystallinity may come from sample weighing (±1%), calibration of peak area using indium (±1%), and integration of peak area by cutting out and weighing (±1%). Thus total errors in the precision of the degree of crystallinity as calculated may be ±3%.

The thermal history of a sample plays a large part in determining the crystallinity and melting point. All samples were given an identical thermal history by holding them at 450K for 5 minutes prior to cooling to 300K at 80°C min^{-1} before running the thermogram.

All measurements were made using a Perkin-Elmer DSC-2.

4.2.2 Results of Differential Scanning Calorimetry

The degree of crystallinity and melting point of the base resin and samples of crosslinked Rigidex 006-60 before and after solvent extraction were determined. To ascertain whether the process of dissolution, and subsequent vacuum drying and heating required by the crosslinking process had any effect on the base resin a number of blanks were prepared which had no dicumyl peroxide added. These were also analysed by differential scanning calorimetry. The results of differential scanning calorimetry are shown in Table 12 and Figures 25-28.

Dicumyl peroxide (%)	Unextracted		Extracted	
	Degree of crystallinity (%)	Melting point (K)	Degree of crystallinity (%)	Melting point (K)
0(1)	75±3	408±1	-	-
0(2)	62±2	408±1	-	-
0.25	55±2	404±1	52±2	401.5±1
0.50	56±2	405±1	56±2	404.5±1
0.74	51±2	401±1	47±2	401±1
1.00	61±2	404±1	57±2	406±1
1.24	56±2	402±1	56±2	406.5±1
1.49	56±2	400±1	58±2	407±1
1.98	49±2	401±1	52±2	402±1
2.96	48±2	401±1	57±2	399.5±1
3.94	51±2	398.5±1	50±2	399.5±1
5.00	48±2	399±1	49±2	401±1
6.01	52±2	401±1	47±2	399±1
6.89	44±2	392.5±1	43±2	395±1
9.84	35±1	389±1	33±1	389±1

(1) Base resin

(2) Blank

Table 12 Results of differential scanning calorimetry

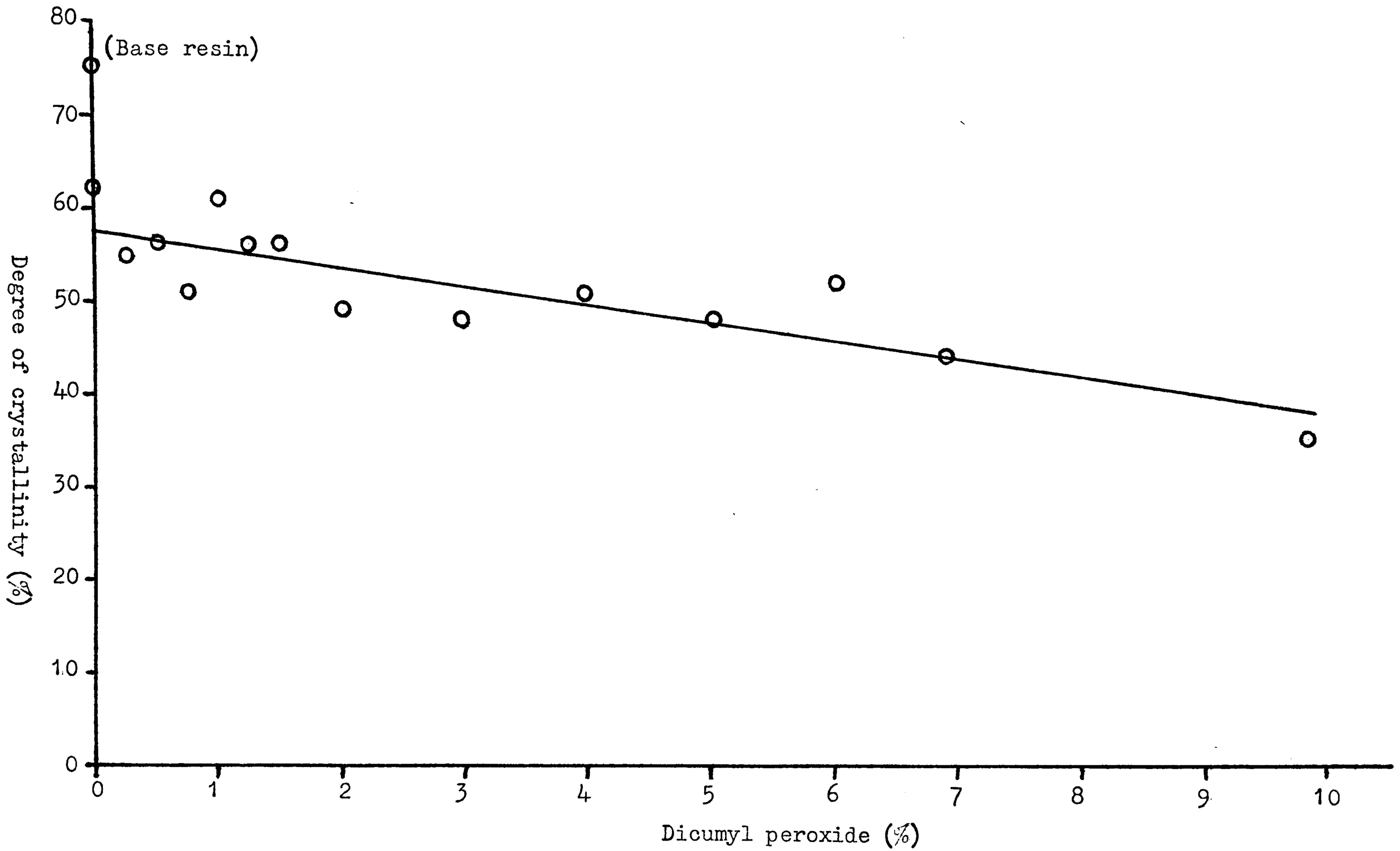

Figure 25 Degree of crystallinity of unextracted samples of crosslinked Rigidex 006-60 vs % dicumyl peroxide used.

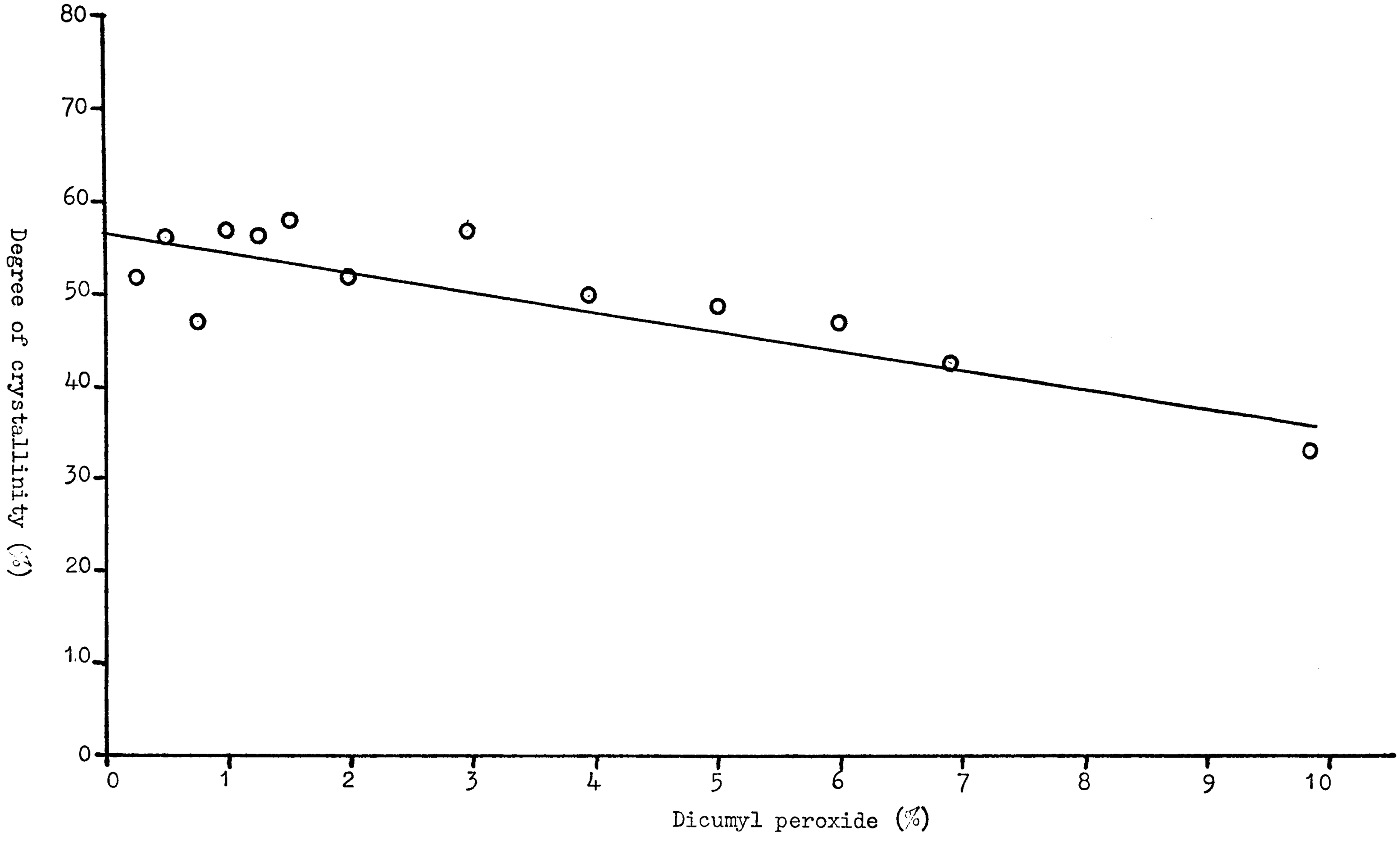

Figure 26 Degree of crystallinity of extracted samples of crosslinked Rigidex 006-60 vs % dicumyl peroxide used.

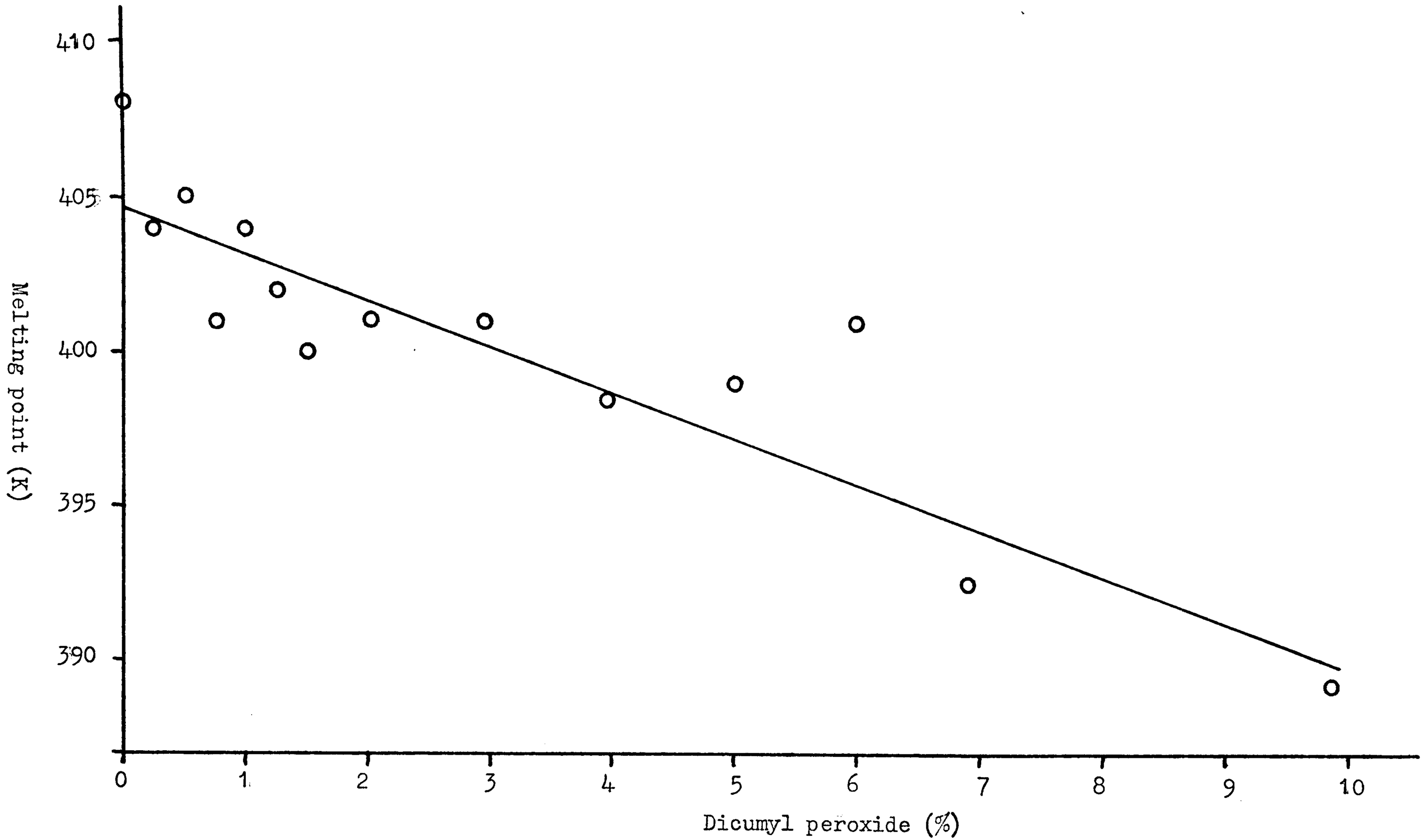

Figure 27 Melting point of unextracted samples of crosslinked Rigidex 006-60 vs % dicumyl peroxide used.

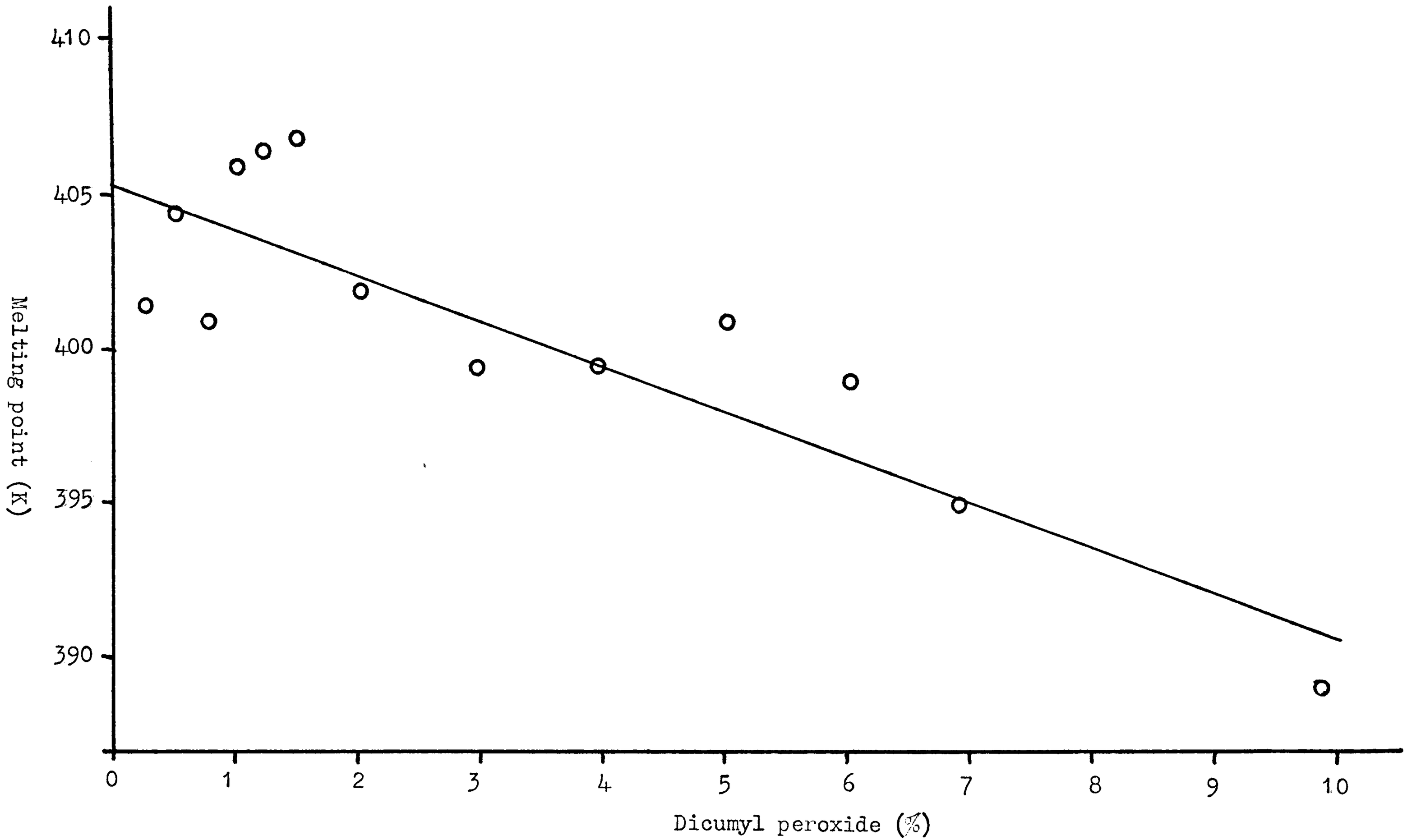

Figure 28 Melting point of extracted samples of crosslinked Rigidex 006-60 vs % dicumyl peroxide used.

As the proportion of crosslinking agent increased, the shape of the thermogram of crosslinked polyethylene changed. The maximum became less sharp with an increased tail towards the lower temperatures; this is shown in Figure 29. This change of shape was not quantified.

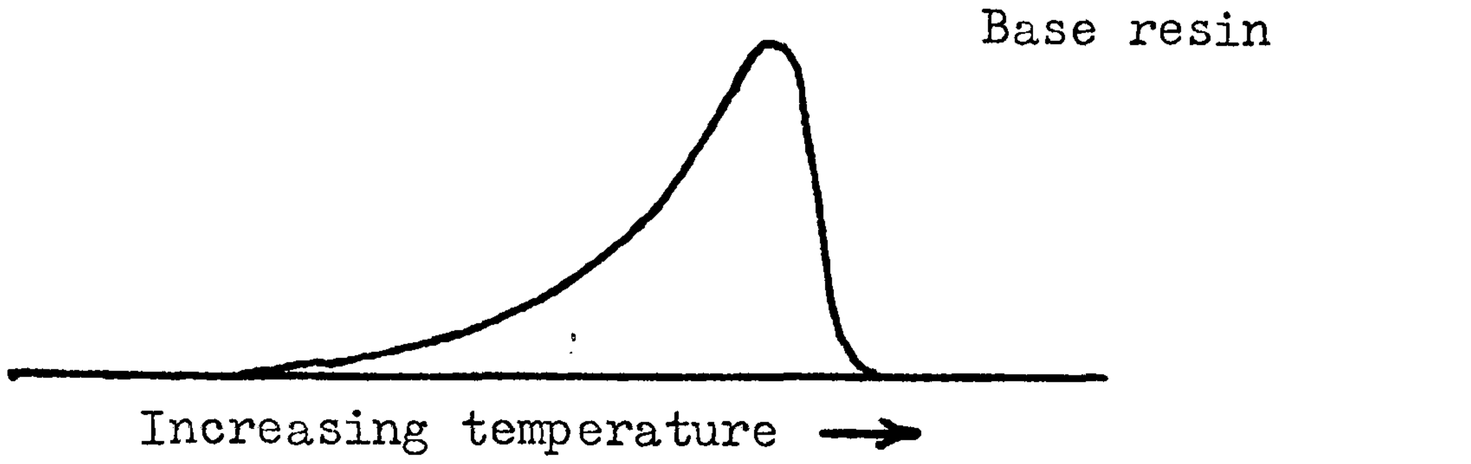

Figure 29 Change of shape of thermogram

From the plots of degree of crystallinity versus % dicumyl peroxide three observations can be made:
1. There is an approximately linear decrease of crystallinity as measured with increasing proportions of dicumyl peroxide.
2. The slopes of unextracted and extracted plots match very closely. 3. The degree of crystallinity decreases by only approximately half when proceeding from no crosslinks to an average separation of crosslinks of approximately 100 methylene groups.

These observations have a number of implications with respect to the morphology of crosslinked polyethylene and polyethylene. The linear decrease in degree of crystallinity implies that there is no clear change of morphology either when the material is crosslinked or as crosslink density increases. In a partially crosslinked material with a low gel content (i.e. $< 1\%$ dicumyl peroxide) one might expect the uncrosslinked chains to crystallize in a different manner to

those that are crosslinked, due to a difference in chain mobility. This does not appear to be the case as there is no difference between the slopes of the extracted and unextracted plots. This strongly suggests that the modes of crystallization for the uncrosslinked and crosslinked materials are similar. As crosslinked chains do not undergo reptation the implication is that neither do uncrosslinked chains, therefore chain folding is not taking place. Particularly at high degrees of crosslinking, gross chain movement is impossible, yet there is still a reasonably high degree of crystallinity when the average separation of crosslinks is approximately 100 methylene group. This evidence favours Flory's model of polyethylene crystallization.

The plots of melting point versus % of dicumyl peroxide serve to reinforce the evidence from the degrees of crystallinity. The extracted and unextracted plots match closely, showing no discontinuities.

The change of shape of the thermograms with increasing degrees of crosslinking indicates that there is gradual change in structure with an increasing spread of crystallite thicknesses. This would not be unreasonable according to Flory's view of crystallization. Varying stem lengths in a crystallite are an inevitable consequence of his model. Crosslinking would restrict the movement of individual chain elements to different degrees according to the separation of crosslinks thus making a spread of stem lengths likely, resulting in a broader endotherm peak.

4.3 LONGITUDINAL ACOUSTIC MODE OF VIBRATION IN CROSSLINKED POLYETHYLENE

4.3.1 Origins of Longitudinal Acoustic Mode

The longitudinal acoustic mode of vibration in polyethylene as recorded by Raman spectroscopy arises from an accordion-like vibration of all trans sequences in crystalline regions.

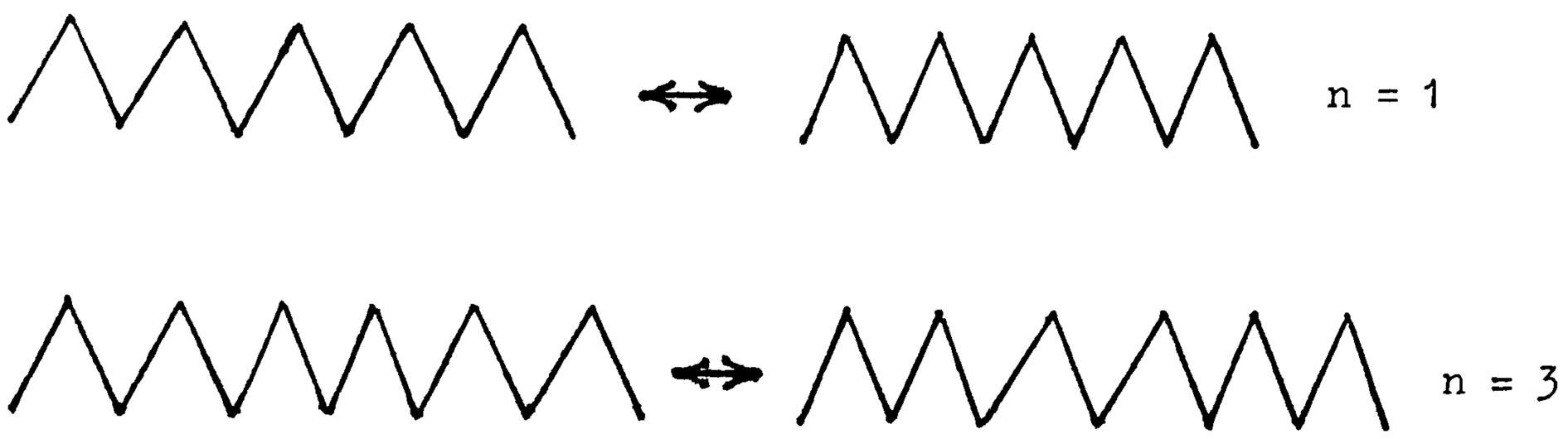

Figure 30 Accordion-like vibrations of all trans sequences

The frequency of the vibration is very low, generally occurring at shifts of $< 30 cm^{-1}$ from that of the exciting radiation. The frequency of vibration for an elastic rod with free ends is readily calculated from classical principles:

$$\nu = \frac{n \left(\frac{Ec}{\rho}\right)^{\frac{1}{2}}}{2cL}$$

where: ν = Frequency of vibration (cm^{-1})

n = Order of vibration (only odd numbers are Raman active)

ρ = Density of rod (gcm^{-3})

c = Speed of light (cms^{-1})

L = Length of vibrating rod (cm)

Ec = Young's modulus of rod (dynes cm^{-2})

In general the longitudinal acoustic mode is only seen for n=1. From a study of the position of the longitudinal acoustic mode bandhead in the Raman spectrum the average all trans stem length in the crystalline regions of polyethylene may be evaluated.

The view of an elastic rod vibrating in the longitudinal acoustic mode producing a single frequency band in the Raman spectrum of polyethylene is simplistic. A number of other factors affecting the band must be considered.

A distribution of lamellar thickness is always found in melt crystallized polyethylene. The relationship between

frequency of vibration and stem length is reciprocal, therefore a broad distribution of stem lengths results in a skewed band (48).

The population of vibrationally excited states is inversely proportional to frequency, hence low frequency bands will be more intense. This situation is further complicated by the effect of temperature which affects the population of vibrational states.

An all trans sequence in a crystalline region cannot be considered simply as an elastic rod as it ignores the effect of the coupling of chains by folds at lamellar surfaces and the effect of the chains in the disordered region to which all trans sequences may be attached. Several models have been proposed which take into account such perturbations. These include perturbed elastic rod models (49,50), the coupled lamellae model (51), and the coupled oscillator model (52). These are illustrated in Figure 31.

Theoretical prediction of the impact of the damping effect based on such models has been variable. However all attempts to demonstrate any effect on the longitudinal acoustic mode of polyethylene by freezing the non-crystalline phases, swelling the non-crystalline phases with solvent, or nitric acid etching have been unsuccessful. This is not so for other polymers, but it is clear that in the case of polyethylene the configurational effects are small.

As all spectra reported here were run at approximately the same temperature and the distribution of chain lengths remains fairly limited it was felt that no correction was needed as all results would be analysed comparatively.

Simple elastic rod

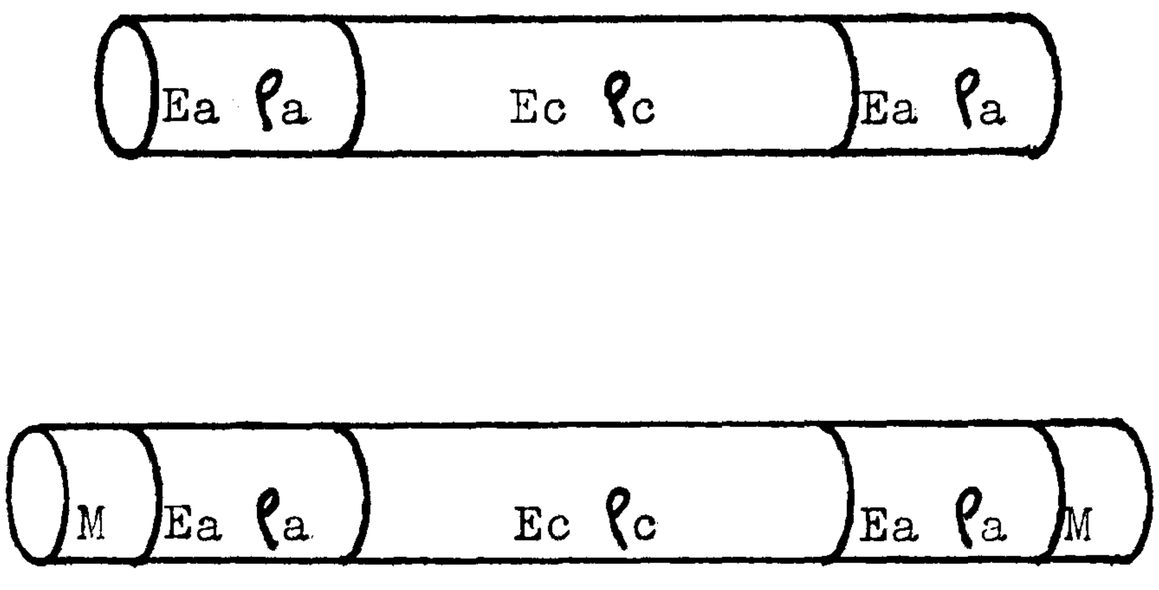

Perturbed elastic rod

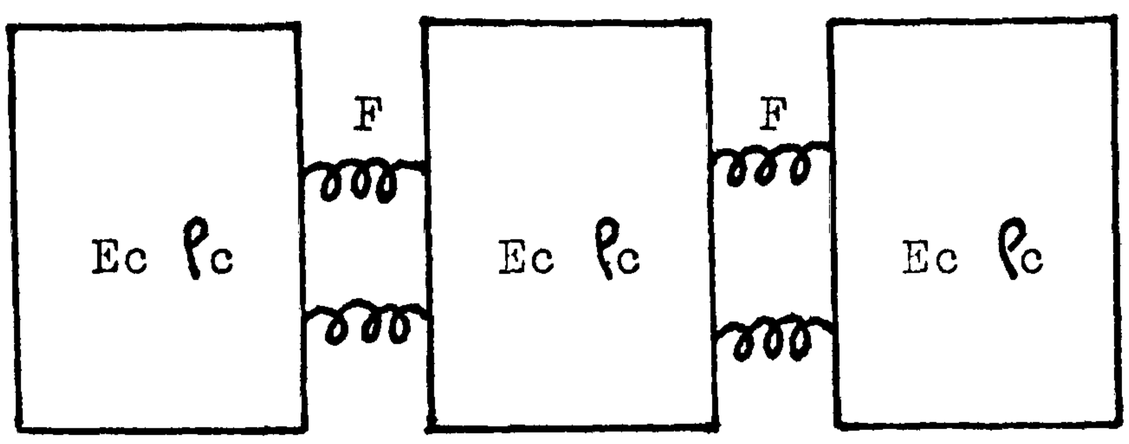

Coupled lamellae

Coupled oscillators

Ec = Youngs modulus of crystalline region

ρc = Density of crystalline region

Ea = Youngs modulus of amorphous region

ρa = Density of amorphous region

F = Interlamellar force

M = Mass of end group

f = Force between monomer units

m = Mass of monomer unit

Figure 31 Models used to explain longitudinal acoustic vibration in polymers.

4.3.2 Determination of Position of Longitudinal Acoustic Mode Bandhead

The low frequency Raman spectra of various specimens of crosslinked Rigidex006-60 were recorded on the Coderg T800 Raman Spectrometer. The power of the exciting laser beam at the sample was typically 100-150mW. Spectra were recorded from a shift of $\sim 5cm^{-1}$ to $50cm^{-1}$ at a scanning speed of $10cm^{-1}$ min^{-1} with all the spectrometer slits set at an identical value of 0.7, 1.0 or $2.0cm^{-1}$.

When recording spectra at such small shifts from the laser frequency the effect of Rayleigh scattering is pronounced. A small slit width reduces the detection of the Rayleigh wing, providing a baseline with a small slope, however this results in a small Raman signal with a concomitant low signal to noise ratio. Opening the slits increases the strength of the Raman signal and hence the signal to noise ratio, but results in a sloping baseline. As the slope of the baseline increases the position of the bandhead is shifted. This state of affairs is illustrated in Figure 32.

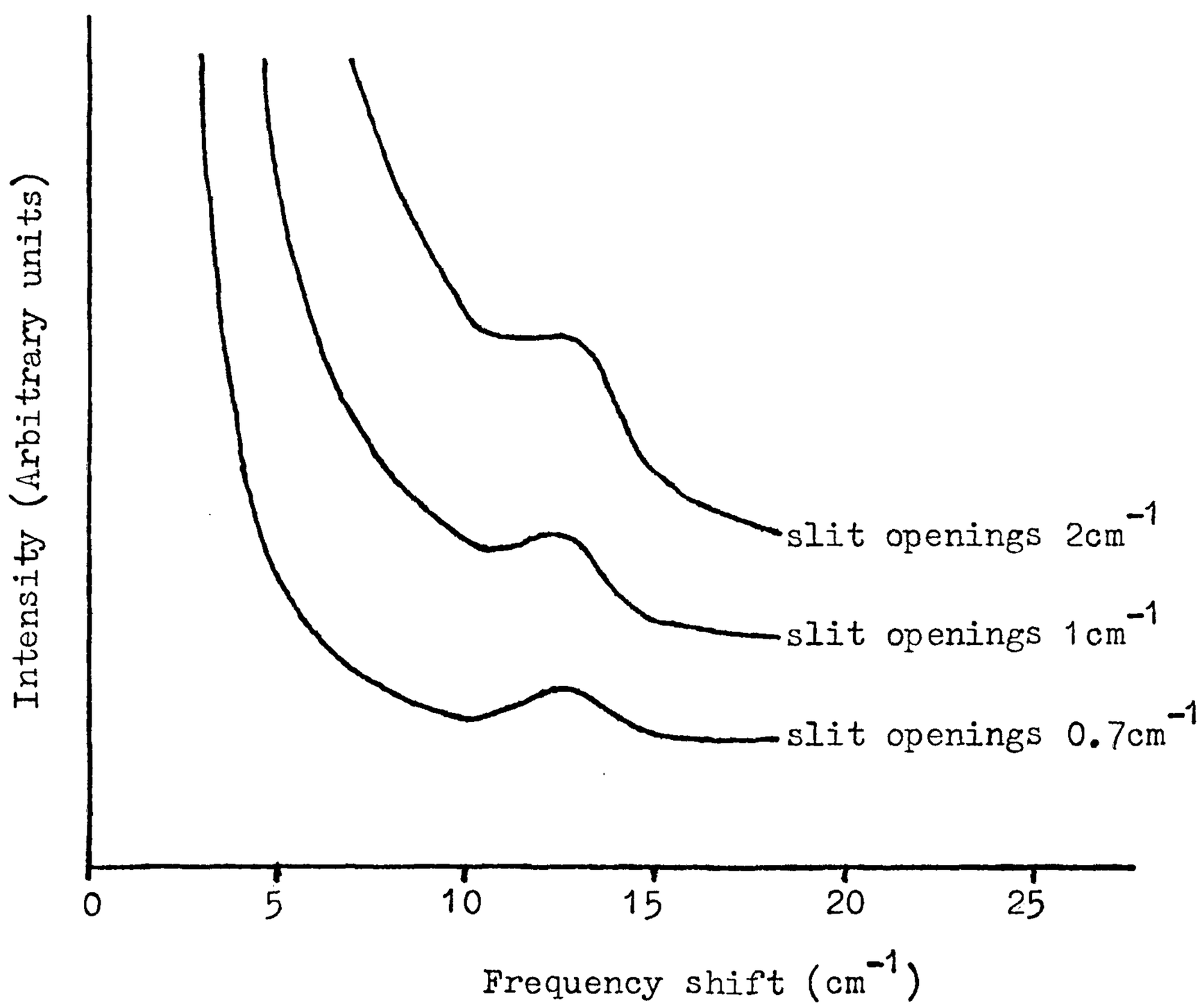

Figure 32 Effect of slit widths on the position of the longitudinal acoustic mode vibration in the Raman Spectrum

It is necessary to deconvolute the peak from the background todetermine the bandhead position. To ensure that this was done with reasonable precision at least two spectra were recorded for each specimen, employing different slit openings. Results after deconvolution of the spectra generally agreed to within $\frac{1}{2}cm^{-1}$.

The most probable value of stem length was calculated from the equation given in 4.3.1 using the parameters:

$$Ec = 2.9x10^{12} \text{ dynes cm}^{-2} \quad (51)$$

$$\rho = 1.00 \text{ g cm}^{-3}$$

$$c = 3.0 \times 10^{10} \text{ cm sec}^{-1}$$

Although no high degree of accuracy is claimed for the most probable stem lengths calculated, the relative values will be in good order.

4.3.3 Results of Longitudinal Acoustic Mode Determination

Samples were conditioned by heating them to 450K, holding them at this temperature for 5 minutes then quenching them directly in liquid nitrogen and finally allowing them to warm up to room temperature. Spectra were run on samples before and after solvent extraction in boiling xylene for 48 hours.

Results for the longitudinal acoustic mode and calculated values for the most probable stem length are given in Table 13 and shown in Figure 33.

The plot of most probable stem length versus % dicumyl peroxide shows a smooth curve with values for the material before and after solvent extraction being similar. The blank specimens have a most probable stem length of $\sim$170Å, this figure gradually decreases with increasing crosslink density to $\sim$95Å for the most highly crosslinked specimen.

It is a generally accepted fact that melt crystallized linear polyethylene has a lamellar morphology. The fact that on lightly crosslinking there is little or no change in the most probable stem length of Rigidex 006-60, indicates that there are no drastic changes in morphology. Increasing degrees of crosslinking show a fairly smooth decrease in the most probable stem length indicating that the morphology undergoes no radical changes. The implication is that crosslinked polyethylene has a lamellar morphology. As reptation cannot take place in a crosslinked network Geil's

Dicumyl peroxide (%)	Unextracted samples		Extracted samples	
	Longitudinal acoustic mode band position (cm^{-1})	Most probable stem length (Å)	Longitudinal acoustic mode band position (cm^{-1})	Most probable stem length (Å)
Blank	$16\frac{1}{2}$,17	172,167	-	-
0.25	$19\frac{1}{2}$,20	146,142	$20\frac{1}{2}$,21	138,135
0.50	$18\frac{1}{2}$	153	17,$17\frac{1}{2}$	167,162
0.54	17,$17\frac{1}{2}$	167,162	-	-
0.74	19,$19\frac{1}{2}$	149,146	$17\frac{1}{2}$	162
1.00	18,$18\frac{1}{2}$	158,153	16,17	177,167
1.49	19	149	$21\frac{1}{2}$	132
1.98	19,$19\frac{1}{2}$	149,146	$19\frac{1}{2}$,20	146,142
2.96	23	123	22,23	129,123
3.94	22,23	129,123	$23\frac{1}{2}$	121
5.00	21,$21\frac{1}{2}$	135,132	25	114
6.01	$23\frac{1}{2}$,$24\frac{1}{2}$	121,116	24,$24\frac{1}{2}$	118,116
6.89	24,$24\frac{1}{2}$	118,116	24,25	118,114
9.84	29,30	98,95	$29\frac{1}{2}$,30	96,95

Table 13 Results of longitudinal acoustic mode analysis

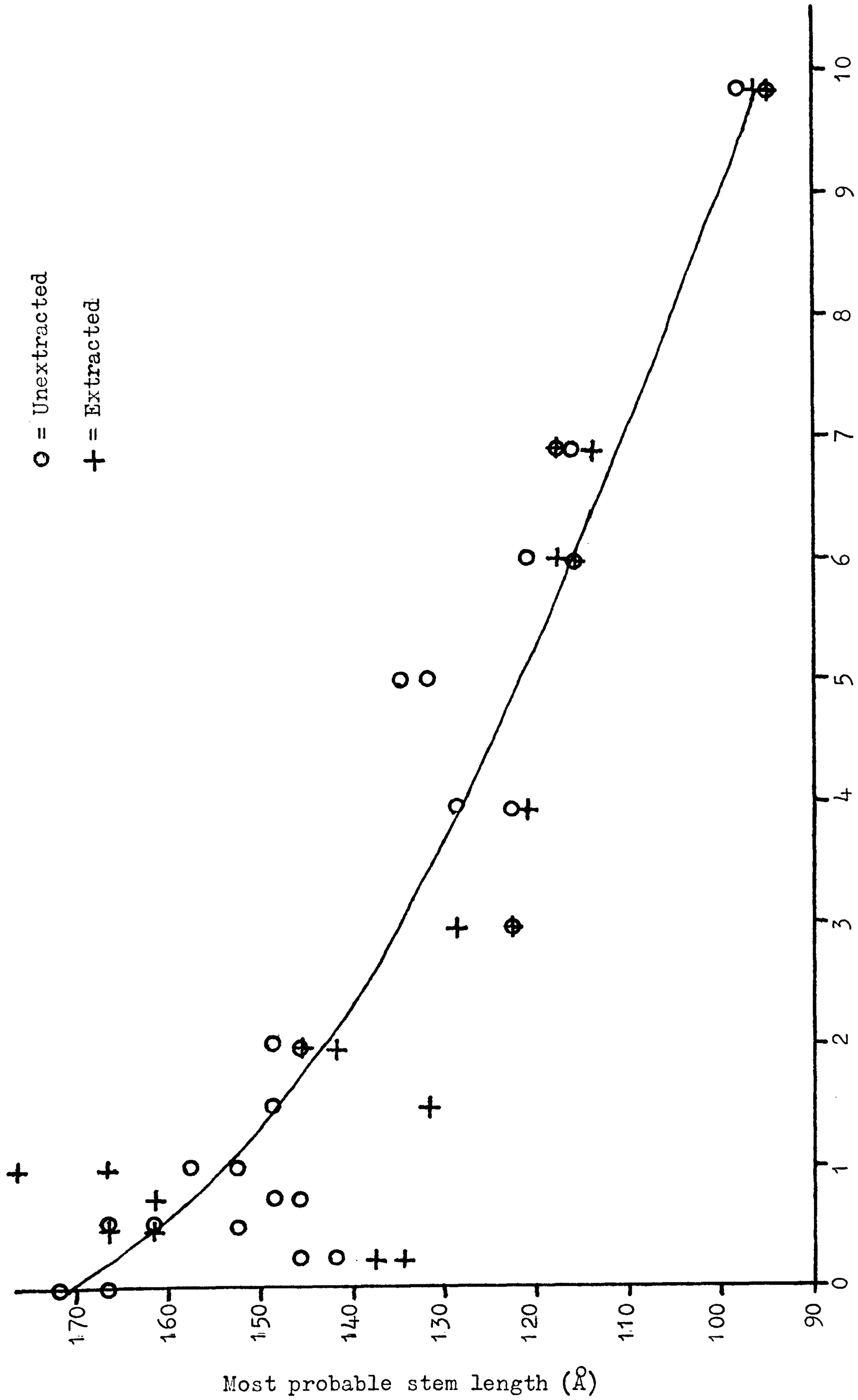

Figure 33 Most probable all trans stem length vs % dicumyl peroxide used.

model for explaining crystallization is inapplicable. The similarity of the plots for the material before and after solvent extraction implies that the modes of crystallization of linear polyethylene and crosslinked polyethylene are similar. Thus Flory's view is strongly favoured.

The restriction of gross movement of chains by crosslinks is consistent with a decrease in the stem length as the crosslink density increases. At all concentrations of dicumyl peroxide the most probable stem length is much less than the average separation of crosslinks. Thus there is no intrinsic reason why crystallization cannot take place in accordance with Flory's view.

4.4 ELECTRON MICROSCOPY OF CROSSLINKED POLYETHYLENE

Using electron microscopy it is possible to observe lamellae in melt crystallized polyethylene - see for example References (53,54). Ordinarily a replica of an etched surface is observed using a transmission electron microscope.

From the results of differential scanning calorimetry and low frequency Raman spectroscopy we know that the morphology of the crosslinked specimens is similar to that of the base resin which is known to be lamellar. An electron microscopic study was undertaken to confirm the previous results.

4.4.1 Experimental

The instrument used in this investigation was a Cambridge Stereoscan S150, a scanning electron microscope. Resolution is theoretically 60Å which would be adequate to observe lamellae. Gratitude is expressed to Mr. E. Heath of the Materials Science Department at the University of Southampton who operated the instrument.

Specimens of the base resin and crosslinked polyethylene of various crosslink densities were studied. Pellets $\sim$2mm thick with a diameter of 10mm were prepared on a hot press at $\sim 180^{\circ}C$ under $\sim$20000 pounds per square inch pressure, these conditions being maintained for 10 minutes to ensure complete homolysis of dicumyl peroxide. This not only moulded the specimens into a convenient form, but also brought about crosslinking at the same time. The pellets were cut in

half and heated to 150°C in an oven, one half of each was quenched in liquid nitrogen and the other was allowed to cool to room temperature at $\sim$1°C min^{-1}. The upper surface was removed to a depth of $\sim$0.25mm using a microtome armed with a freshly prepared fractured glass knife. The specimens were etched in a 7% weight to volume solution of potassium permanganate in concentrated sulphuric acid according to the method of Olley et al (53). Etching selectively destroys the disordered regions rather than the crystalline regions to leave crystallites standing proud. Specimens were mounted in the conventional manner on "buttons" and were finally coated with a thin layer of gold in a vacuum chamber.

Obtaining low resolution scanning electron micrographs of crosslinked polyethylene and the base resin presents no problems. However as resolution is increased the electron beam must be focussed more finely on the specimen; this leads to difficulties. The focussed beam caused substantial damage to the samples. Cracks and degradation of structure occurred as the sample was moved through the beam. This meant that interesting structures literally disintegrated before one's very eyes. Resolution was reduced from a theoretical 60Å to $\sim$300Å; this was galling to say the least.

4.4.2 Results of Scanning Electron Microscopy

Specimens investigated were the base resin - Rigidex 006-60 - and 3 samples of crosslinked polyethylene, crosslinked with approximately 1, 7 and 10% dicumyl peroxide.

Generally specimens displayed a dominant large scale morphology with various inhomogeneities scattered at random. A spherulitic structure was found to be the dominant morphology for all quenched specimens, and for the slow cooled base resin and most lightly crosslinked specimens. The range of sizes of spherulites varied little between different specimens, being $\sim$10-20μm in diameter, see Figure 34.

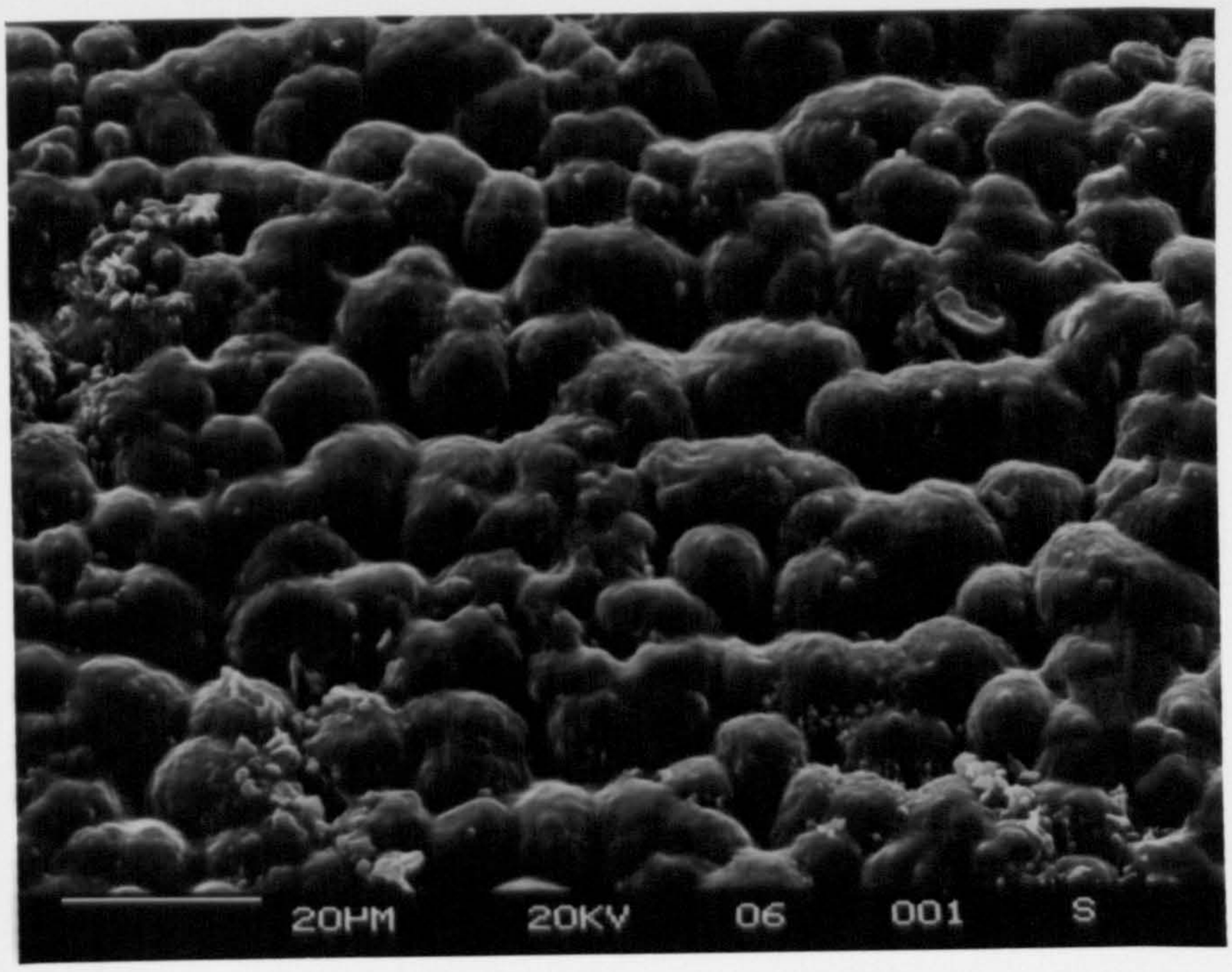

Figure 34 Typical scanning electron micrograph of spherulites in crosslinked polyethylene.

The two most heavily crosslinked specimens on slow cooling showed irregular structures, examples of which are depicted in Figure 35. No explanation is offered for these structures except to say that they appear to be evidence of some kind of large scale order. No reports of similar structures have been found in the available literature.

Due to the difficulties inherent in high resolution work it was not possible to ascertain with certainty the presence or otherwise of lamellae. There appeared to be some form of small scale stratification but the quality of the photographs is such that few would be convinced of the presence of lamellae.

Due to these difficulties attention was turned to alternative methods of examining crosslinked polyethylene.

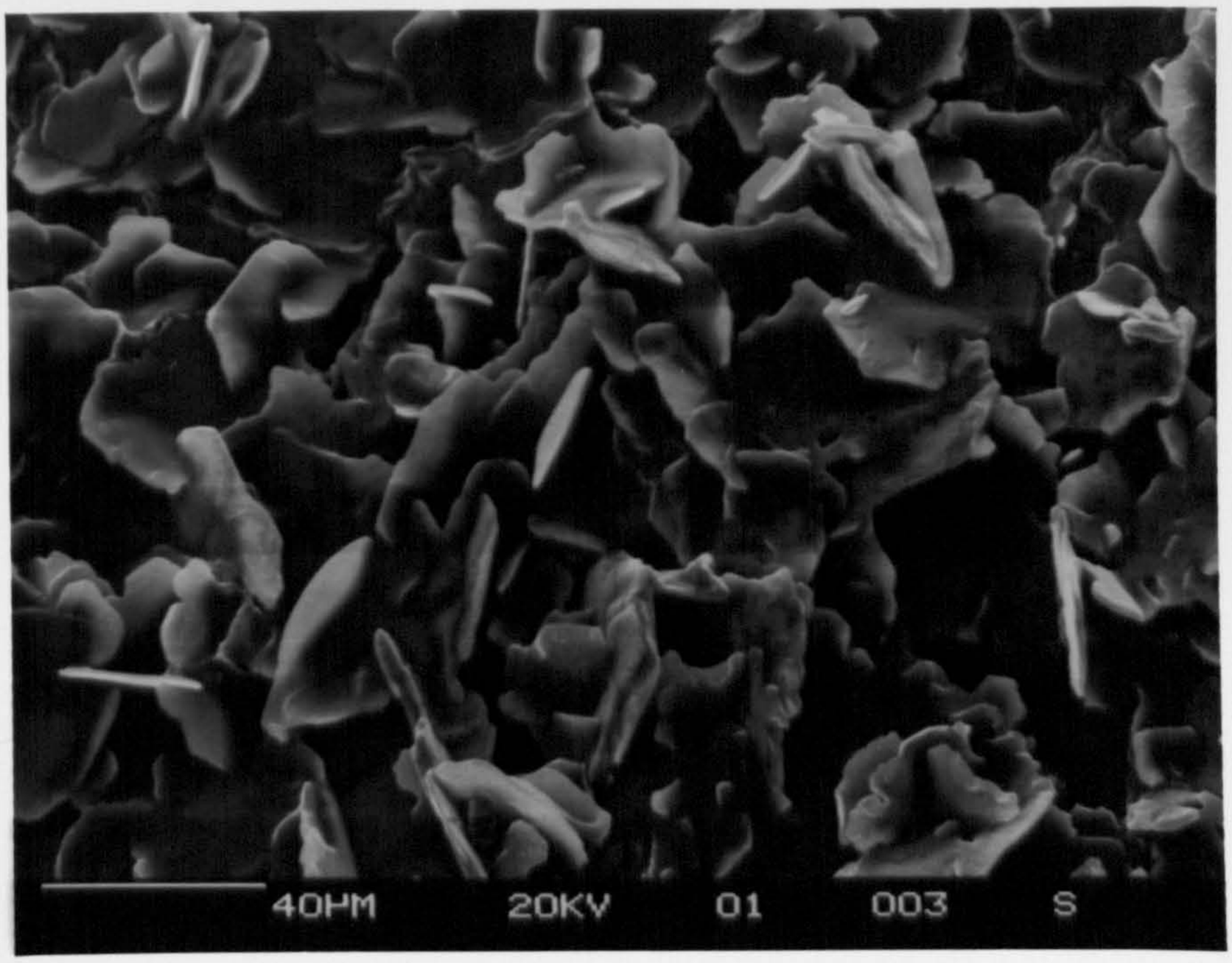

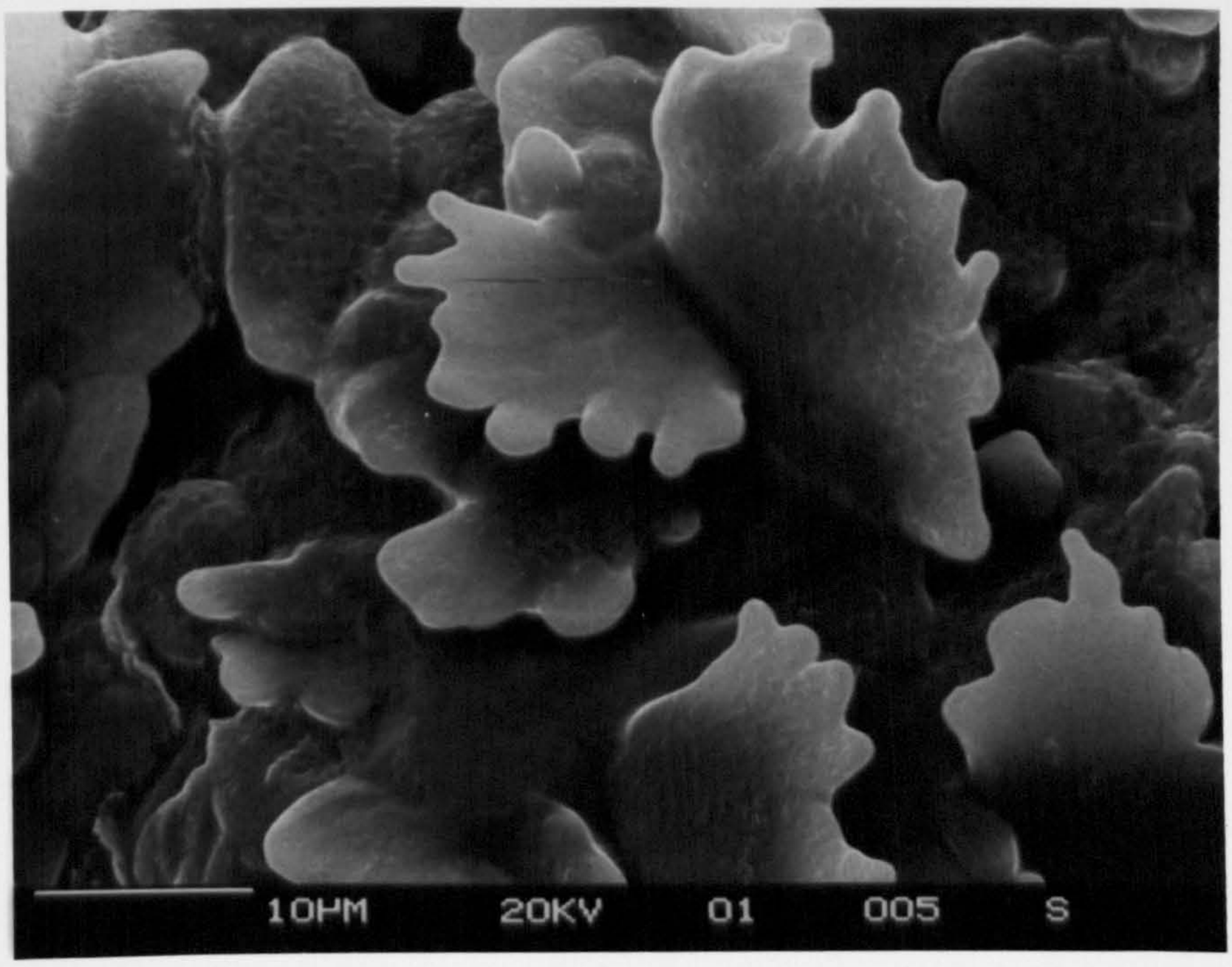

Figure 35 Examples of unexplained irregular structures in slow cooled crosslinked polyethylene.

4.5 SMALL ANGLE LIGHT SCATTERING

4.5.1 Theory and Technique

The average size of spherulites in a semi-crystalline polymer may be determined from the scattering pattern produced when a collimated beam of monochromatic polarized light strikes an unoriented thin film (55). The experimental arrangement is illustrated in Figure 36.

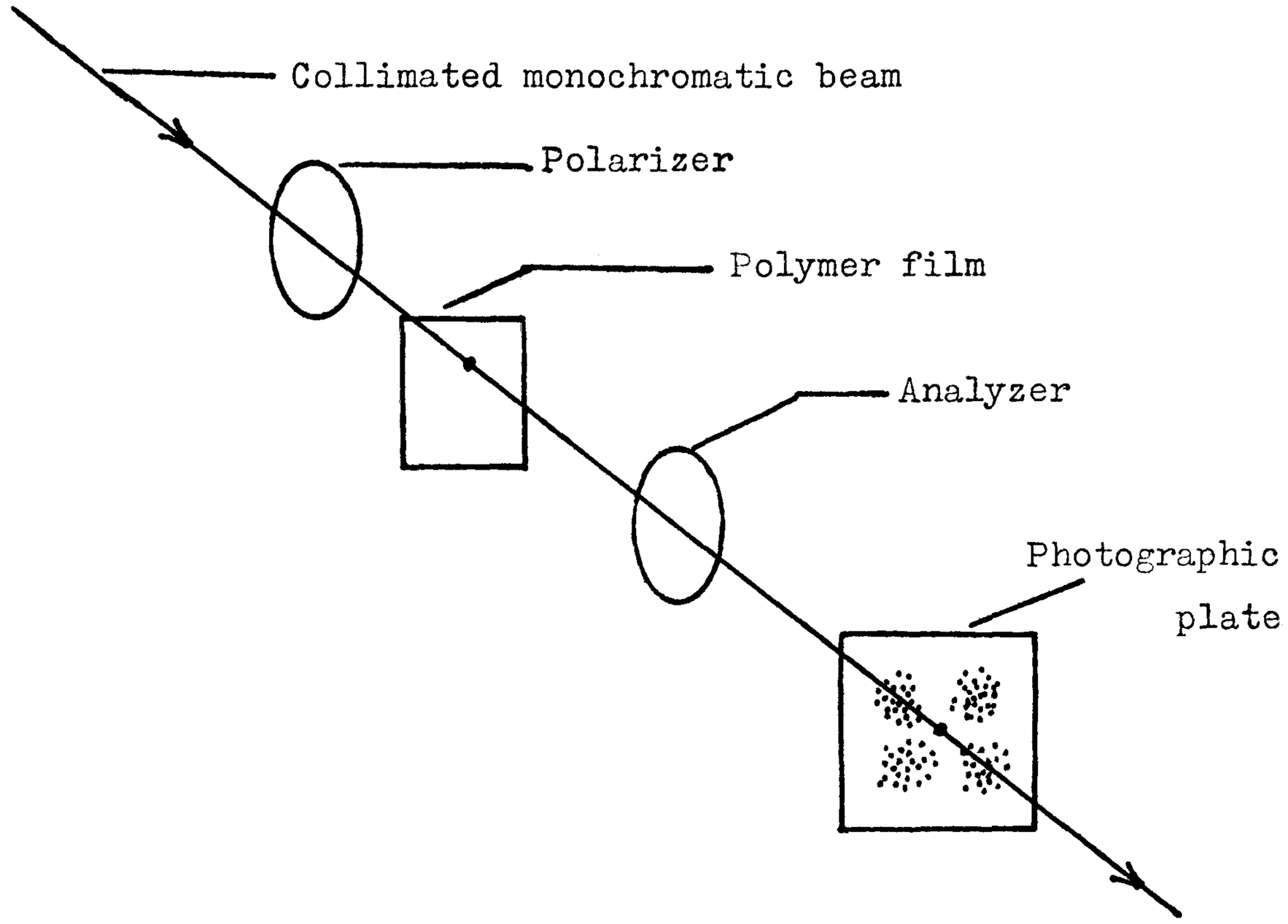

Figure 36 Arrangement for recording small angle light scattering

When a photon strikes an electron in a spherulite a dipole is induced. The observed scatter for an unoriented film when the polarizer and analyser are both vertical corresponds to the tangential component of polarization giving rise to scatter as shown in Figure 37.

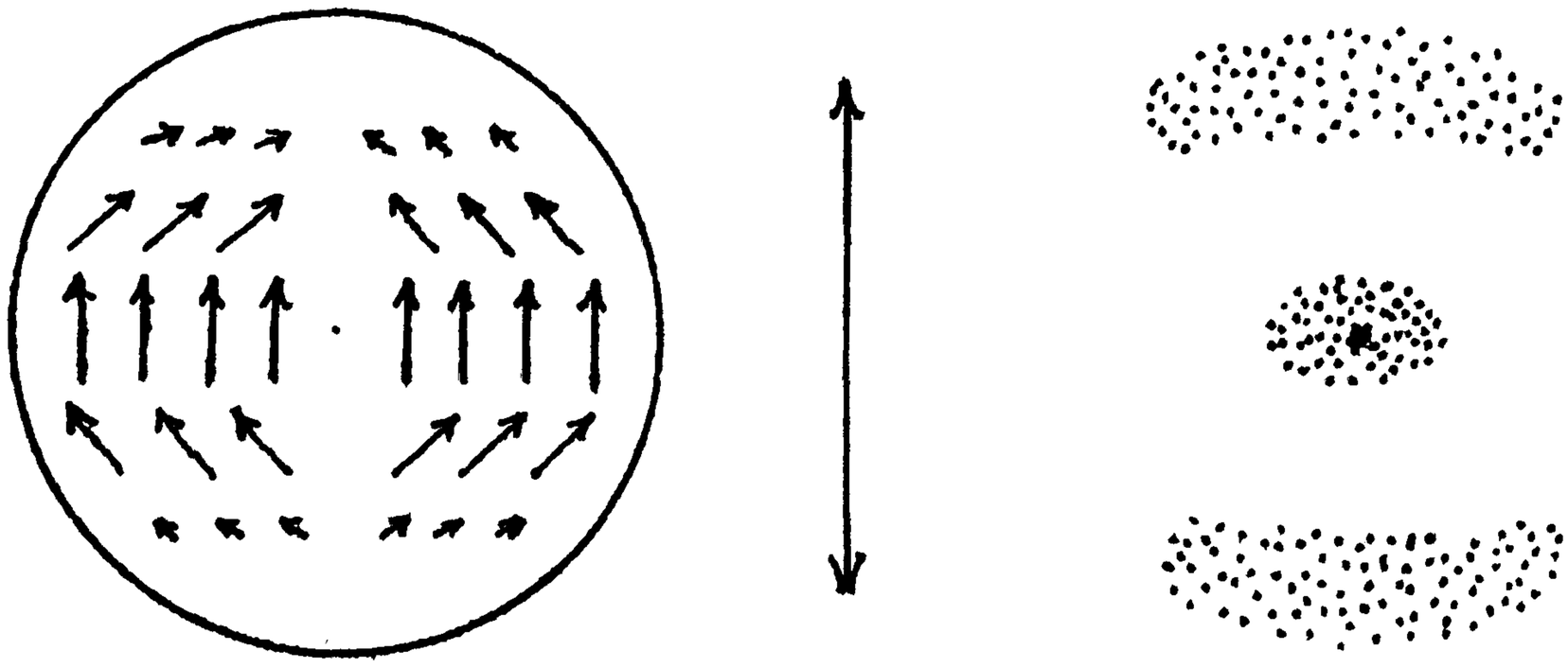

Figure 37 Light scattering arising from tangential polarization in spherulites.

As may be seen from the diagram the induced dipoles have a horizontal vector as well as a vertical one, except at the equator of the spherulite. If the analyser is now turned through 90^{o} into the horizontal position the scatter from the equator is nullified and reduced to a lesser extent towards the poles. The result is the pattern illustrated in Figure 38. This pattern is clear evidence of spherulitic morphology.

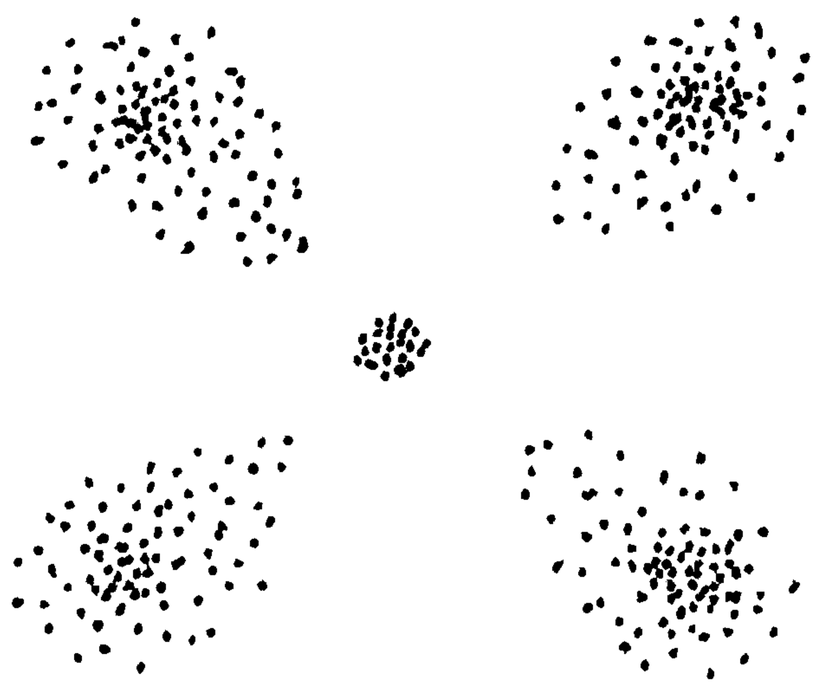

Figure 38 Light scattering pattern produced by spherulites with crossed polarizers.

The amplitude of the scattered beam in any direction is a function of the distance of the scattering electrons from the spherulitic centre, the direction of the scatter and the wavelength of the incident light in the polymer. The integrated scatter can be calculated (55), and the resulting formula used to evaluate the average spherulitic size from the azimuthal angle of the maximum scattering intensity.

$$R = \frac{\lambda}{\pi \sin \vartheta/2}$$

where: R = Average radius of spherulites

λ = Wavelength of light in polymer

ϑ = Azimuthal angle of maximum scatter

In melt crystallized linear polyethylene the spherulites are made up from lamellae arranged in such a way that they extend away from the nucleus like ribbons as illustrated in Figure 39.

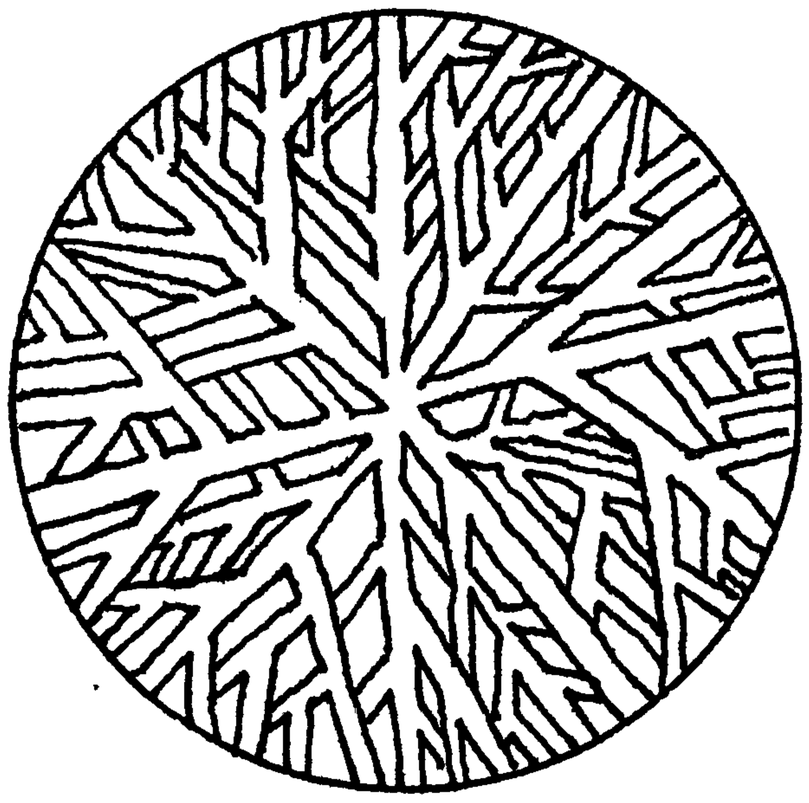

Figure 39 Arrangement of lamellae in a polyethylene spherulite.

The existence of spherulites in crosslinked polyethylene would indicate a lamellar morphology.

Apart from information on spherulites, small angle light scattering can also yield information on molecular orientation in anisotropic samples.

4.5.2 Results of Small Angle Light Scattering

Investigation of the small angle light scattering of crosslinked polyethylene was carried out using equipment in the laboratories of Pirelli General Cable Works PLC at Eastleigh in Hampshire. Gratitude is expressed to the company for extending this facility.

The incident light beam was provided by a helium/neon laser operating at a wavelength of 632.8nm at a power of $\sim$1mW. Scattering patterns were recorded on negative Polaroid film. Films of crosslinked polyethylene were prepared on a hot press as described in Section 2.3. Films were cooled to room temperature in air, taking $\sim$1 minute to cool from $\sim$180°C to 50°C.

A number of specimens of crosslinked polyethylene were studied. These varied from a lightly crosslinked sample with an average separation of crosslinks of $\sim$100000 molecular weight units to a heavily crosslinked sample with an average separation of crosslinks of $\sim$3000 molecular weight units.

All samples gave a similar pattern, a typical example of which is shown in Figure 40. The typical light scattering pattern for a specimen of melt crystallized linear polyethylene is shown in Figure 41 (this scattering pattern was recorded on 35mm negative film).

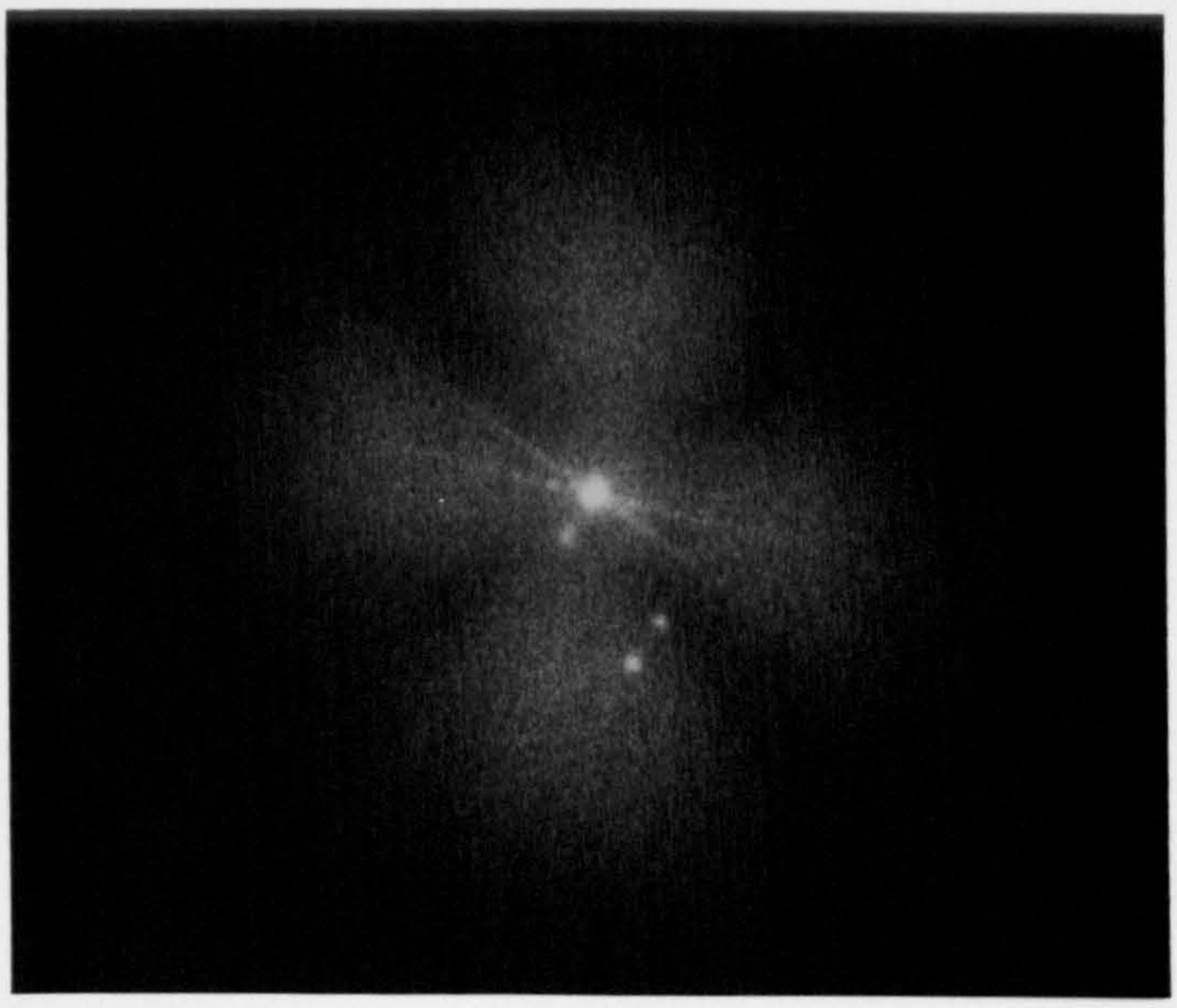

Figure 40 Typical small angle light scattering pattern from crosslinked polyethylene

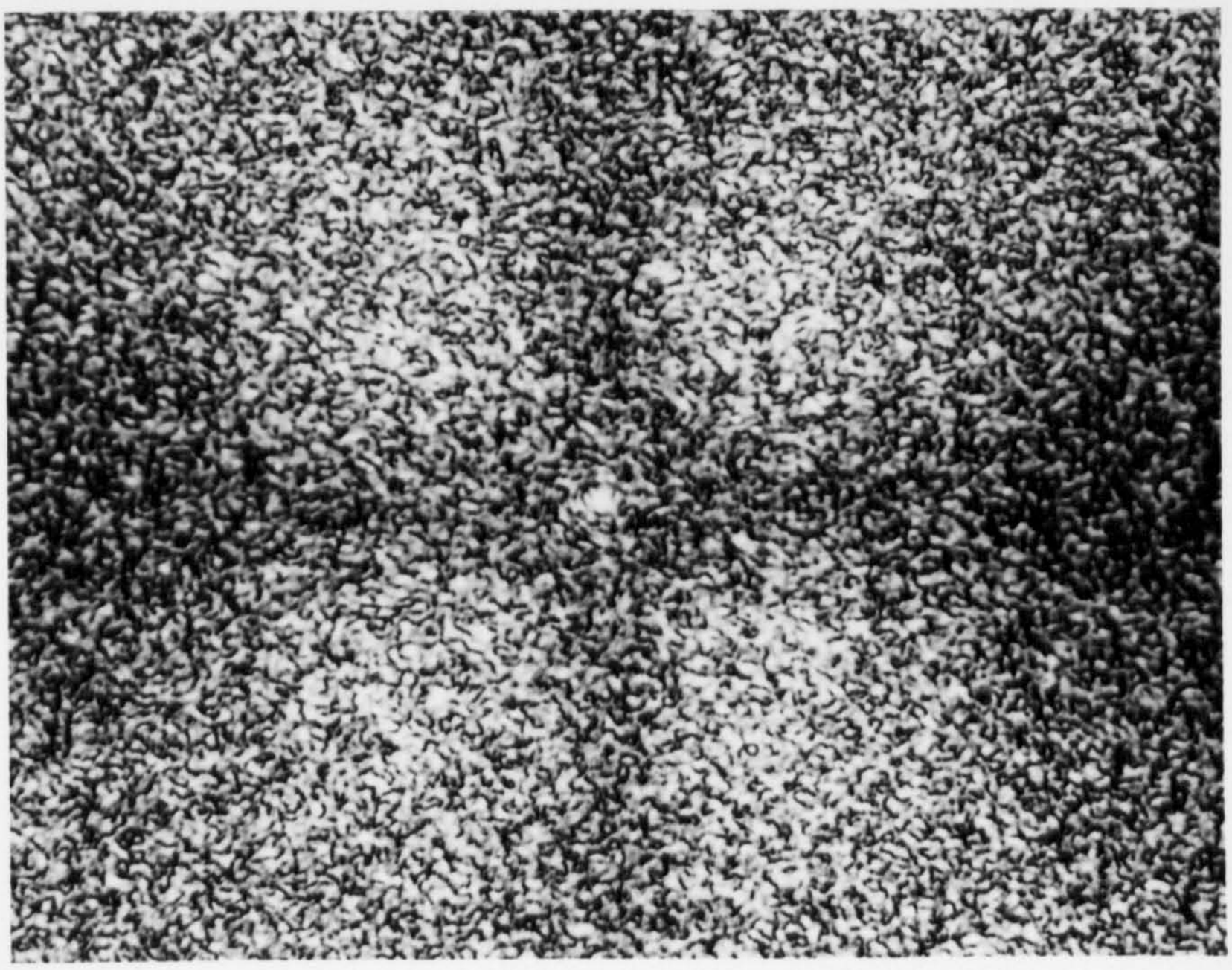

Figure 41. Typical small angle light scattering pattern from linear polyethylene.

There are no definable nodes in the small angle light scattering pattern of crosslinked polyethylene as there are for linear polyethylene, but all specimens gave the distinctive 'X' configuration. The explanation for this is that spherulites are present in a broad range of sizes, including many of such a size that the scattering angle is $<1^{o}$. Such small scatterings make distinguishing scatter originating from spherulites, from the effect of dispersion of the laser beam difficult. However it is possible to state with certainty that specimens of crosslinked polyethylene contain spherulites. The inference of this is that crosslinked polyethylene has a lamellar morphology.

4.6 SOLID STATE NUCLEAR MAGNETIC RESONANCE SPECTROSCOPY OF CROSSLINKED POLYETHYLENE

Fourier transform pulsed nuclear magnetic resonance spectroscopy on solid samples of polyethylene was carried out in the School of Chemical Sciences at the University of East Anglia, to whom gratitude is expressed. Four samples were

investigated, the base resin, and three samples of crosslinked polyethylene with average separation of crosslinks of ∼21000, ∼2000 and ∼1400 molecular weight units. The results of relaxation measurements are shown in Table 14.

Dicumyl peroxide (%)	Average separation of crosslinks (molecular weight)	T1 (Seconds) *	T1ρ (ms) †	Population (%)	Degree of crystallinity (%)(1)
Base resin		0.537	77.5 8.78 2.62	48.8 27.6 23.6	75
1.24	∼21000	0.357	56.4 8.93 2.49	25.0 30.4 44.6	56
6.89	∼2000	0.405	47.1 7.51 2.50	21.1 38.1 40.8	44
9.84	∼1400	0.232	29.2 4.33 1.30	6.2 63.1 30.8	35

(1) As calculated from differential scanning calorimetry

Table 14 Results of solid state ^{1}H nuclear magnetic resonance.

Each sample shows three distinct relaxation times, indicative of a three phase morphology (56). The longer the relaxation time, the more ordered is the phase in any given sample. This is considered to be consistent with Flory's view of crystallization; apart from the crystalline and disordered phases there is a partially ordered transition phase between the other two at lamellar surfaces. See Figure 42.

* Relaxation time of ^{1}H in the laboratory frame of the experiment.

† Relaxation time of ^{1}H in the rotating frame of the experiment.

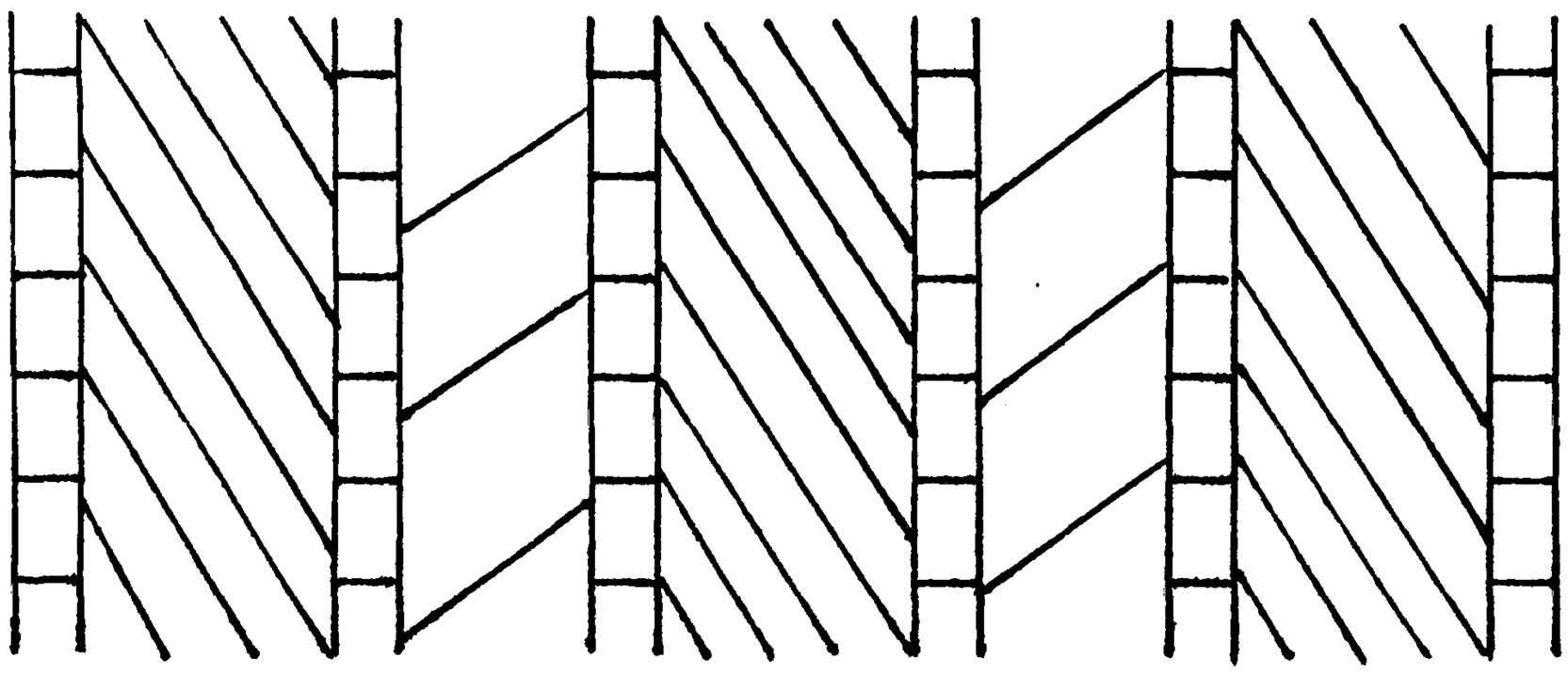

Figure 42 Three zone structure of semi-crystalline polyethylene (56).

The population fractions show an increase in the partially ordered zone as crosslink density increases, and a decrease in the proportion of crystalline material. The population in the disordered region at first increases with increasing crosslink density then decreases. These observations may be explained in terms of decreasing chain mobility with increasing crosslink density. Initially, with a low crosslink density crystallization is hindered to some extent due to restrictions of movement imposed on long sections of the chain, however small scale movement and vibration in the disordered region is still allowed to a great extent. As the crosslink density increases, crystallization is further hindered reducing the degree of crystallinity and lamellar thickness. The intermediate zone increases in size as chains try to take up a crystalline structure, but are prevented from doing so completely by crosslinks disrupting the lattice, and restrictions in conformation caused by crosslinks. Finally, at high crosslink density very few chains have sufficient freedom of conformation

to adopt a perfectly crystalline configuration. A high proportion of units in the chain are influenced by close proximity to crosslinks resulting in greatly restricted movements, giving rise to an increased figure for the population in the intermediate zone. The effect of proximity to crosslinks may be likened to the effect on a chain as it leaves the crystalline zone; a crosslink restricts the movement of the chain elements near it as does attachment to a crystalline lattice.

The discrepancy between the value of degree of crystallinity evaluated by differential scanning calorimetry and the population of the crystalline lattice indicated by nuclear magnetic resonance spectroscopy increases with increased crosslink density. As detailed in Section 4.2, differential scanning calorimetry measures the amount of energy required to raise the temperature of the sample, thus a crystalline region requires more energy than a partially ordered region which in turn requires more than a disordered region. The model of morphology used for calculating crystallinity is two phase. This is necessitated because the differential scanning calorimetry endotherm does not distinguish between energy input to disorder a crystalline lattice from that used to disorder a partially ordered region. In reality the endotherm is made up of contributions from the disordering of the crystalline and intermediate phases, thus giving an anomalously high value to the degree of crystallinity.

4.7 SUMMARY OF RESULTS OF INVESTIGATION INTO THE MORPHOLOGY OF CROSSLINKED POLYETHYLENE AND IMPLICATIONS WITH REGARD TO THE MORPHOLOGY OF MELT CRYSTALLISED LINEAR POLYETHYLENE

Differential scanning calorimetry shows that crosslinked polyethylene is semi-crystalline in nature and that its morphology does not differ greatly from that of linear polyethylene. Similarity between the plots of melting point and degree of crystallinity versus % dicumyl peroxide for specimens before and after solvent extraction provide evidence that the manner of crystallisation of crosslinked polyethylene is similar to that of linear polyethylene.

Low frequency Raman spectroscopy shows that no radical changes occur in the morphology of linear polyethylene on crosslinking, or as the degree of crosslinking increases. The similarity of the plots of most probable stem length versus % dicumyl peroxide for solvent extracted and unextracted specimens indicates that the process of crystallization of linear polyethylene is similar to that of crosslinked polyethylene.

Scanning electron microscopy of etched samples indicates the presence of spherulites in crosslinked polyethylene. This is indicative of a lamellar morphology.

Small angle light scattering experiments confirms the existence of spherulites in crosslinked polyethylene, adding weight to evidence in favour of lamellae being present.

Nuclear magnetic resonance spectroscopy shows clear evidence of three phase morphology in linear and crosslinked polyethylene. This is consistent with an intermediate partially ordered zone lying between the crystalline lamellae and the amorphous regions.

The implication of this evidence is clear. Crosslinked polyethylene chains cannot undergo reptation during crystallization. Linear polyethylene crystallizes by the same process as crosslinked polyethylene. Therefore linear polyethylene chains do not undergo reptation during crystallization. Chain folding in melt crystallized linear polyethylene is thus untenable.

All observations may be explained with reference to Flory's model of melt crystallization.

Chapter 5

SPECTROSCOPY OF HOT STRETCHED CROSSLINKED POLYETHYLENE

5.1 INTRODUCTION

Part of the continuing research work of the Polymer Properties Group at the University of Southampton concerns the morphology of flowing polymer melts. As a contribution to this effort it was decided to attempt to model flowing polymer using hot stretched crosslinked polyethylene. Above its crystalline melting point crosslinked polyethylene behaves as a rubber. Stretching this rubber effectively induces shear into the material, analogous, in certain respects, to that experienced by flowing polyethylene. This effect was investigated using the techniques of Raman and infra-red spectroscopy.

5.2 RAMAN SPECTROSCOPY OF CROSSLINKED POLYETHYLENE

5.2.1 Experimental Methods for Recording Raman Spectra of Hot Stretched Crosslinked Polyethylene

The requirements for conducting this experiment are straightforward; a film of crosslinked polyethylene must be heated to a constant temperature above the melting point of polyethylene and then stretched, whereupon a Raman spectrum is recorded. Reality - as is often the case - was not as simple as this.

A heated chamber was designed to fulfil the experimental requirements. With only minor refinements it performed well. This chamber is illustrated in Figure 43 in place on the Anaspec LR-36 Raman spectrometer.

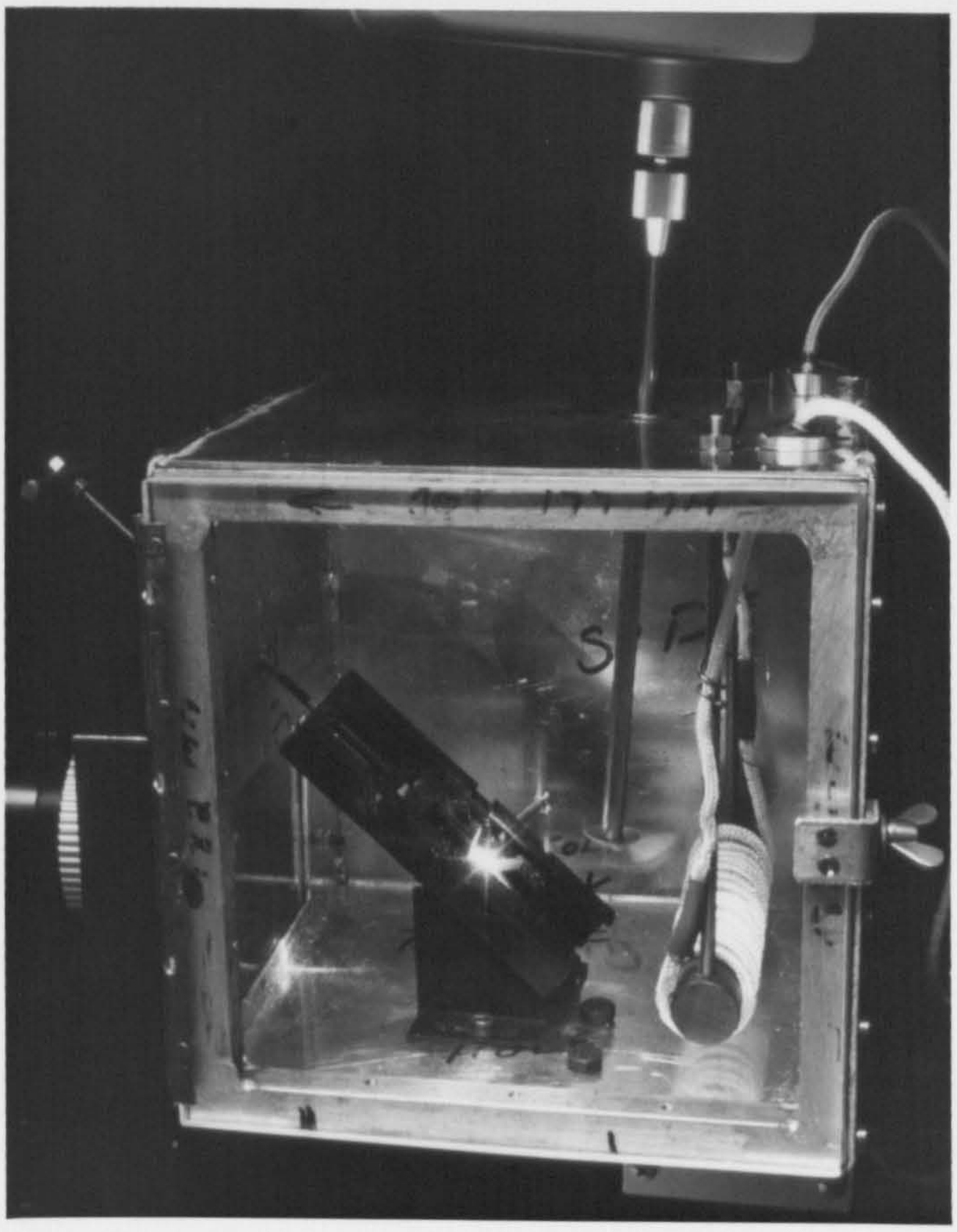

Figure 43 Heated chamber for Raman study of stretched crosslinked polyethylene.

The exciting laser radiation enters the chamber through a window in its base and strikes the sample at an angle of $\sim 45^{\circ}$. The inelastic Raman scatter is collected by the instrument through the glass window shown on the left of the illustration. The chamber is heated by a flexible heating cord wrapped round a steel bar. A high speed stirrer motor fitted with a propeller blade circulates the air. The temperature was controlled by a proportionating temperature controller regulating the current to the heater. The temperature of the specimen itself was measured with a chromel/alumel thermocouple (not shown), standardised with a cold junction in an ice/water mixture. The temperature of the specimen was maintained to $\pm$ 1 $^{\circ}$C. Strain was applied to the specimen by means of a clamping device with

a moveable jaw; illustrated in Figure 44. Approximate strain was measured by counting the revolutions of the threaded rod.

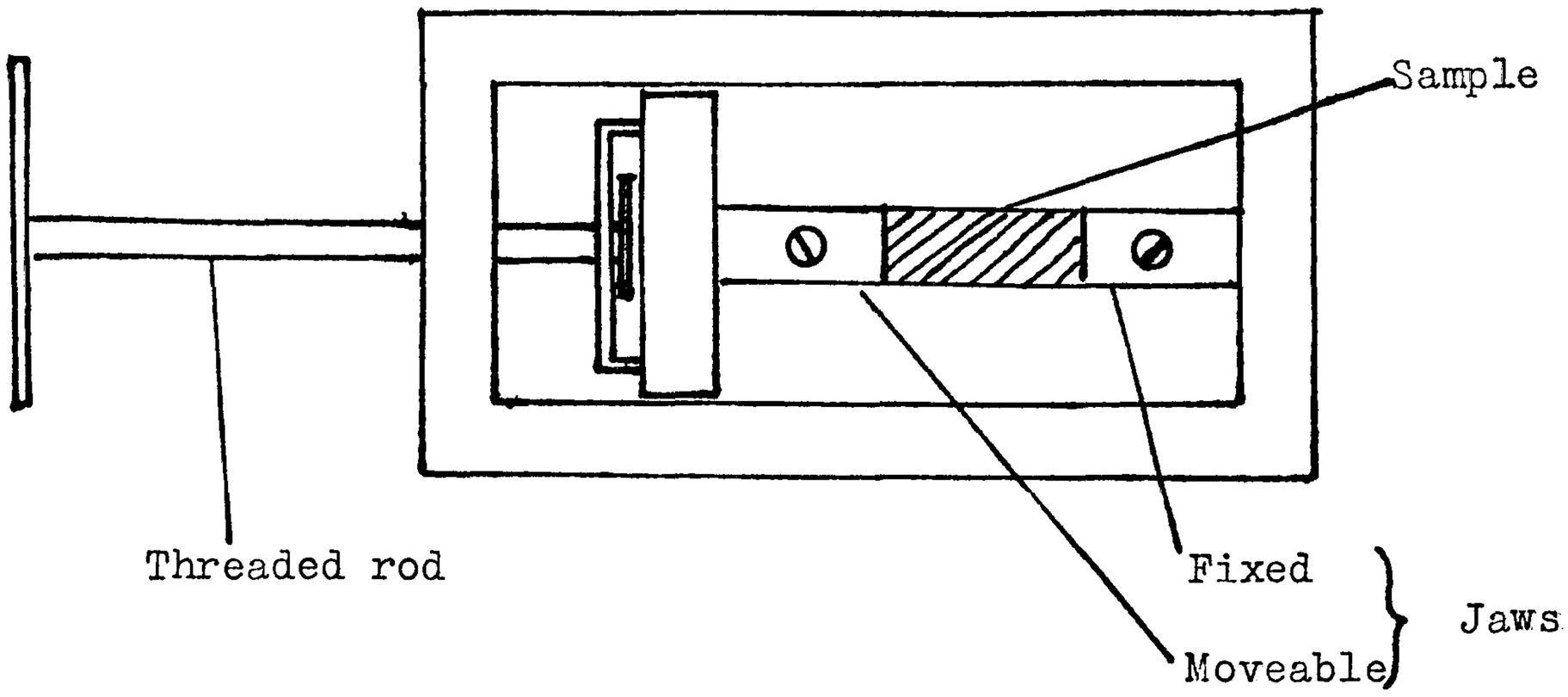

Figure 44 Stretching apparatus.

Alignment of the sample in the spectrometer at the common focus of the collection and incident lenses was effected by moving the whole chamber using the 3-dimensional controllers of the instrument.

The chamber was so designed that it could be mounted in either the Anaspec LR-36 or the Coderg T800. Spectra recorded on the Anaspec instrument were of very poor quality. All the work reported below was carried out on the Coderg T800, despite the relatively slow scan rate required. Typically the scan rate was 50cm^{-1} min^{-1}.

Specimens of crosslinked polyethylene were prone to fluorescence in the laser beam which could overwhelm the Raman signal. This problem could only be overcome by "burning out" the fluorescence in the sample by leaving it aligned in the laser beam for half an hour or more until it had decayed to a tolerable level. Samples of crosslinked polyethylene tended to deteriorate while being held at elevated temperatures for sufficiently long times, to "burn out" the fluorescence in the unstretched material, record a reference spectrum under these conditions, stretch the specimen, and "burn out" again, prior to recording a spectrum of the hot stretched sample. The normal evidence of deterioration was a sudden loss of

Raman signal as the specimen snapped. This difficulty made the recording of a series of spectra on the same sample impossible. Invariably a specimen would snap if an attempt was made to stretch it further after a spectrum had been recorded. By this time the specimen would have been held at a temperature of $\sim 140^{\circ}C$ in excess of one and a half hours.

Due to the limited timescale imposed on the recording of spectra only a limited range of the spectrum could be studied. The region of 1000-1500cm^{-1} is that most commonly studied with regard to conformational effects on polyethylene as it contains a wealth of information (57).

5.2.2 Results of Raman Spectroscopy of Crosslinked Polyethylene

The material used in this investigation was lightly crosslinked Rigidex 006-60 containing approximately 1 crosslink per 7000 methylene groups. Specimens were $\sim 0.25mm$ thick and had not been solvent extracted.

The signal to noise ratio of the spectra was not as good as would have been desired, being typically of the order of 4-10:1. A thicker specimen would have improved the signal to noise ratio; however thicker specimens have a larger number of defects in a given length, which promotes premature failure of the sample under extension.

Spectra were recorded with the sample relaxed at room temperature, relaxed at $\sim 140^{\circ}C$, and stretched to twice its original length at $\sim 140^{\circ}C$. Examples of these spectra are shown in Figures 45, 46 and 47 respectively. Approximate positions of bandheads and an estimate of intensity for these and other spectra are given in Table 15.

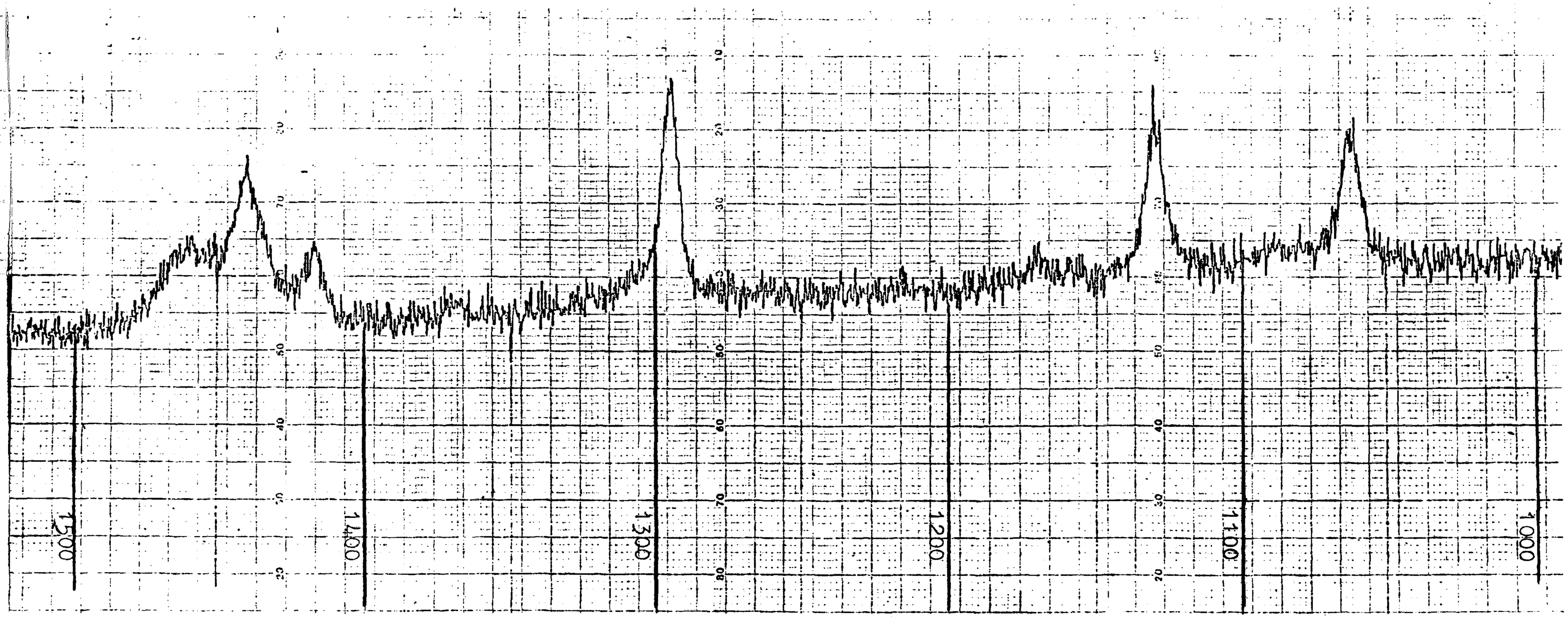

Figure 45 Raman spectrum of relaxed crosslinked polyethylene at room temperature

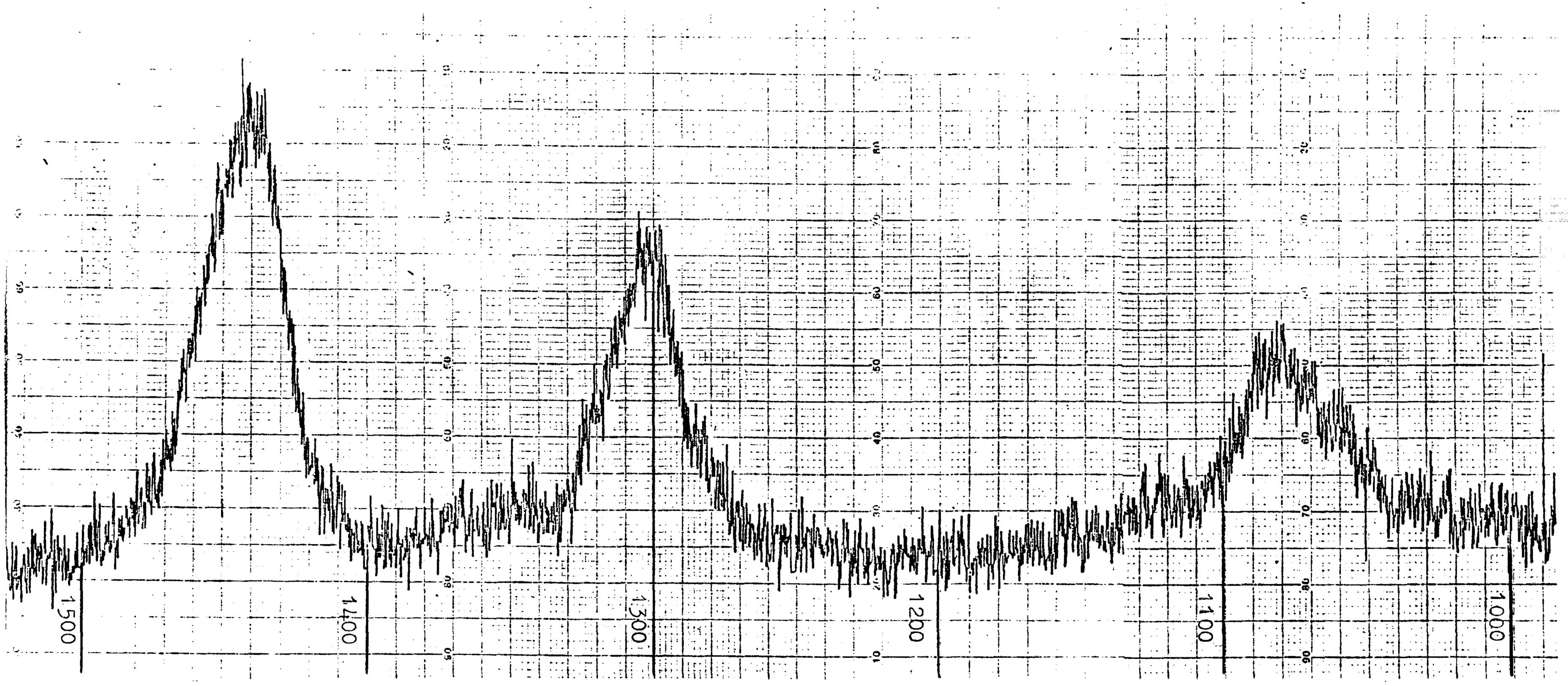

Figure 46 Raman spectrum of relaxed crosslinked polyethylene at $\sim 140^{\circ}C$

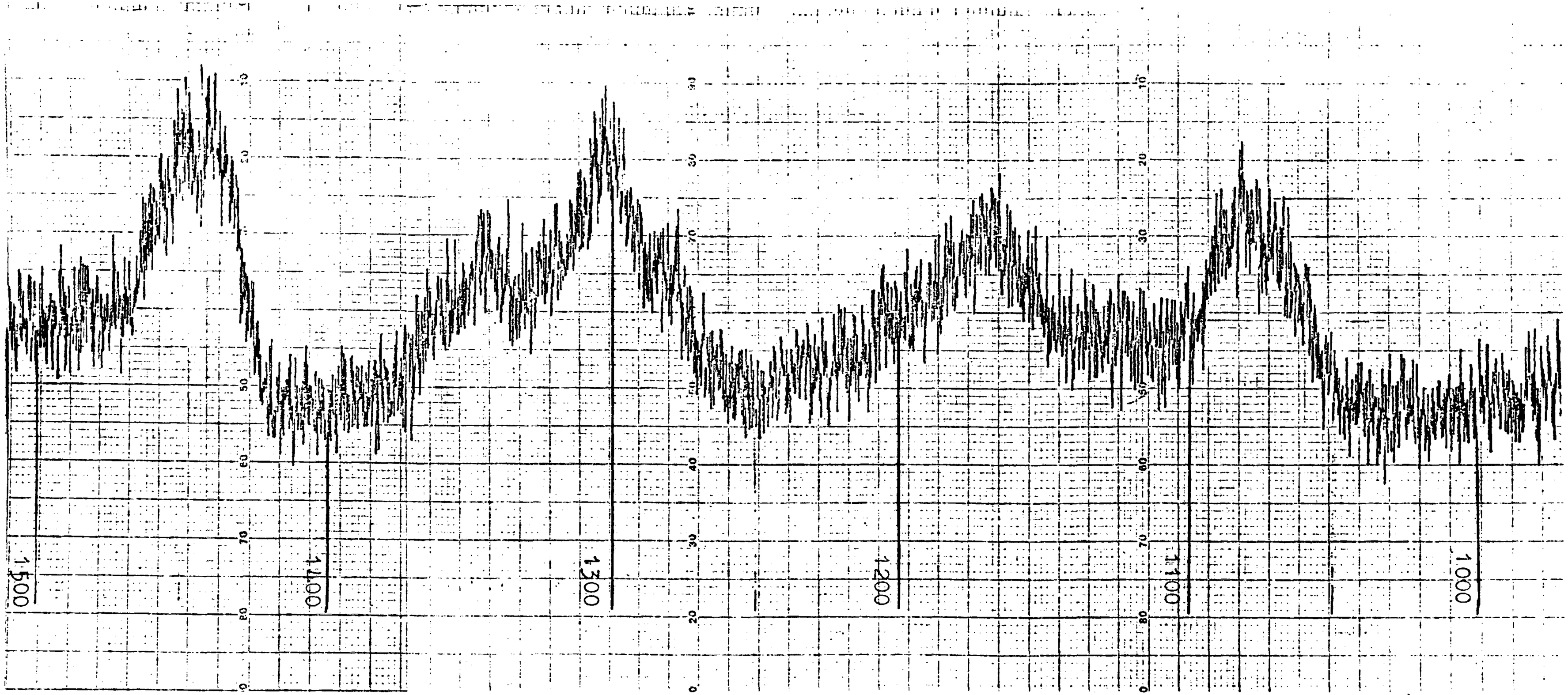

Figure 47 Raman spectrum of crosslinked polyethylene at ~140°C stretched ~2:1

Sample	Condition	Peak positions and approximate intensity with respect to methylene twist at 1300cm^{-1}					
1	Room temperature relaxed	1400-1500 Triplet (2.5)	1360 (0.1)	1296 (1.0)	1169 (0.2)	1129 (0.6)	1060 (0.6)
1	140°C Relaxed	1443 (1.3)	1361 (0.1)	1306 (1.0)			1088 (1.0)
1	140°C Stretched 2:1	1442 (1.1)	1373 (0.2)	1307 (1.0)	1163 (0.6)	1123 (0.2)	1082 (1.1)
2	Room temperature relaxed	1400-1500 (2.5)	1360 (0.1)	1294 (1.0)	1171 (0.1)	1124 (0.6)	1059 (0.6)
2	140°C Relaxed	1438 (1.4)	1365 (0.1)	1299 (1.0)			1081 (1.0)
2	140°C Stretched 2:1	1441 (1.0)	1345 (0.2)	1302 (1.0)	1163 (0.8)	1121 (0.2)	1072 (0.8)

Table 15 Results of Raman spectroscopy on crosslinked polyethylene.

5.2.3 Discussion of Raman Spectroscopy of Crosslinked Polyethylene

The bands in the range 1000-1500cm^{-1} in the Raman spectrum of polyethylene may be divided into three groups: 1000-1150cm^{-1}, due to the skeletal optical modes of vibration, 1150-1400cm^{-1}, due to vibrations of the methylene unit, and 1400-1500cm^{-1}, accounted for by C-H bending modes.

5.2.3.1 Changes in the Raman Spectrum of Crosslinked Polyethylene on Heating to 140°C.

In solid crosslinked polyethylene the bands at ~1125 and 1060cm^{-1} are due to the C-C stretch in the trans configuration in phase and out of phase respectively within the unit cell (58, 59). As the crystallinity breaks down the intensity of these bands decreases to zero and a broad band situated around 1080cm^{-1} replaces them. The new band is due to C-C vibrations of the gauche configurations. The ratio of the intensity of the bands at 1125 and 1060cm^{-1} to that of the band at 1080cm^{-1} yields a measure of the proportion of gauche bonds (60), as shown in Figure 48.

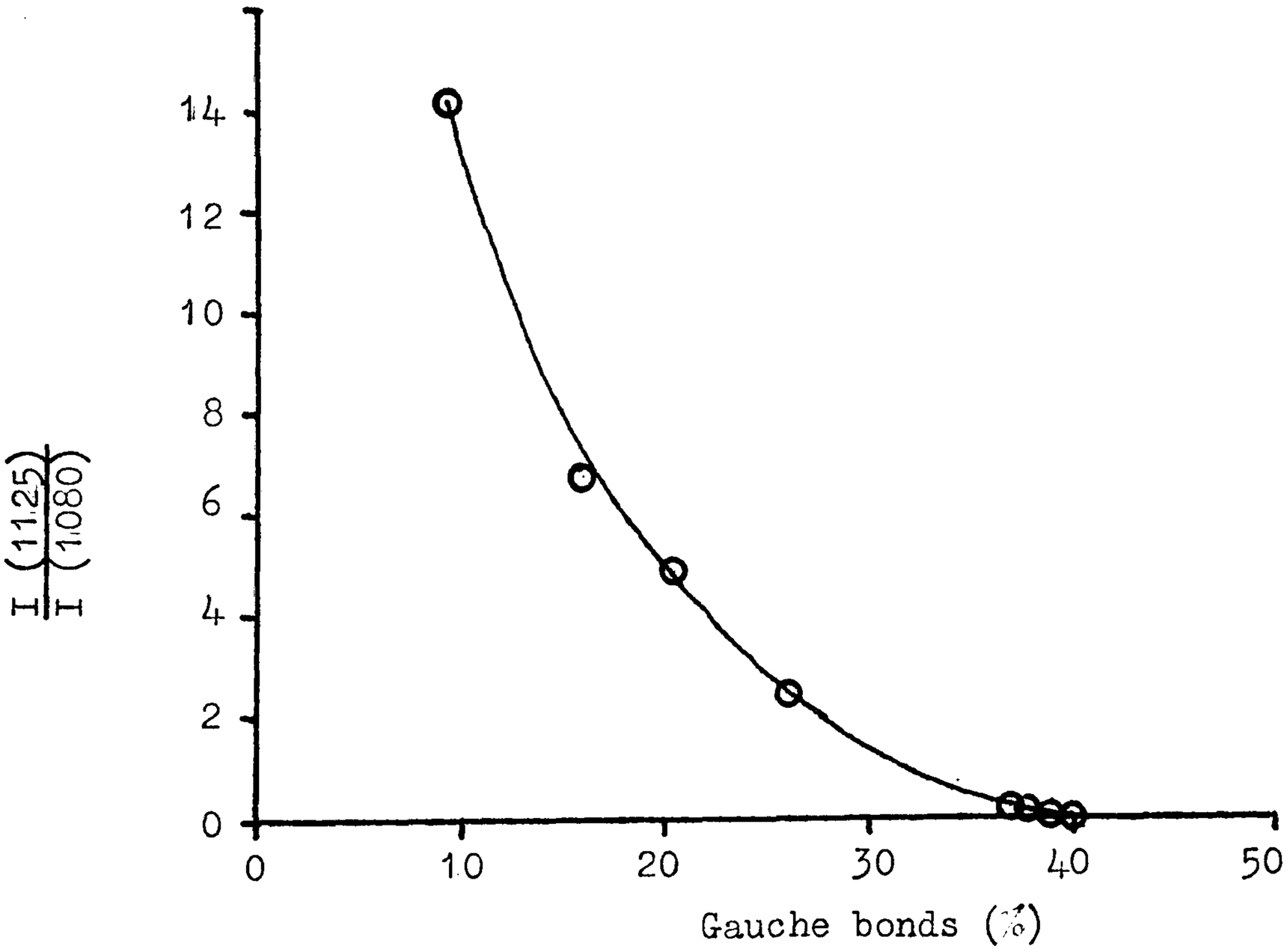

Figure 48 Ratio of intensities of bands at 1125 and 1080cm^{-1} versus % gauche bonds (after Wunder (60)).

The band that appears at 1170cm^{-1} is due to the fundamental rock of methylene groups (61), and increases as the number of all trans sequences increases (58). Thus it disappears on melting.

The methylene twisting band at 1295cm^{-1} present at room temperature broadens on melting and moves to a position of ~1305cm^{-1}. This band's position at 1296cm^{-1} is due to the crystalline morphology. The broad band at 1305cm^{-1} (which is also present to a small degree at room temperature) is characteristic of the gauche-trans-gauche configurations (60,62). The integrated intensity of the methylene twisting bands remains constant throughout (61), and it is against this band that others are compared in Table 15.

The small band at ~1370cm^{-1} is due to the fundamental wag of the methylene group (63,64). On melting it retains approximately the same position and intensity. Snyder (63) suggests that the intensity of this band increases as the number of extended chains increases. The fact that it does not appear to fall on melting crosslinked polyethylene is not surprising due to the error associated with estimating the intensity of such a small peak. Possibly the constraints imposed by crosslinks help to maintain the number of extended chains.

The triplet of bands centred around 1440cm^{-1} at room temperature is due to the C-H bending vibration. A fundamental vibration at 1442cm^{-1} is crystal field split to give vibrations at 1418 and 1449cm^{-1}. The vibration at 1449cm^{-1} reacts via Fermi resonance with the overtone of the infra-red active rocking fundamental at 720cm^{-1} to give bands at 1440 and 1462cm^{-1} (60). As crystallinity falls the crystal field splitting is destroyed and the triplet is replaced by a single broad band at ~1440cm^{-1}.

Thus far, all changes described are similar to those reported elsewhere for polyethylene going from the solid to the melt (60,61,62).

In addition to these changes it was noted that the longitudinal acoustic mode disappears on melting.

5.2.3.2 Changes in the Raman Spectrum of Crosslinked Polyethylene on Stretching at 140°C.

On stretching crosslinked polyethylene in its rubbery state the Raman spectrum changes. The manner of its change is such that there is no parallel reported elsewhere.

The single broad band found at 1080/1088cm^{-1} decreases in intensity and shifts to a lower frequency at 1072/1082cm^{-1}. A new broad band appears at 1163cm^{-1} of a similar intensity to that at 1072/1082cm^{-1}. A small band appears at ~1122cm^{-1}. The band at ~1305cm^{-1} remains constant. The band originally at ~1363cm^{-1} increases greatly in intensity and moves, in one case to ~1373cm^{-1}, and in the other to ~1345cm^{-1}. The broad band centred at ~1440cm^{-1} shows no change in position or shape, but exhibits a loss of intensity. These observations are tentatively accounted for below.

The appearance of a band at ~1122cm^{-1} indicates that the number of methylene groups in the trans configuration has increased. A corresponding band at ~1060cm^{-1} would be expected to appear, but in this case is overwhelmed by the broad, intense amorphous C-C stretching band. The effect of a band at ~1060cm^{-1} might account for the shift of the 1080/1088cm^{-1} band to a lower frequency. From Figure 48 it would appear that the proportion of gauche bonds drops about 3% from 40% to 37% on stretching.

Snyder (63) notes that the bands at 1170 and 1370cm^{-1} are of similar intensity in his oriented specimens at room temperature. This situation seems to apply in hot stretched crosslinked polyethylene. As both vibrations involve vibration of the methylene group one is tempted to postulate that there is a freeing of the environment surrounding a proportion of the methylene groups. Both vibrations have been related to the extended chain (57,58,63). A possible explanation for the increase in intensity of these bands lies in the effect of crosslinks. It seems highly probable that certain effective chains will be subject to a far greater extensional force than most others, due to the positioning of crosslinks in relation to one another. This would result in complete extension of these lengths of chain, while others remain only partially aligned. This would account for a slightly increased trans/

gauche ratio and the increase in intensity of bands associated with chain extension. The specimens under investigation had a gel content of $\sim$55%. Thus almost half of the material consists of chains with a large degree of freedom which are unlikely to be affected grossly by extension of the sample.

For a fully gelled material, extension to a fair degree might result in a liquid crystal type morphology. Still further extension might result in strain induced crystallization as found in stretched natural rubber.

5.3 INFRA-RED SPECTROSCOPY OF CROSSLINKED POLYETHYLENE

5.3.1 Experimental Method for Recording Infra-Red Spectra of Hot Stretched Crosslinked Polyethylene

The requirements of this experiment are similar to those of the equivalent Raman one. A heated chamber was designed and made, to fit into the sample area of the Nicolet MX-1 Fourier transform infra-red spectrometer. This chamber is illustrated *in situ* in Figure 49.

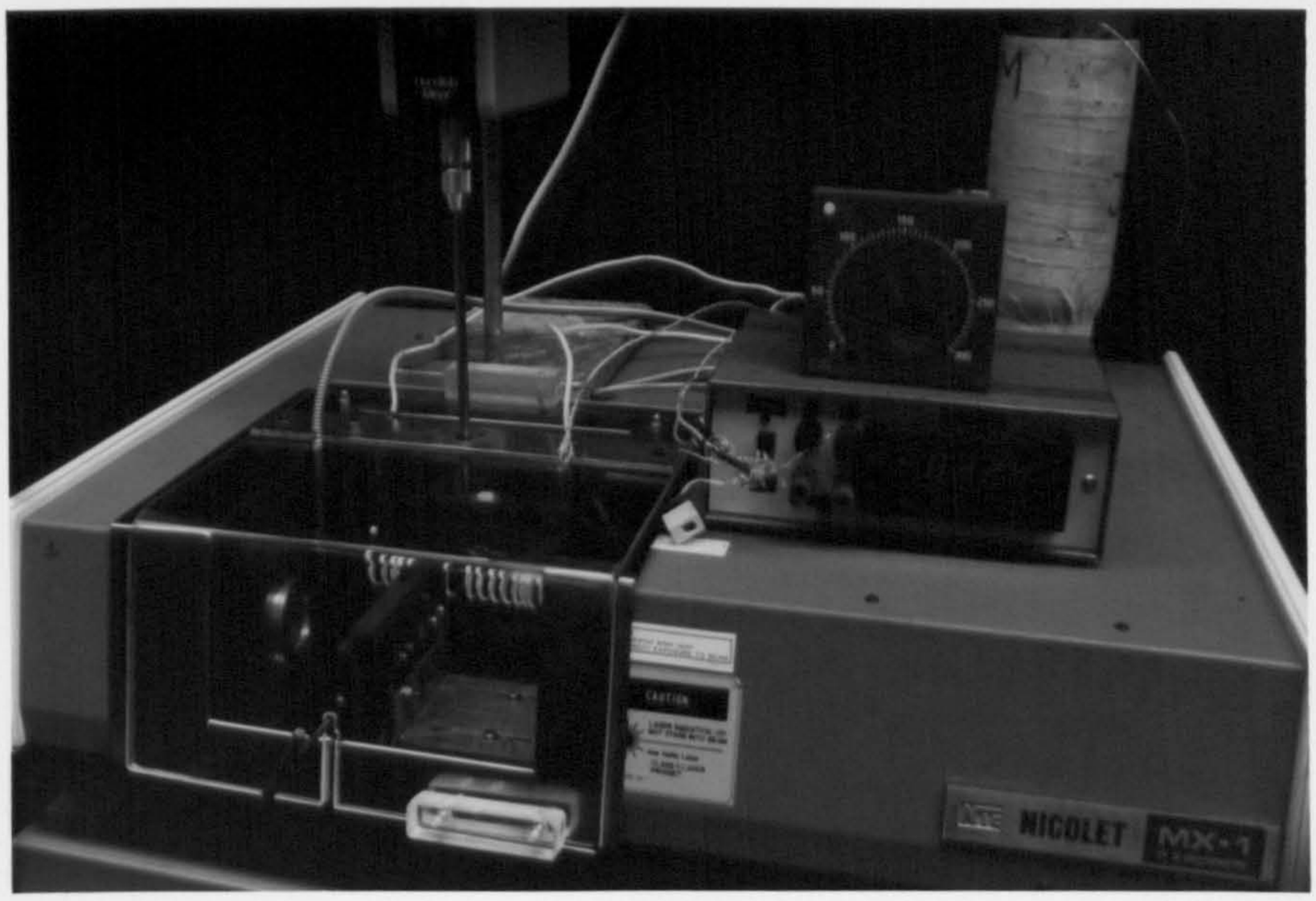

Figure 49 Heated chamber for infra-red study of stretched crosslinked polyethylene.

The windows of the chamber are made of polished sodium chloride. The stretching apparatus was similar to that used for the Raman experiment. The temperature measurement and control was the same as adopted for the Raman experiment. Temperature stability was $\pm 1\,^{o}C$.

The only major modification to the chamber as illustrated in Figure 49 was the replacement of the polymethylmethacrylate cover with one of glass. After prolonged times at elevated temperature the plastic cover suffered distortion.

The resolution and acquisition time used to record spectra were $2cm^{-1}$ and 1 minute respectively.

5.3.2 Results and Discussion of Fourier Transform Infra-Red Spectroscopy of Crosslinked Polyethylene

Recording Fourier transform infra-red spectra of crosslinked polyethylene provided few difficulties. It was possible to record spectra at extensions of up to $3\frac{1}{2}:1$ at $150\,^{o}C$. The specimens used were cut from the same sheet of crosslinked polyethylene that furnished samples for the equivalent Raman experiment.

The vibrational spectrum of molten polyethylene and the assignment of bands to specific vibrations is covered exhaustively by Snyder (65). It is from this paper that all assignments quoted below are drawn.

The infra-red spectrum of relaxed crosslinked polyethylene at $150\,^{o}C$ closely matches that recorded by Snyder for molten linear polyethylene. Spectra were recorded for samples at extensions of 2:1, 3:1 and $3\frac{1}{2}:1$. At a glance these spectra failed to reveal any marked differences between extended and unextended specimens. Closer inspection however revealed a few subtle changes in the fine structure.

In the light of results from the equivalent Raman experiment the small changes in the infra-red spectra can be explained. From the Raman results it was suggested that only certain chains take up an extended configuration, and that the proportion of gauche configurations drops by only $\sim 3\%$ from 40%. The calculated position of the methylene rocking mode which appears in the infra-red spectrum varies with

the number of consecutive trans configurations, asymptoting to a value of 718.5cm^{-1} (as shown in Figure 50). Therefore even a fully extended chain of infinite length will give rise to a peak indistinguishable in position from that produced by only 5 or 6 consecutive trans conformations. On stretching the hot crosslinked polyethylene, the profile of this methylene rocking band changed very slightly, but its position did not alter distinguishably.

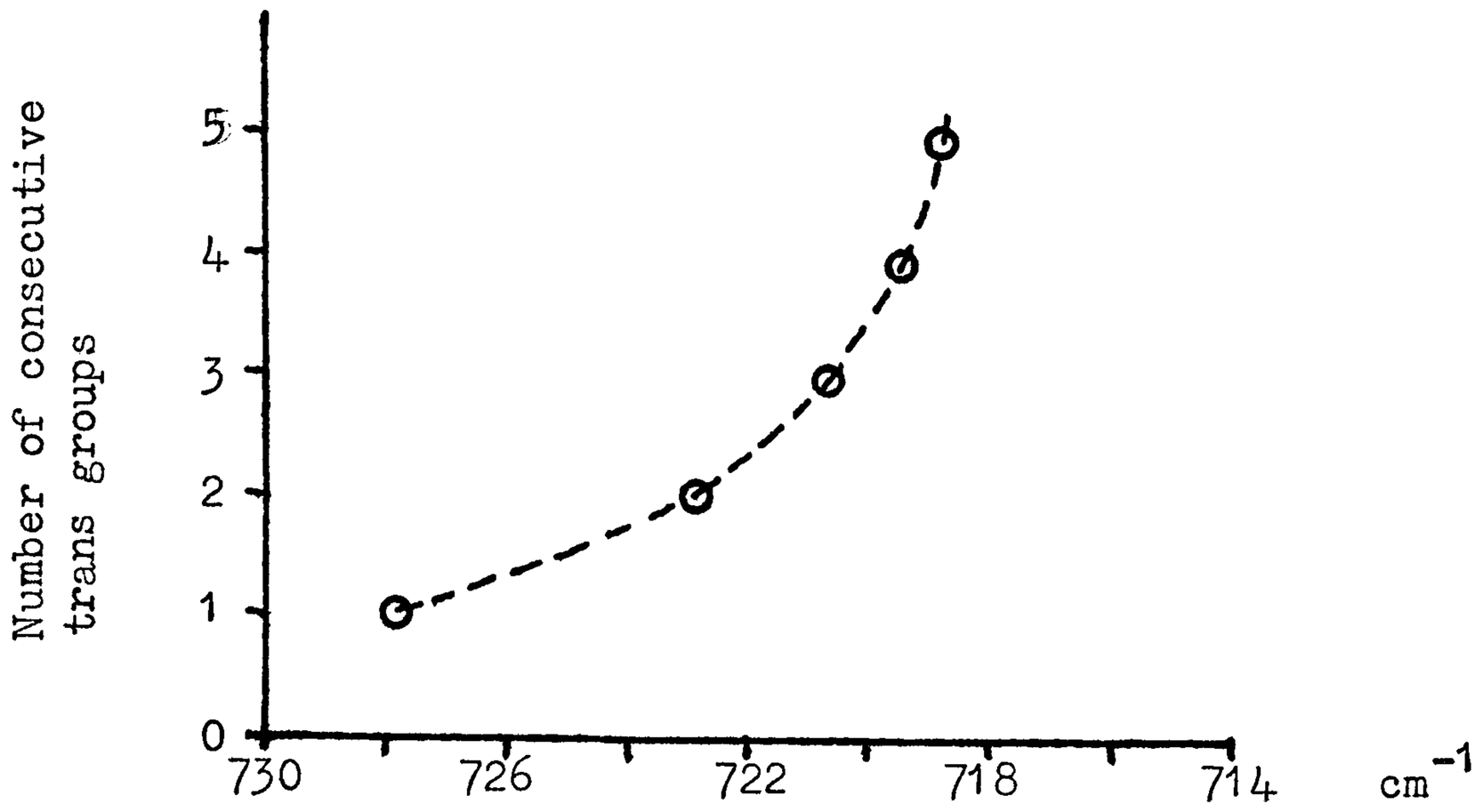

Figure 50 Number of consecutive trans groups versus methylene rocking mode frequency in polyethylene (after Snyder (65)).

The numbers of gauche-gauche and gauche-trans-gauche configurations would be expected to fall slightly as the samples are extended, resulting in a decrease in intensity of the bands associated with methylene wag at 1352, 1367 and 1305cm^{-1} and with methylene rock at 745cm^{-1}. Two factors mitigate against a large decrease in intensity of these bands; the sample is only 55% gelled, so many free chains exist, and also, even in the semi-crystalline state at room temperature these bands retain ~50% of their intensity found in the rubbery state. It is therefore not surprising that the intensities of these bands show a decrease of only ~5% on stretching to $3\frac{1}{2}$:1. This fall is not unreasonable compared with the fall in concentration of gauche configurations estimated as 3% from the Raman results.

5.4 SUMMARY OF RAMAN AND INFRA-RED STUDIES OF HOT STRETCHED CROSSLINKED POLYETHYLENE

The two methods of vibration spectroscopy used to study hot stretched crosslinked polyethylene indicate that only a small proportion of all chains adopt an extended form. Other chains retain their disordered arrangement, with only a slight decrease in gauche configurations.

Similar experiments on fully crosslinked samples would be expected to exaggerate the observed effects.

Chapter 6

RAMAN SPECTROSCOPY OF FLOWING POLYMER MELTS

6.1 DESIGN OF EXTRUDER DIES FOR RAMAN SPECTROSCOPY

The Polymer Properties Group at the University of Southampton had previously carried out Raman spectroscopic study of a polymer melt flowing in circular tubes (66). It was proposed that this work be continued and experimental techniques refined.

The requirements for an extrusion die for Raman spectroscopy fall into two categories; primary, which must be fulfilled, and secondary which potentially improve the quality of the results. The primary requirements are simply that there must be a window to admit the exciting laser beam, a window to view the inelastic light scatter, and that the die must be able to withstand the temperatures and pressures required for extrusion in safety and without leaking. Secondary requirements include: accurate measurement of the temperature and pressure of the flowing melt, accurate location of the laser beam, the ability to study all parts of the channel along which the polymer flows, and the facility to change the cross-section of the channel.

The original die used for this work comprised a glass tube, through which the polymer flowed, surrounded by a heated steel cylinder with appropriate holes to allow the introduction of the laser beam and the collection of the scattered light. This die is illustrated in Figure 51.

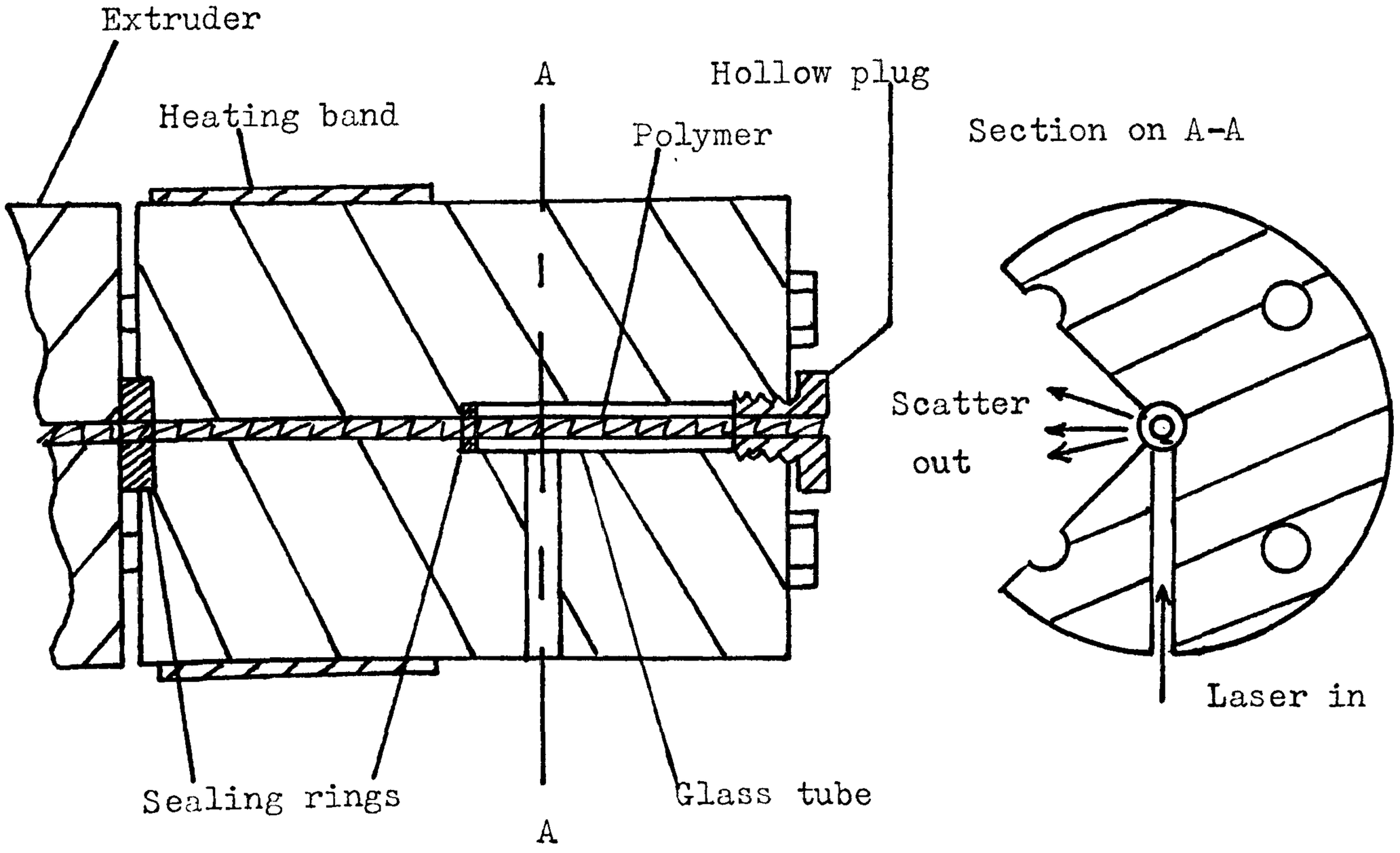

Figure 51 Diagram of original die.

This die suffered from the major drawback that it was not possible to determine, or duplicate, the exact point illuminated by the laser beam. It was therefore decided to develop a die that would avoid this problem, and fulfil as many of the secondary requirements as possible. To this end, a new die was designed, which is described below.

The new die (Mk II) departed entirely from the design of its predecessor. The principle adopted was that polymer should flow along a channel, one side of which consisted of a glass plate. This die was kindly made in the workshops of Imperial Chemical Industries Plastics Division at Welwyn Garden City, to whom thanks are expressed. This die is illustrated in Figure 52.

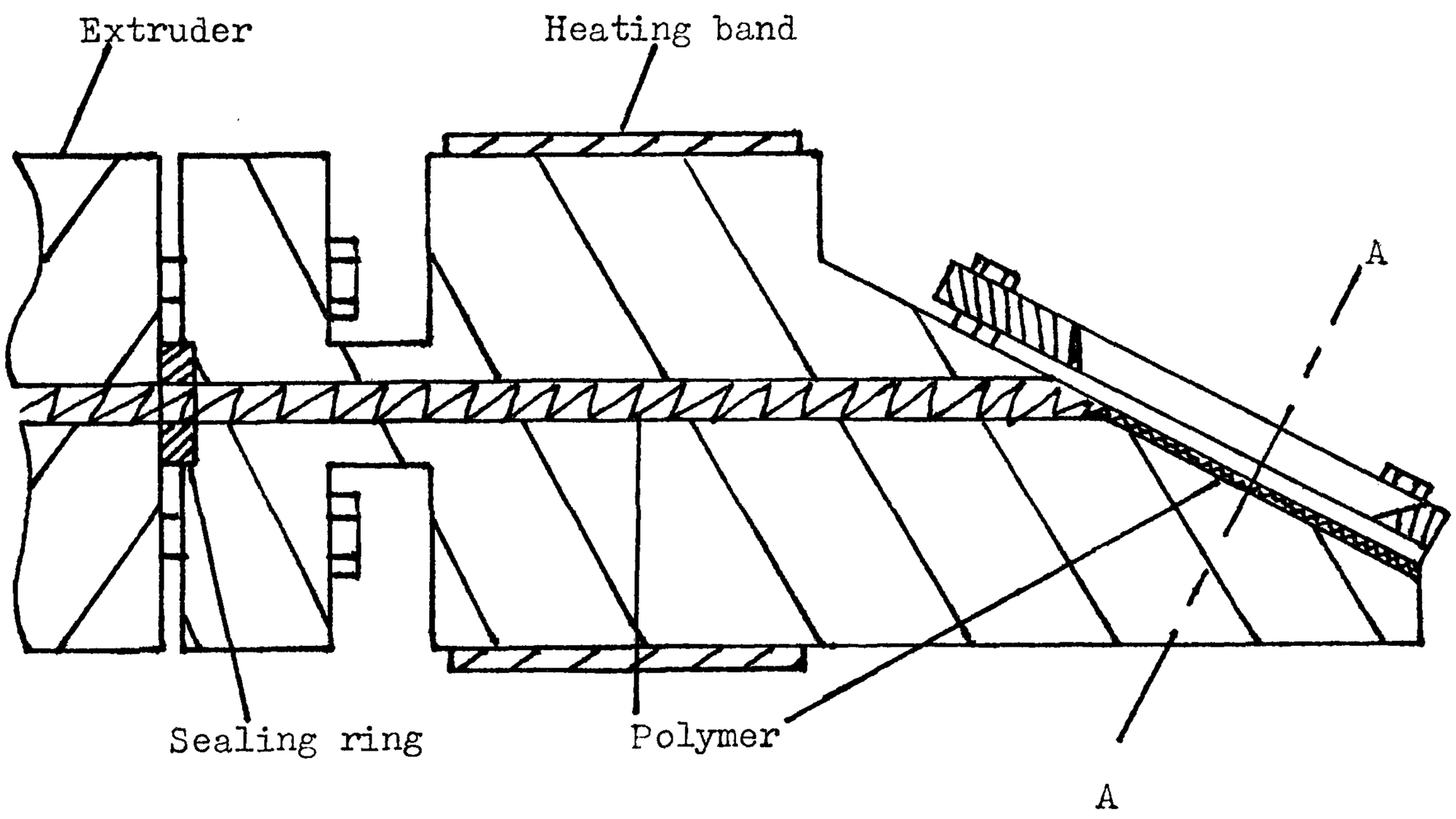

Figure 52 Diagram of die Mk II.

The glass plate is held in place by a cover plate with a chamfered slot cut into it; this allowed the entry of the laser beam and the collection of the scattered light. To record spectra it was necessary to orientate the die carefully with respect to the spectrometer. To facilitate this a flexible coupling was made to transport molten polymer from the extruder to the die. The flexible coupling consisted of a copper tube connected to flanges at either end by Wade Couplings. The flanges were bolted to the extruder and the die. The tube was heated by a pair of heating cords tightly wrapped around it, control was by means of a variac. For higher pressure work it was found to be necessary to use a seamless stainless steel tube. As the pressure was further increased it became necessary to solder part of the couplings into place on the tube.

The new die proved to be of limited use. Its major faults were that the glass window was prone to break and that the channel down which the polymer flowed was fixed in cross-section and was of a rheologically awkward nature for which accurate shear rate data could not be calculated. However the spectra recorded using it were of sufficiently high quality that further development was thought to be worthwhile.

The next die design (Mk III), allowed for a readily variable channel profile. In principle this die was similar to die Mk II. The channel was formed by an interchangeable slotted plate sandwiched between the main part of the die and a glass plate. This die is shown in Figure 53.

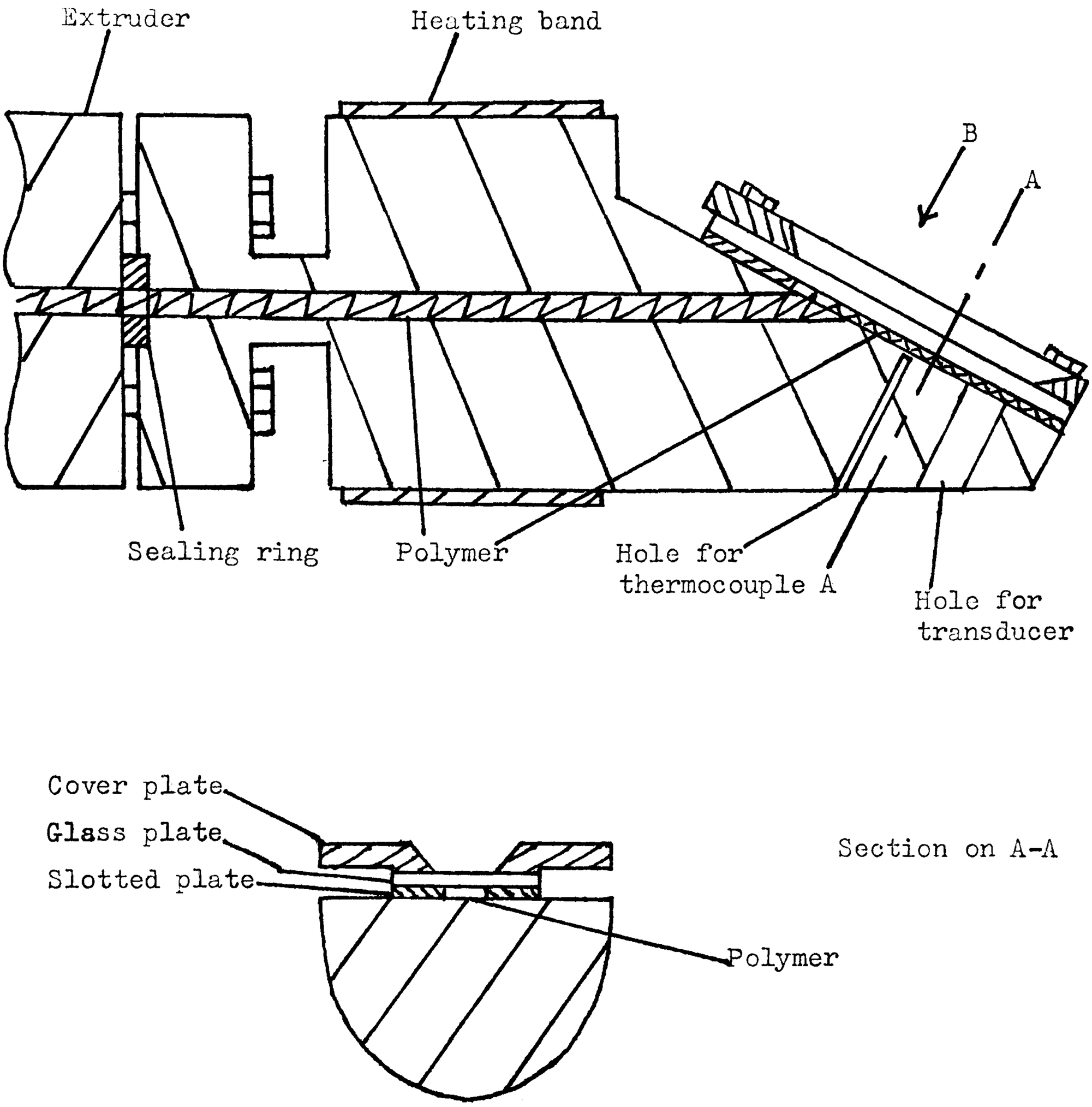

Figure 53 Diagram of die Mk III.

Other refinements included the provision of a tapped hole to accept a pressure transducer, and a blind hole approaching to within 2mm of the channel to accommodate a thermocouple. Facility was also included for the provision of a change of channel profile at a point accessible to the laser beam. This arrangement is shown in Figure 54.

View on B of figure 53

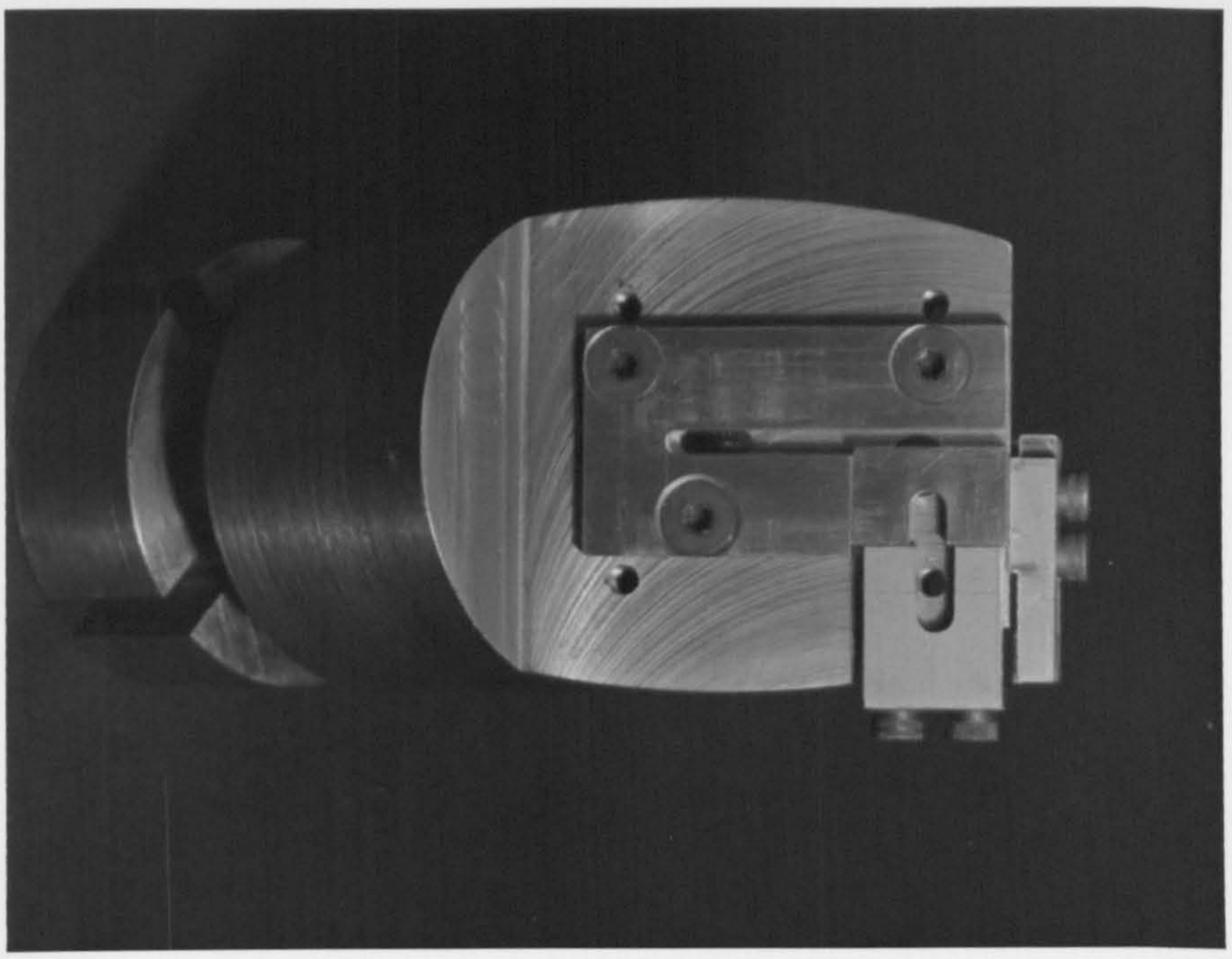

Figure 54 Arrangement for changing channel profile on die Mk III

The assembly of this die required a "delicate touch" to ensure a good seal. With so many mating surfaces it was necessary to ensure that each surface was perfectly flat, cleaned and polished before assembly. This was accomplished by polishing each metal face with 1200 grit "wet and dry" emery paper attached to a piece of plate glass. A good joint was ensured by the use of "Red Hermatite" (a proprietary jointing compound, beloved of all amateur engine rebuilders). Tightening down the cover plate had to be accomplished in a perfectly even manner if leaks were to be prevented and the glass plate not broken.

At first this die suffered from two inter-related problems, the glass plate was prone to break under pressure, and it was very difficult to get a signal out of the slotted cover plate. If the thickness of the glass plate was increased refraction prevented any signal being recorded as no scattered light could then be collected. See Figure 55.

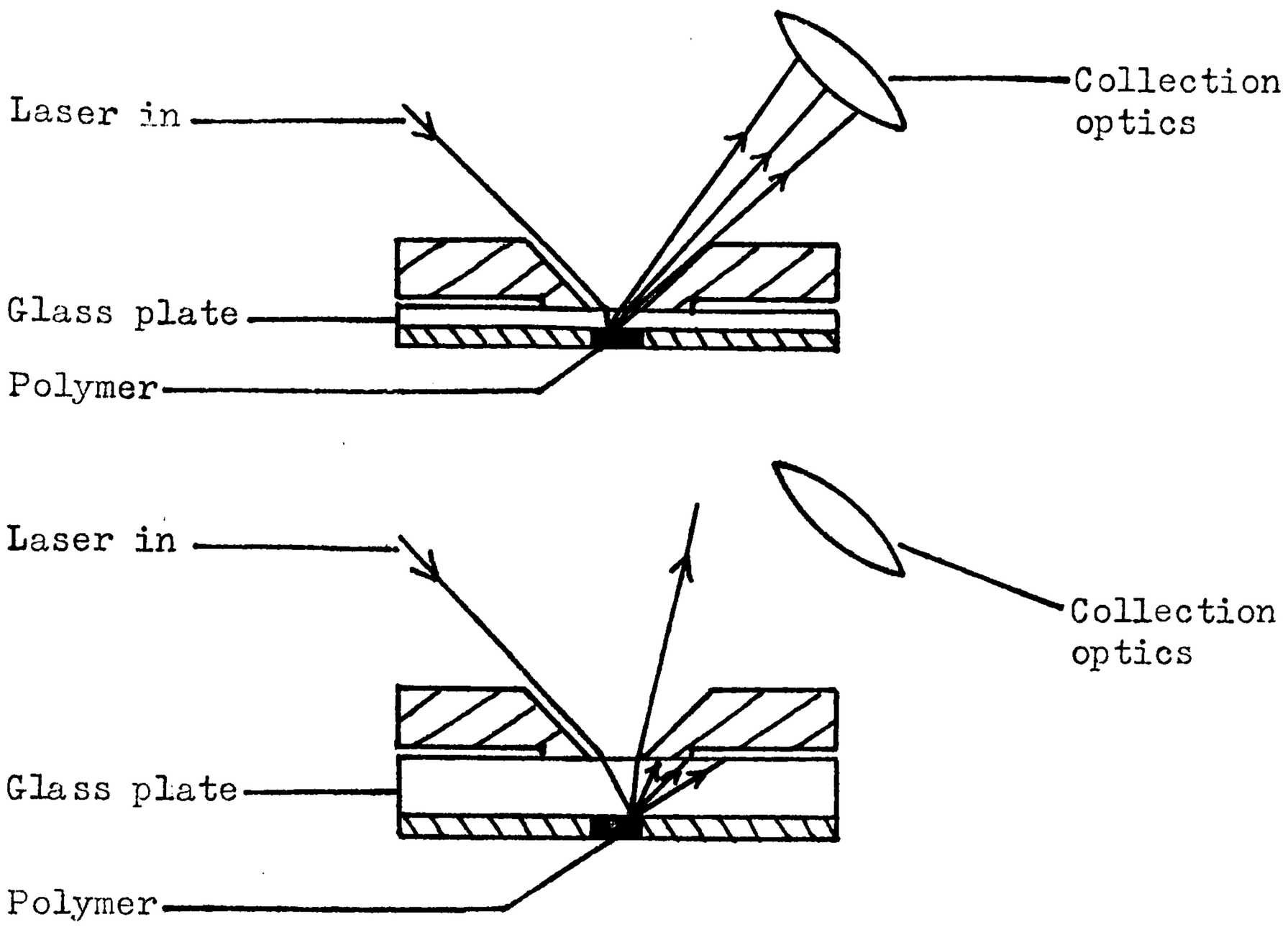

Figure 55 Effect of increased glass thickness on signal collected.

The glass plate most frequently broke when the pressure exerted by the extruder was increased or decreased. The usual point of fracture was at the point where the polymer first makes contact with the glass. It was decided to reduce the slot in the cover plate to a truncated conical hole, as shown in Figure 56.

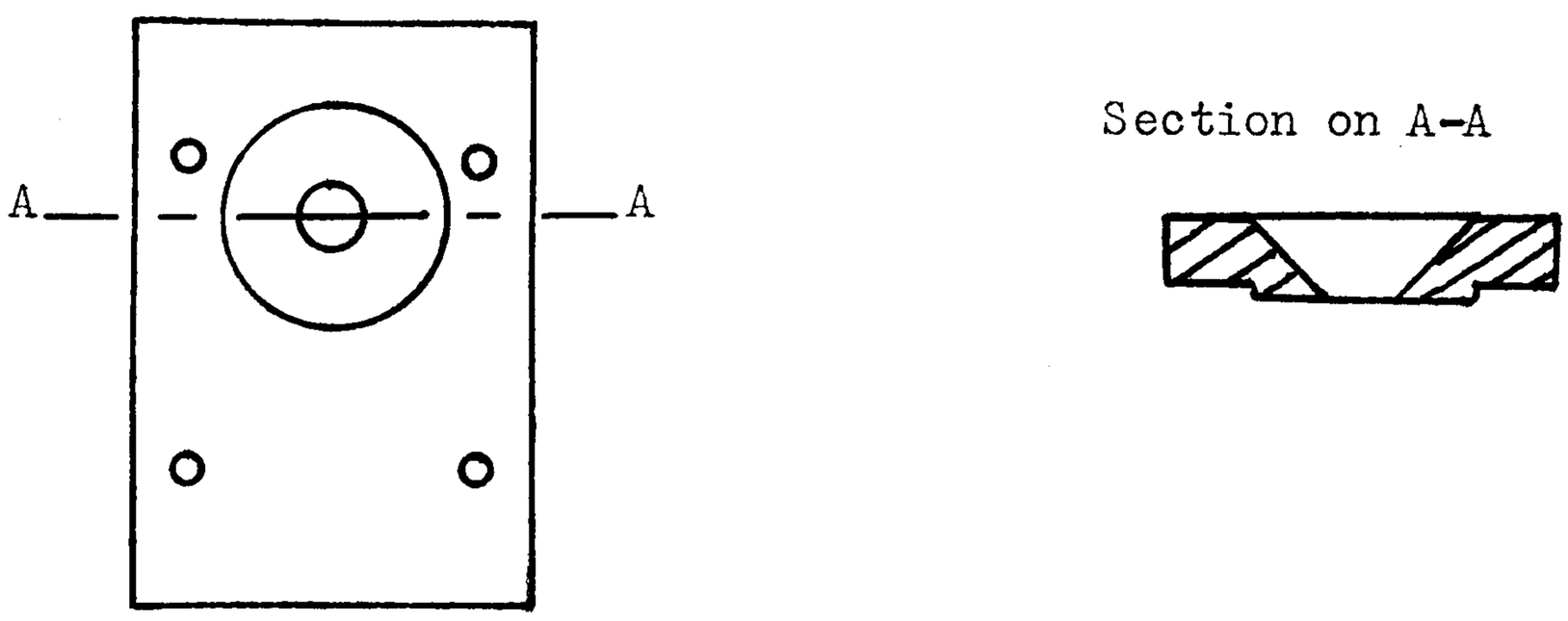

Figure 56 New cover plate.

This solved the problem of the window breaking, but reduced the area observable effectively to a point. This situation was unacceptable. After some thought was given

to the physical strength of glass, and the performance required of it, a solution was found. The breaking of the glass plate may be considered as the breaking of a very wide beam. The strength of a beam increases as a power of 3 as its thickness increases, whereas refraction effects are directly proportional to the thickness of the glass. Hence, all that is required is to increase the thickness of the glass plate dramatically and to dispense with the cover plate replacing it with a pair of stiff beams positioned in such a way that they do not impinge on the optical path. This arrangement is shown in Figure 57.

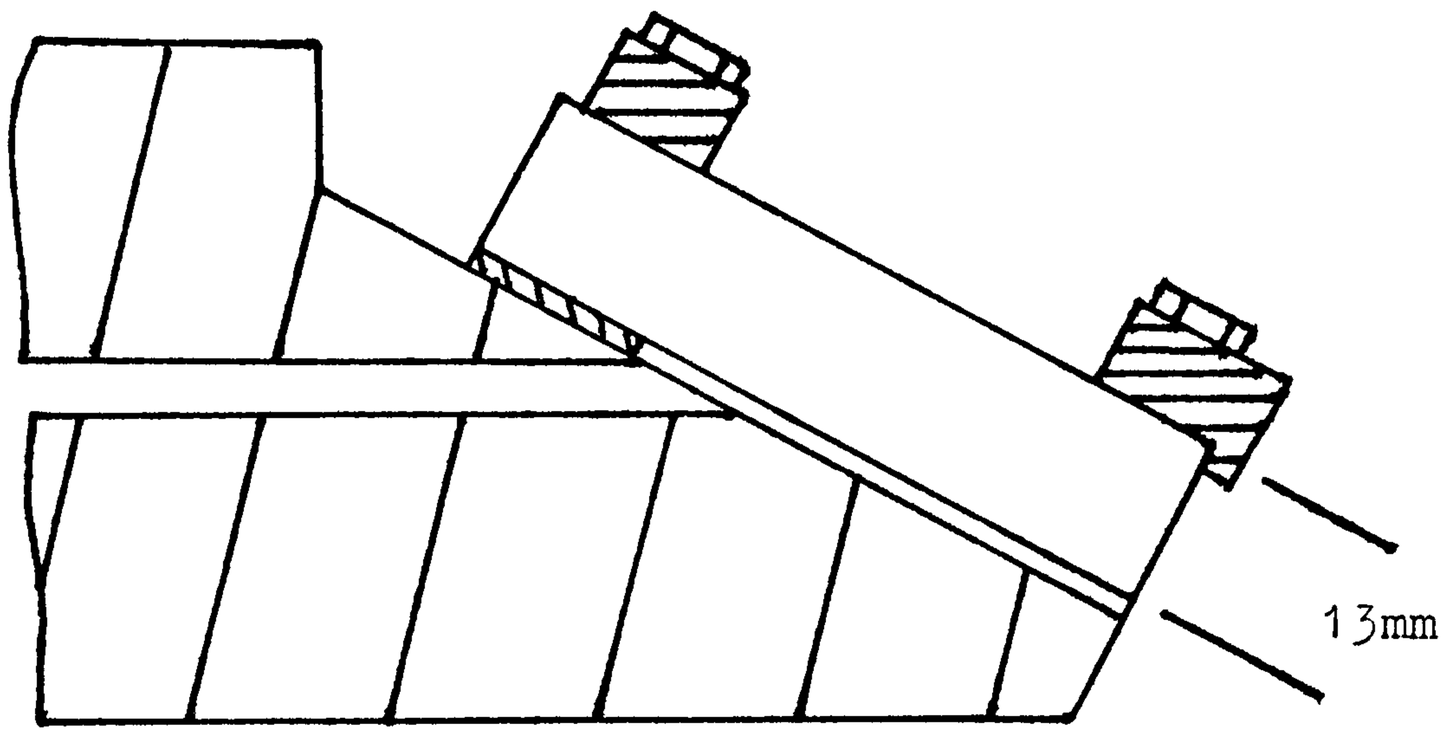

Figure 57 Arrangement of successful glass window on die Mk III

With this final modification the die performed well.

6.2 RECORDING RAMAN SPECTRA OF FLOWING POLYMER MELTS

Raman spectra of flowing polymer melts were recorded on the Anaspec LR-36. This instrument was chosen in preference to the Coderg T800 because of its rapid data acquisition and excellent data handling capabilities.

Four commercially available polymers were investigated; Rigidex 50, a high density grade of polyethylene manufactured by British Petroleum PLC; Propathene PXC 2090, an isotactic polypropylene manufactured by Imperial Chemical Industries PLC; polyethylene terephthalate grade B73 manufactured by Imperial Chemical Industries PLC; and Maranyl, a grade of nylon-6 manufactured by Imperial Chemical Industries PLC.

Great difficulties were encountered when recording spectra of flowing polymer melts. The signal to noise ratio was variable in the extreme. This made the accurate determination of peak position and intensity impossible in many cases. However, some series of spectra were recorded which exhibited an acceptable signal to ratio over a range of shear rates. The cause of the low signal to noise ratio was generally a combination of the effects of fluorescence and mechanical vibration from the extruder. Polymer samples generally fluoresce at high temperatures, the degree of fluorescence is also dependent upon the length of time the polymer resides in the hot extruder, and thus is related to the output rate. In many cases the fluorescence was more than 20 times as strong as the most intense Raman signal. Theoretically the fluorescent background can be removed by subtraction on the LR-36. This is dependent on being able to produce a matching fluorescent background to subtract from the raw data. A reasonable match could generally be achieved for the static melt, but when the screw was started the fluorescent background changed, thus an acceptable signal to noise ratio may be obtained at low shear but not at high shear. Varying the shear rate required altering the screw speed of the extruder. The faster the screw speed the greater is the mechanical vibration experienced by the die. Vibration causes deterioration of the alignment of the die in the spectrometer. The flexible coupling helped to alleviate this problem, but did not remove it entirely.

6.3 RESULTS OF RAMAN SPECTROSCOPY ON FLOWING POLYMER MELTS

Overall results were fairly disappointing. The different polymers studies will b e discussed in turn.

6.3.1 High Density Polyethylene

Spectra were recorded for this material at shear rates at the tube wall of up to $340s^{-1}$ at 150°C, and $925s^{-1}$ at 182°C. The quality of the spectra decreased with increasing shear rate and temperature.

As far as could be ascertained there were no changes in peak position as the polymer was sheared. Nor did any new peaks appear as they did in the stretched crosslinked polyethylene experiment. Intensities remained constant as far as could be

estimated within the large experimental errors.

6.3.2 Isotactic Polypropylene

Spectra of this material proved to be very difficult to obtain, even as a static melt. The signal to noise ratio was at best 5:1 dropping to 1:1. As far as could be seen (which admittedly was not very far!) no changes occurred in the spectrum as the melt was sheared.

Experiments on this material were terminated at a preliminary stage.

6.3.3 Nylon-6

The quality of the spectra obtained for this polymer was very poor. A very high degree of fluorescence overwhelmed all spectral detail.

Experiments on this material were terminated at a preliminary stage.

6.3.4 Polyethylene Terephthalate

By far the majority of experiments on flowing melts was carried out on polyethylene terephthalate.

It was necessary to dry the polymer chips prior to extrusion. Neglect of this precaution resulted in premature degradation of the polymer in the extruder. Over zealous drying resulted in increased fluorescence. The polymer was dried for 24 hours at 80°C in a vacuum oven before extrusion.

Spectra recorded for polyethylene terephthalate were invariably of better quality than those recorded for the other three polymers investigated. Signal to noise ratio could drop as low as 5:1 at high shear, but was generally 15:1 or better. A good example of a spectrum of flowing polyethylene terephthalate is shown in Figure 58.

The use of polyethylene terephthalate was facilitated by the fact that it can be extruded at supercoolings of up to 20°C below its melting point of 260°C.

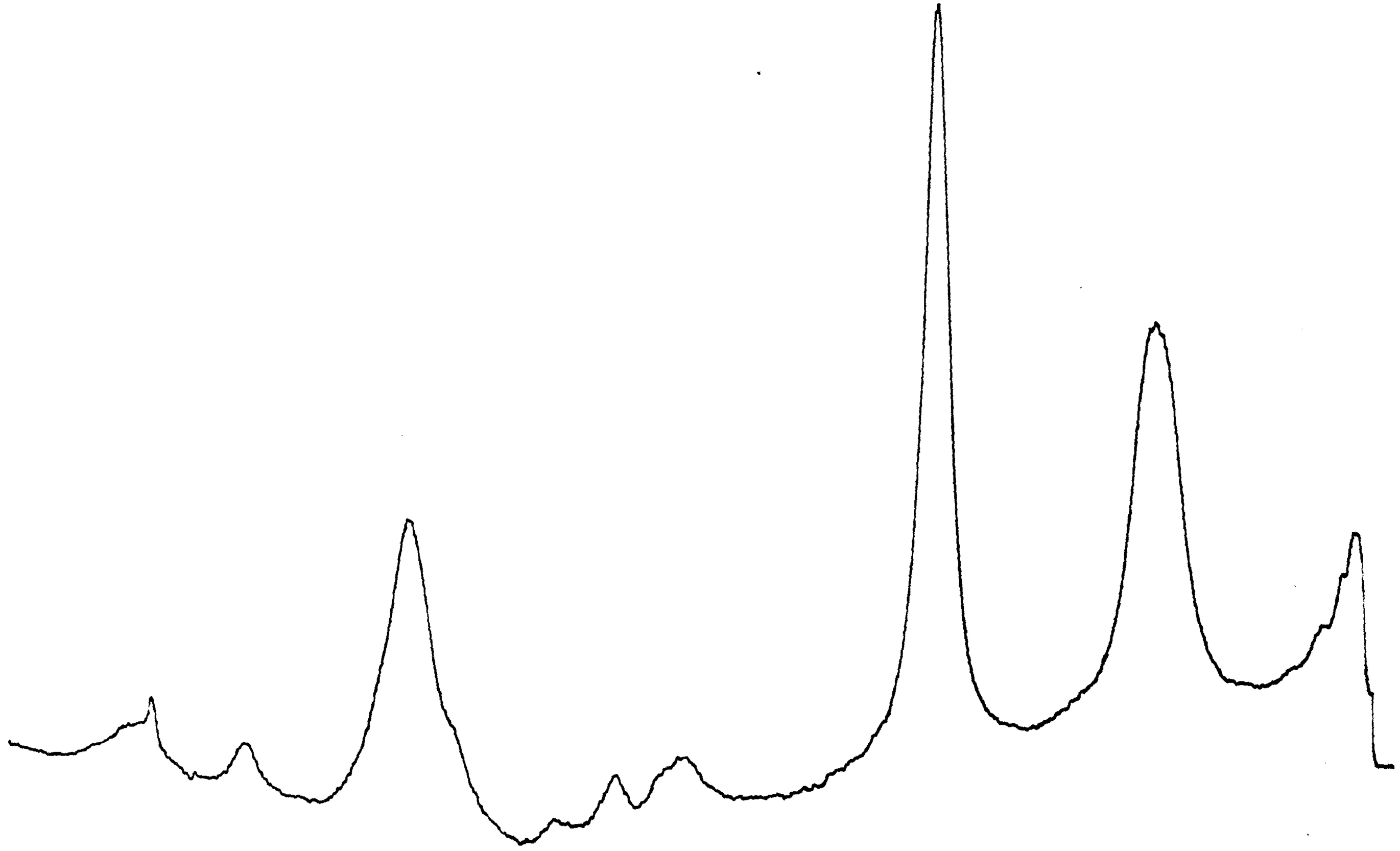

Figure 58 Raman spectrum of flowing polyethylene terephthalate

An exhaustive series of experiments was carried out on flowing polyethylene terephthalate varying: temperature (240-300°C), shear rate at wall (0-500s^{-1}), size and shape of die channel, and the position of the exciting laser beam with respect to changes in the cross-section of the die channel. This was all to no avail, all peaks remained in the same positions and of the same intensities (as far as could be ascertained) as those found in the static melt at the same temperature.

6.4 DISCUSSION OF RESULTS

The results obtained for flowing polyethylene terephthalate are at variance with those previously reported (66) where shear effects were noted in the spectrum of molten polyethylene terephthalate. The major experimental difference is that of die channel cross-section. The previous work was carried out using a circular cross-section glass die, in which the laser beam was positioned at the extreme edge of the tube where the shear is greatest. In the work reported here the laser beam enters the melt at an angle, therefore sampling a volume of polymer extending further into the melt than in the earlier configuration. This is illustrated in Figure 59.

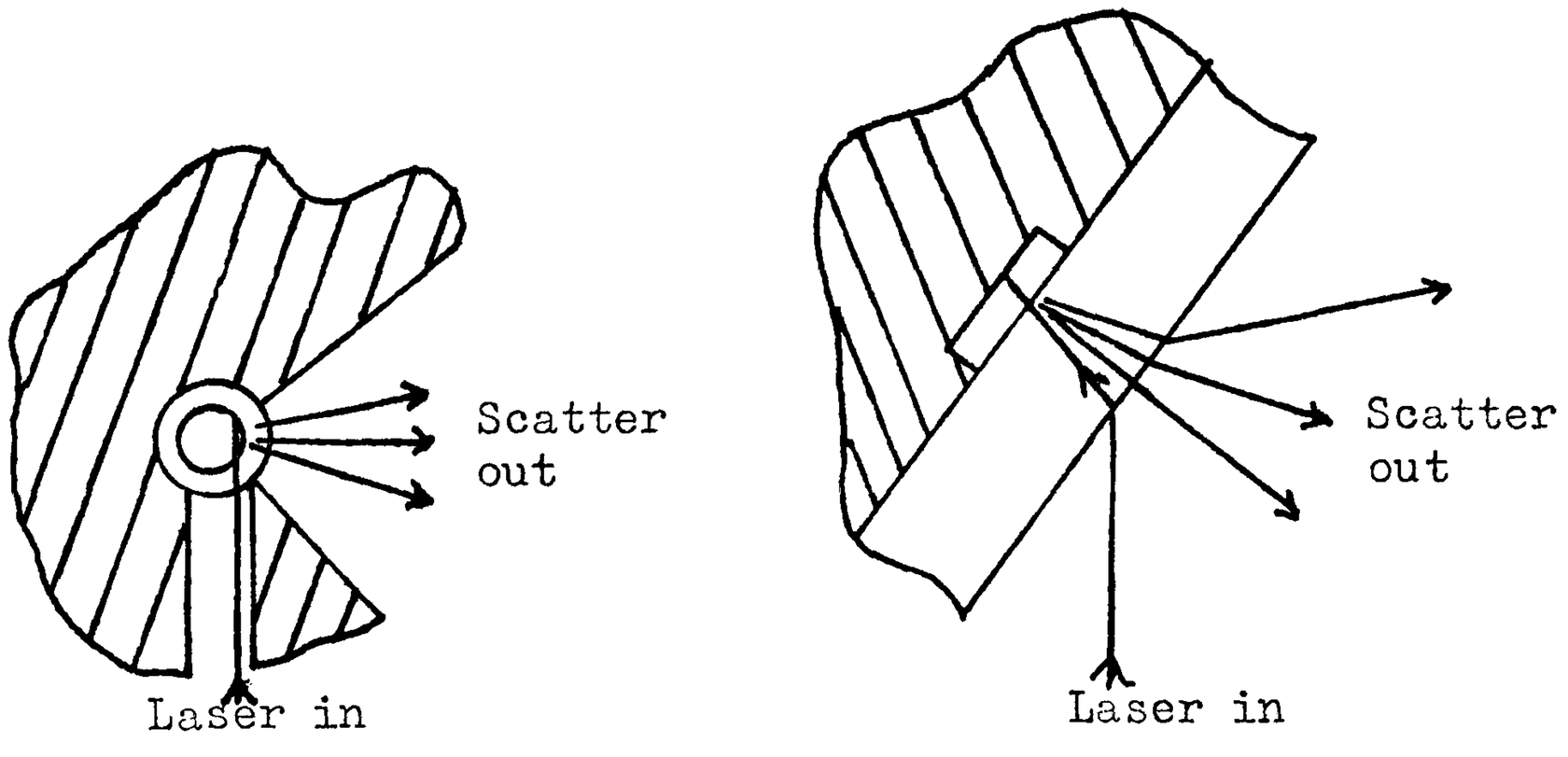

Figure 59 Configurations for studying flowing melts.

It is possible that such a configurational difference accounts for the discrepancy between results.

The investigation reported here was far more exhaustive than that conducted previously, and the quality of spectra was much higher. The fact that no change at all was noticed in the present work as shear increases leads one to believe that configurational differences between the two experiments cannot account wholly for the lack of agreement between data. Doubt is therefore cast upon the previous work.

From the results of the Raman investigation of polyethylene and polyethylene terephthalate one is led to the conclusion that the alignment of molten polymer molecules flowing along a tube at the shear rates used is very slight. This conclusion is in agreement with parallel work being carried out on the X-ray diffraction of flowing melts by other members of the Polymer Properties Group (67).

This conclusion is disquieting in the light of accepted explanations of rheological phenomena. The mechanism of die swell is usually explained in terms of shear extended chains adopting a random coil configuration, thus bringing about shortening of the extrudate. Such extension is not detectable by Raman spectroscopy although die swell under certain conditions is very marked. Extrudates usually contain oriented crystalline regions: does this orientation only occur on crystallization? Many other questions are also posed.

Chapter 7

CONCLUSION

Historically the research of the Polymer Properties Group under Dr. Hendra has been concerned with the morphology of thermoplastics. The intention of the work described in this thesis was to continue and refine previous lines of research and open new areas by the use of novel techniques of specimen preparation and well established experimental techniques.

Three lines of research were originally postulated. The first involved continuation of research into the Raman spectra of flowing melts with particular emphasis on improving experimental techniques. As an aid to this work it was decided to model flowing polymer with crosslinked polyethylene stressed above its crystalline melting point. The final line of research originally suggested, was the study of various properties of crosslinked polyethylene as the degree of crosslinking was varied, in an attempt to improve our understanding of the morphology of semi-crystalline polymers. The crosslinking reaction also came under scrutiny after anomalies in the crosslinking reaction were noted.

The outcome of this research covers various areas:

1. Reproducible methods for crosslinking high density polyethylene have been developed.
2. The efficiency of the crosslinking reaction has been determined.
3. Certain morphological properties of crosslinked polyethylene have been explained as a function of crosslink density.
4. The technology of recording Raman spectra of flowing melts has been improved.
5. Raman spectra have been recorded for a variety of flowing melts.
6. Methods have been developed for recording vibrational spectra of crosslinked polyethylene at high temperature under large extensions.
7. Vibrational spectra of hot stretched crosslinked polyethylene have been used to elicit the structure of stretched rubber.

As a result of the information provided by this research, three major conclusions have been reached.

1. The chain folded model of crystallization of polyethylene is untenable.
2. The change of molecular order consequent upon polymer flow is slight overall.
3. Stress applied to a rubber causes preferential alignment of certain chains, overall ordering remains slight.

The work reported here poses a number of questions, as well as answering others. It would appear that fruitful lines of research leading from these results include:

1. Analysis of flowing melts by means of a semi-microscopic probe e.g. optical fibres.
2. Polarization experiments involving infra-red and Raman spectroscopy of stretched crosslinked polyethylene.
3. Analysis of other rubber systems by vibrational spectroscopy.
4. Use of a pulsed laser and synchronised data gathering to avoid fluorescence effects when carrying out Raman spectroscopy on flowing polymer melts and hot polymers.
5. Effects of entanglements on flowing polymer melts.

References

(1) European Plastics News, April 1984

(2) P.H. Till, J.Polym.Sci.,24,301 (1957)

(3) A. Keller, Phil.Mag.,2,1171 (1957)

(4) D.C. Bassett, F.C. Frank and A. Keller, Phil.Mag.,8,1753 (1963)

(5) E.W. Fischer and R. Lorenz, Kolloid-Z:Z. Polymere,189,97 (1963)

(6) J.B. Jackson, P.J. Flory and R. Chiang, Trans.Far.Soc.,59, 1906 (1963)

(7) T. Kawai, Makromol.Chem.,90,288 (1966)

(8) E.W. Fischer, Z. Naturforsch., 12a,753 (1957)

(9) R. Eppe, E.W. Fischer and H.A. Stuart, J.Polym.Sci.,34,721(1959)

(10) C. Sella and J.J. Trillat, Compt.Rend.,248,410 (1959)

(11) P.H. Geil, J.Polym.Sc.,47,65 (1960)

(12) P.J. Flory, J.Amer.Chem.Soc.,84,2857 (1962)

(13) F.C. Frank, Far.Disc.Chem.Soc.,No.68,7 (1979)

(14) J.Schelten, D.G.H. Ballard,G.D. Wignall,G. Longman and W. Schmatz, Polym.,17, 751 (1976)

(15) D.Y. Yoon and P.J. Flory, Polym.,18, 509 (1977)

(16) D.Y. Yoon, J.Appl.Cryst.,11,531 (1978)

(17) D.Y. Yoon and P.J. Flory, Far.Disc.Chem.Soc.,No 68,288 (1979)

(18) J.D. Hoffman,Polym.,23, 656 (1982)

(19) P.G. De Gennes, J.Chem.Phys.,55(2), 572 (1971)

(20) J.D. Hoffman, C.M. Guttman and E.A. Di Marzio, Far.Disc.Chem. Soc.,No.68, 177 (1979)

(21) C.M. Guttman, E.A. Di Marzio and J.D. Hoffman,Polym., 22, 597, (1981)

(22) D.M. Sadler and A. Keller, Polym.,17, 37 (1976)

(23) J. Petermann and H. Gleister, Kolloid-Z:Z. Polymere,251, 850 (1973)

(24) B.S. Bernstein, S.P.E. Eastern New England Section,TETEC Conf., p117, March 1975

(25) V.V. Vasilenko, E.R. Klinshpoint and V.K. Milinchuk, Polym. Sci. USSR,20, 503 (1978)

(26) M. Dole,Polym.Plast.Technol. and Engng.,13, 41 (1979)

(27) A. Keller and G.M. Patel, J.Polym.Sci.Polym.Phys.Ed., 13(2), 323 (1975)

(28) F.C. Frank, Polym.,15, 679 (1977)

(29) Technical Information on Noury Initiators supplied by Akzo Chemie.

(30) G.E. Hulse, R.J. Kersting and D.R. Warfel, J.Polym.Sci. Polym.Chem.Ed.,19, 655 (1981)

(31) R.D. Mair and A.J. Graupner, Anal.Chem.,36, 194 (1964)

(32) G. Herzberg, "Infrared and Raman Spectra of Polyatomic Molecules", D. Van Nostrand Co., Princeton,N.J. (1945)

(33) P.J. Hendra and T. Gilson, "Laser Raman Spectroscopy", J. Wiley Interscience,London (1970)

(34) D.J. Cutler, P.J. Hendra and G. Fraser, "Developments in Polymer Characterisation-2", (Edited by J.V. Dawkins), Applied Science Publishers Ltd. (1980)

(35) R.J. Bell, "Introductory Fourier Transform Spectroscopy", Academic Press, New York (1972)

(36) P.R. Griffiths "Chemical Infra-Red Fourier Transform Spectroscopy", Wiley-Interscience,New York (1975)

(37) E.M. Dannenberg, M.E. Jordan and H.M. Cole, J. Polym. Sci.,31, 127 (1958)

(38) D.Simunkova, R. Rado and O. Mlejnek, J. Appl.Polym.Sci., 14, 1825 (1970)

(39) J.D. Van Drumpt and H.H.J. Oosterwyk, J.Polym.Sci.Polym. Chem.Ed.,14, 1495 (1976)

(40) A.J. Peacock,M.Sc. Thesis, Lancaster (1981)

(41) A.M. Ryke and L. Mandelkern, Macromol.,4(5), 594 (1971)

(42) P.J. Flory and J. Rehner,J.Chem.Phys.,11, 512 (1943)

(43) P.J. Flory,J.Chem.Phys.,18, 108 (1950)

(44) P.J. Flory,Ind.Engng.Chem.,38, 417 (1946)

(45) L. Mullins,J.Polym.Sci.,19, 225 (1956)

(46) Q.A. Trementozzi,J. Polym.Sci.,23, 887 (1957)

(47) L.H. Tung, J.Polym.Sci.,24, 333 (1957)

(48) R.G. Snyder and J.R. Scherer, J.Polym.Sci.Polym.Phys.Ed., 18, 421 (1980)

(49) S.L. Hsu and S. Krimm,J.Appl.Phys., 47, 4265 (1976)

(50) S.L. Hsu and S. Krimm.J.Appl.Phys., 48, 4013 (1977)

(51) G.R. Strobl and R. Eckel,J.Polym.Sci.Polym.Phys.Ed., 14, 913 (1976)

(52) G. Minoni and G. Zerbi, J.Phys.Chem.,86, 4791 (1982)

(53) R.H. Olley, A.M. Hodge and D.C. Bassett, J.Polym.Sci. Polym.Phys.Ed.,17, 627 (1979)

(54) D.C. Bassett and A.M. Hodge,Proc.R.Soc.Lond., A377,25 (1981)

(55) R.S. Stein and M.B. Rhodes,J.Appl.Phys.,31, 1873 (1960)

(56) K.J. Packer, J.M. Pope, R.R. Yeung and M.E.A. Cudby, J. Polym.Sci.Polym.Phys.Ed., in press.

(57) J. Maxfield, R.S. Stein and M.C. Chen, J.Polym.Sci.Polym. Phys.Ed.,16, 37 (1978)

(58) J.L. Lippert and W.L. Peticolas,Proc.Nat.Acad.Sci. USA, 68, 1572 (1971)

(59) H. Tanaka and T.Takemura,Poly.J.,12, 355 (1980)

(60) S.L. Wunder,Macromol.,14, 1024 (1981)

(61) G.R. Strobl and W. Hagedorn,J.Polym.Sci.Polym.Phys.Ed., 16, 1181 (1978)

(62) R.G. Brown,J.Chem.Phys.,38,221 (1963)

(63) R.G. Snyder,J.Mol.Spectry.,31, 461 (1969)

(64) V.B. Carter,J.Mol.Spectry.,34, 356 (1970)

(65) R.G. Snyder,J.Chem.Phys.,47, 1316 (1967)

(66) P.J. Hendra, D.B. Morris, R.D. Sang and H.A. Willis, Polym.,23, 9 (1982)

(67) M.A. Taylor, unpublished data